

Surface Parameter Estimation: Basics and Advanced Concepts

Irena Hajnsek



Earth Observation and
Remote Sensing

Institute of Environmental Engineering, ETH Zürich
Microwaves and Radar Institute, DLR Oberpfaffenhofen

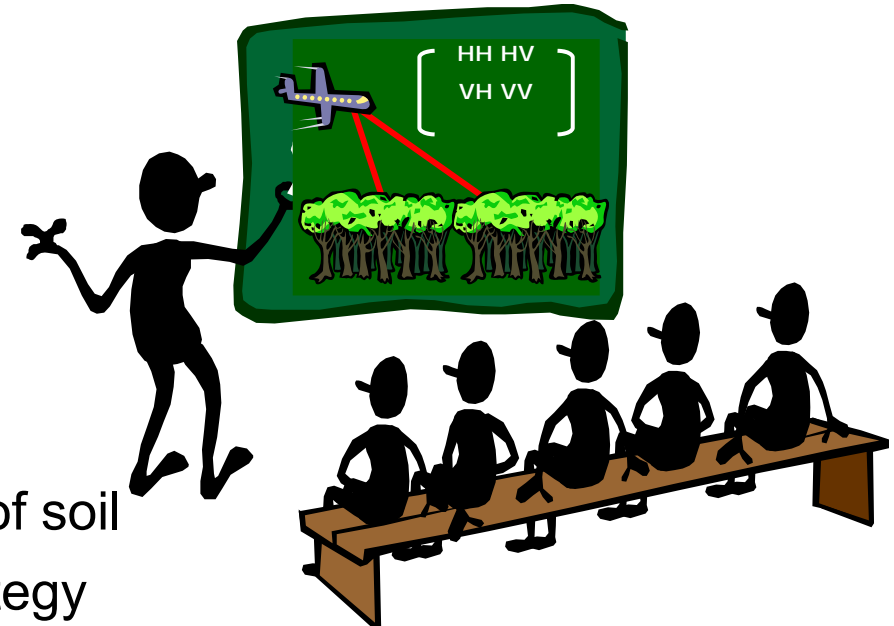


Knowledge for Tomorrow

Overview

Part I: Theory and basics

- › Introduction into SAR polarimetric observables
- › Decomposition techniques
- › Introduction into material properties of soil
- › Model description and inversion strategy

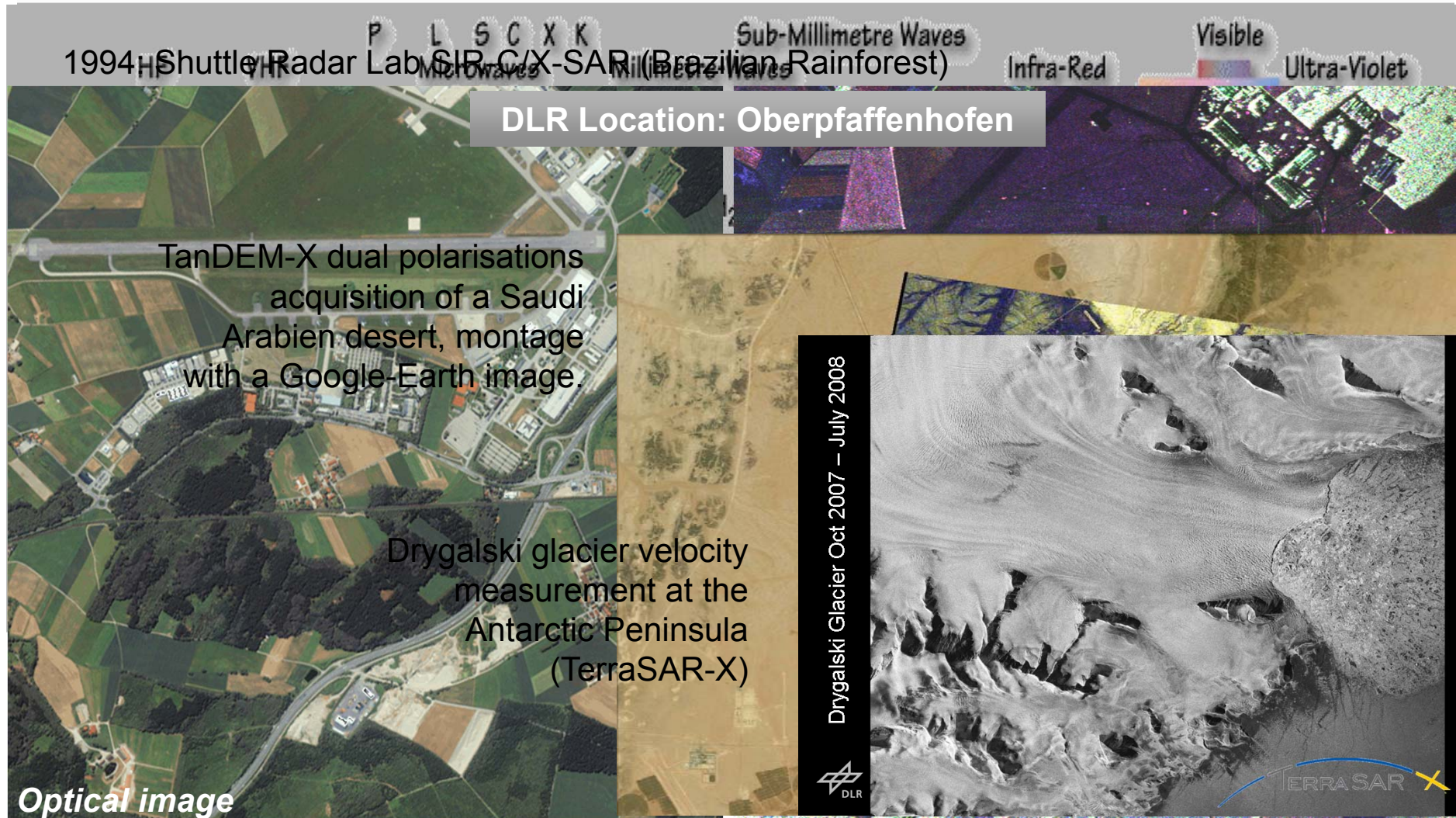


Part II: Exercises with L-band airborne data

- › Read the data
- › Speckle filtering
- › Oh, Dubois and X-Bragg inversion

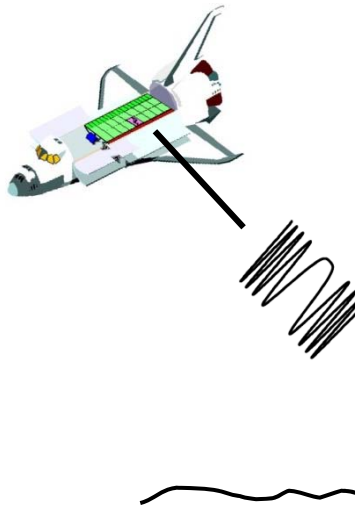
Motivation of Radar Remote Sensing

- Independent from Weather
 - Data acquisition during cloud cover, rain, ...
- Radar is complementary to optics



What does the Radar measure ?

Radar reflectivity (backscattered signal) of the target as a function of position.

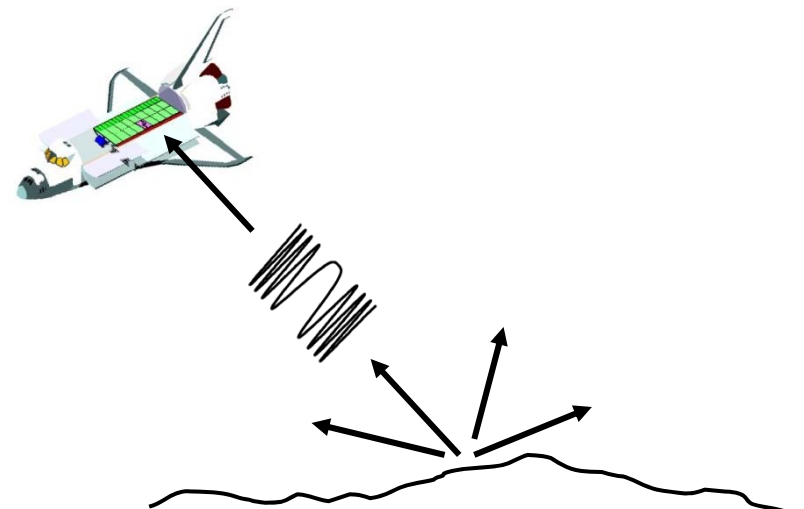


**radar transmits a pulse
(travelling velocity is equal to velocity of light)**

some of the energy in the radar pulse is reflected back towards the radar.

This is what the radar measures.

**It is known as radar backscatter σ_0
(sigma nought or sigma zero).**



What does the Radar measure ?

Normalized radar cross-section (backscattering coefficient) is given by:

$$\sigma_0 \text{ (dB)} = 10 \cdot \log_{10} \text{(energy ratio)}$$

whereby

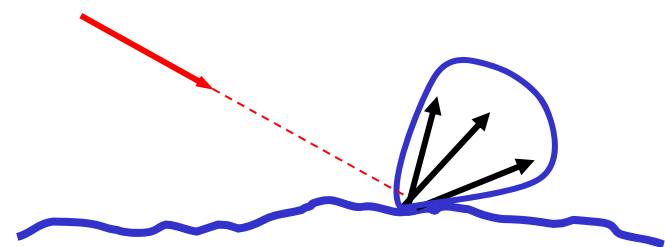
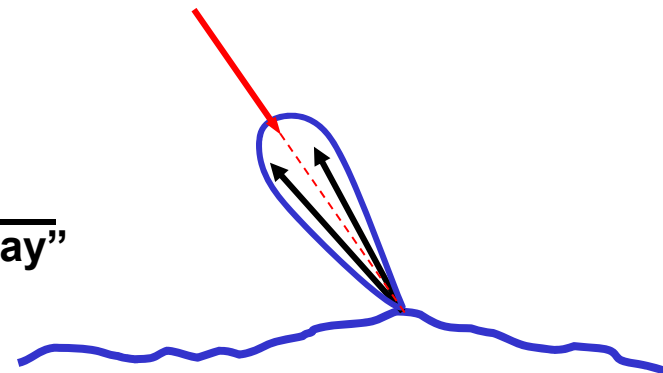
$$\text{energy ratio} = \frac{\text{received energy by the sensor}}{\text{"energy reflected in an isotropic way"}}$$

i.e.

The backscattered coefficient can be a positive number if there is a focusing of backscattered energy towards the radar

or

The backscattered coefficient can be a negative number if there is a focusing of backscattered energy away from the radar (e.g. smooth surface)



Backscattering Coefficient σ_o

<i>Levels of Radar backscatter</i>	<i>Typical scenario</i>
Very high backscatter (above -5 dB)	<ul style="list-style-type: none">➢ <i>man-made objects (urban)</i>➢ <i>terrain slopes towards radar</i>➢ <i>very rough surface</i>➢ <i>radar looking very steep</i>
High backscatter (-10 dB to 0 dB)	<ul style="list-style-type: none">➢ <i>rough surface</i>➢ <i>dense vegetation (forest)</i>
Moderate backscatter (-20 to -10 dB)	<ul style="list-style-type: none">➢ <i>medium level of vegetation</i>➢ <i>agricultural crops</i>➢ <i>moderately rough surfaces</i>
Low backscatter (below -20 dB)	<ul style="list-style-type: none">➢ <i>smooth surface</i>➢ <i>calm water</i>➢ <i>road</i>➢ <i>very dry terrain (sand)</i>



Commonly Used Frequency Bands

<i>Frequency band</i>	<i>Frequency range</i>	<i>Application examples</i>	<i>Typical frequency for soil parameter inversion</i>
VHF	300 KHz - 300 MHz	foliage/ground penetration, biomass	
P-Band	300 MHz - 1 GHz	soil moisture, biomass, penetration	
L-Band	1 GHz - 2 GHz	agriculture, forestry, soil moisture	
C-Band	4 GHz - 8 GHz	ocean, agriculture	
X-Band	8 GHz - 12 GHz	agriculture, ocean, high resolution radar	
Ku-Band	14 GHz - 18 GHz	glaciology (snow cover mapping)	
Ka-Band	27 GHz - 47 GHz	high resolution radar	



Environmental Sensing from Air and Space

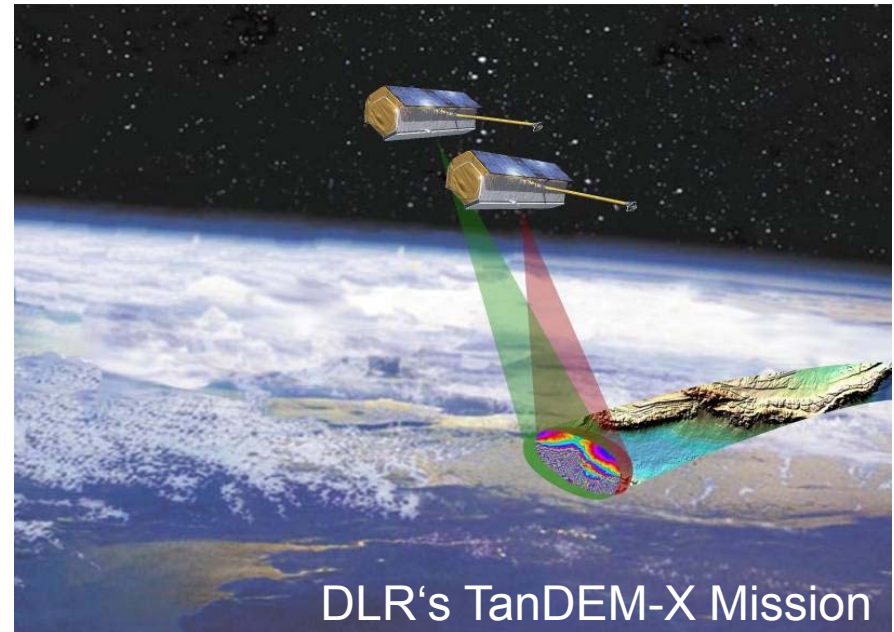
Airborne measurements

- ↗ Highly flexible operation
- ↗ Coverage of dedicated areas
- ↗ Experimental configuration
- ↗ Sensor specific data formats
- ↗ Short re-visit times

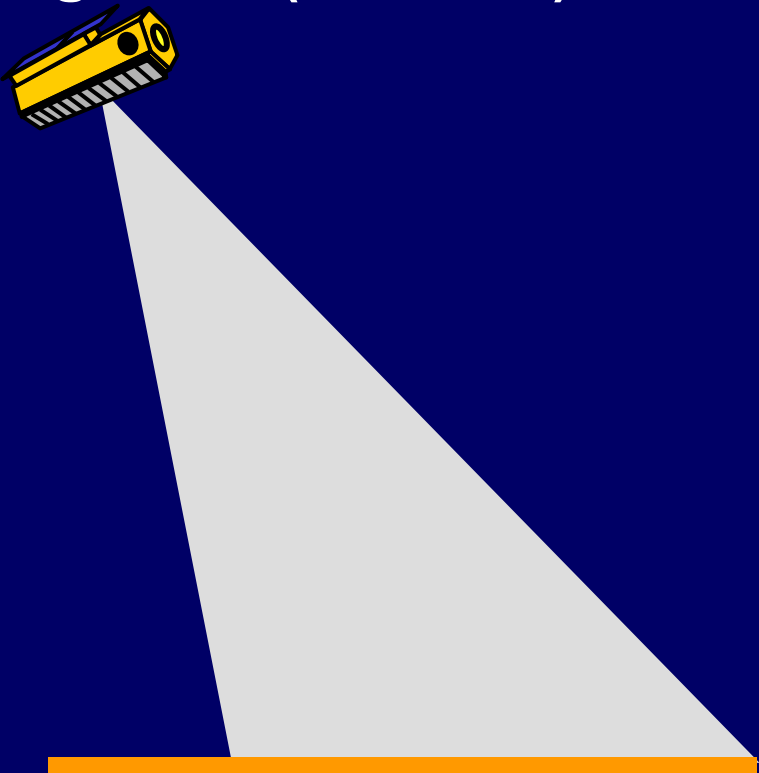


Spaceborne measurements

- ↗ Highly regular observation
- ↗ Wide area coverage
- ↗ Highly operational & reliable
- ↗ Standard product delivery
- ↗ Long term observations



Single Pol (Channel) SAR



Observation Space

Distributed Scatterers:

- Norm. Backscattering Cross Section σ^0 ;
- Texture (σ^0 statistics).

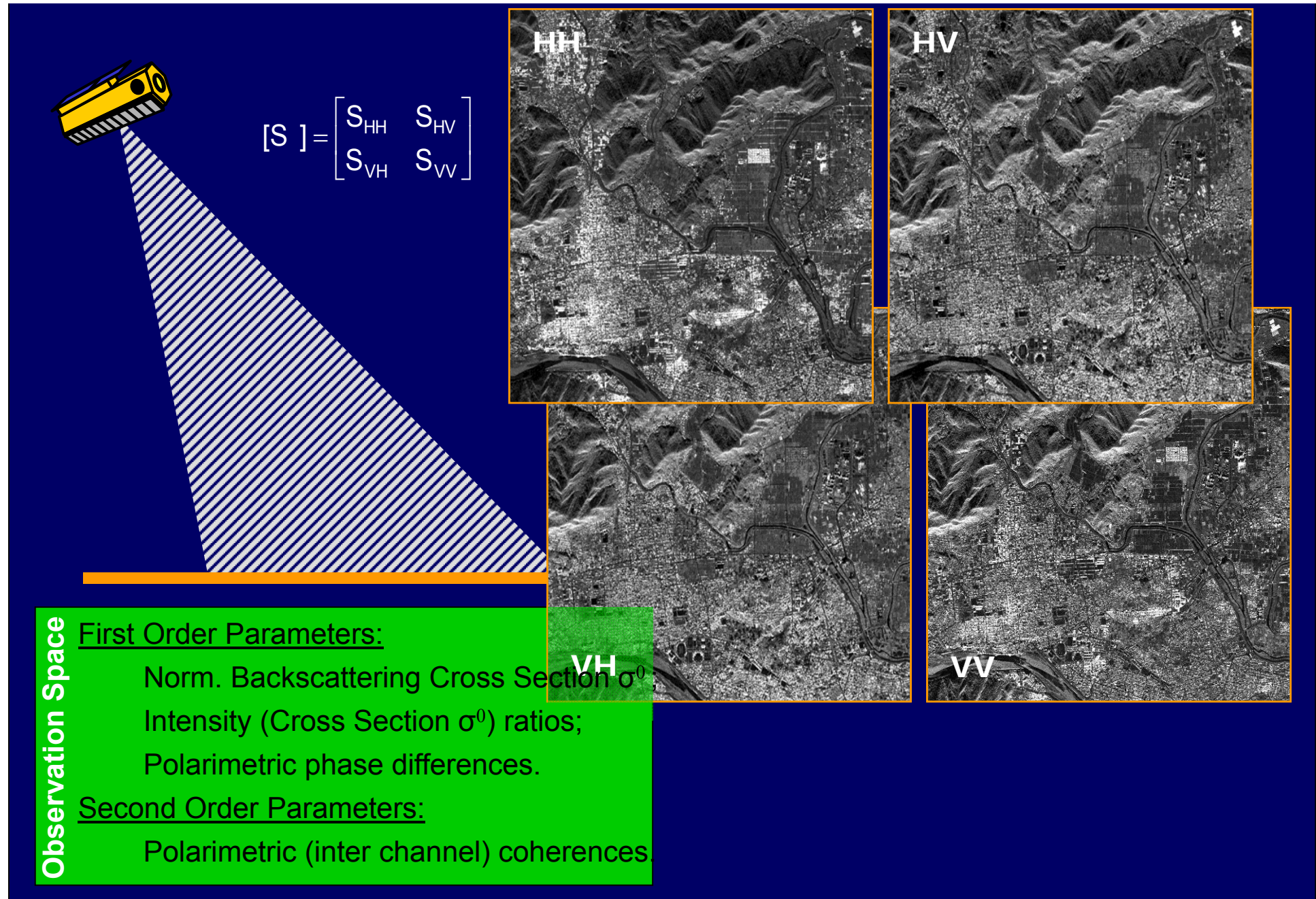
Deterministic Scatterers:

- Radar Cross Section (RCS) ;
- Phase of the SAR signal.

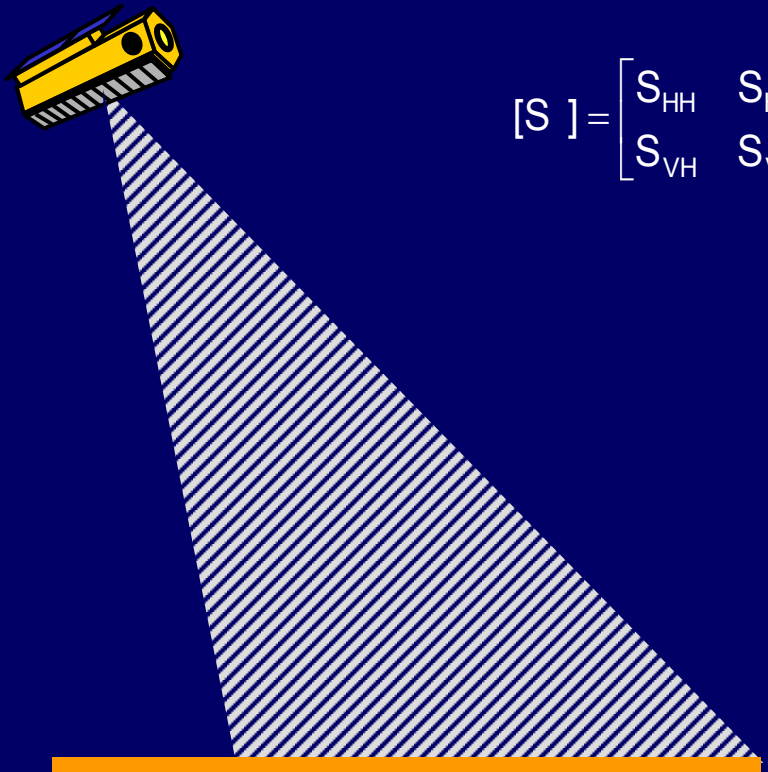


Applications

- Classification/Segmentation (Texture);
- Change detection (Multi temp. analysis);
- Glacier velocities (Feature tracking);
- Mapping (Feature extraction/Bordering);
- Ocean wave/Wind mapping;
- Coherent scatterers (CSs).

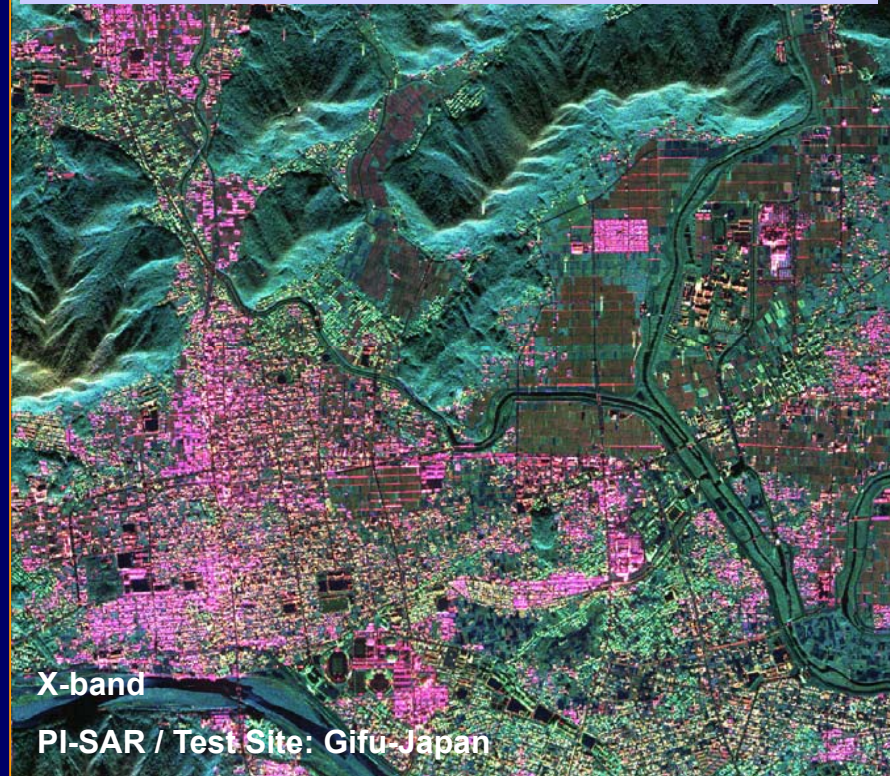


Polarimetric SAR



$$[S] = \begin{bmatrix} S_{HH} & S_{HV} \\ S_{VH} & S_{VV} \end{bmatrix}$$

R:HH-VV G:HV+VH B:HH+VV



Observation Space

First Order Parameters:

- Norm. Backscattering Cross Section σ^0 ;
- Intensity (Cross Section σ^0) ratios;
- Polarimetric phase differences.

Second Order Parameters:

- Polarimetric (inter channel) coherences

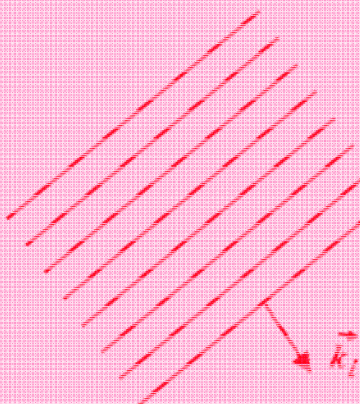
Applications

- Soil moisture/roughness estimation;
- Wetland/Veg. characterisation/mapping;
- Snow & Ice mapping (type classification);
- Ship & Oil spill detection;
- Classification/Segmentation (Pol based).

The Polarimetric Scattering Problem

Incident (Plane) Wave

$$\vec{E}_{hv}^i(\vec{r}) = \begin{bmatrix} E_h^i(\vec{r}) \\ E_v^i(\vec{r}) \end{bmatrix}$$



(Jones Vector Representation)

Scattered Field

In the far zone region
($|\vec{r}| \gg \lambda$ $|\vec{r}| \gg |\vec{r}'|$)

$$\vec{E}_{hv}^s(\vec{r}) = \begin{bmatrix} E_h^s(\vec{r}) \\ E_v^s(\vec{r}) \end{bmatrix}$$

(Jones Vector Representation)

Scatterer

Transforms the incident
into the scattered wave



2x2 Complex Scattering Matrix

$$\begin{bmatrix} E_h^s(\vec{r}) \\ E_v^s(\vec{r}) \end{bmatrix} = \frac{\exp(i\kappa r)}{r} \begin{bmatrix} S_{HH}(\vec{r}) & S_{HV}(\vec{r}) \\ S_{VH}(\vec{r}) & S_{VV}(\vec{r}) \end{bmatrix} \begin{bmatrix} E_h^i(\vec{r}) \\ E_v^i(\vec{r}) \end{bmatrix}$$

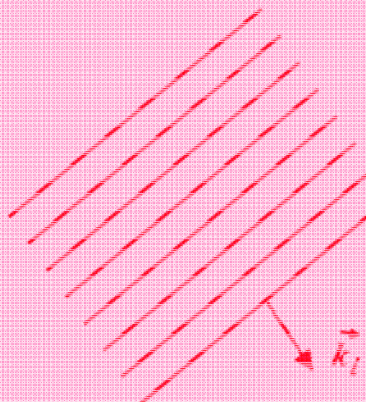
Mapping of the 2-dim incident vector $\vec{E}_{hv}^i(\vec{r})$ into the 2-dim scattered vector $\vec{E}_{hv}^s(\vec{r})$



The Polarimetric Scattering Problem

Incident (Plane) Wave

$$\vec{E}_{hv}^i(\vec{r}) = \begin{bmatrix} E_h^i(\vec{r}) \\ E_v^i(\vec{r}) \end{bmatrix}$$



(Jones Vector Representation)

Scattered Field

In the far zone region
 $(|\vec{r}| \gg \lambda \quad |\vec{r}| \gg |\vec{r}'|)$

$$\vec{E}_{hv}^s(\vec{r}) = \begin{bmatrix} E_h^s(\vec{r}) \\ E_v^s(\vec{r}) \end{bmatrix}$$

(Jones Vector Representation)

Scatterer

Transforms the Incident
into the scattered wave

- 1: Changes the polarisation state of the incident wave
- 2: Changes the degree of polarisation of the incident wave

2x2 Complex Scattering Matrix

$$\begin{bmatrix} E_h^s(\vec{r}) \\ E_v^s(\vec{r}) \end{bmatrix} = \frac{\exp(i\kappa r)}{r} \begin{bmatrix} S_{HH}(\vec{r}) & S_{HV}(\vec{r}) \\ S_{VH}(\vec{r}) & S_{VV}(\vec{r}) \end{bmatrix} \begin{bmatrix} E_h^i(\vec{r}) \\ E_v^i(\vec{r}) \end{bmatrix}$$

Mapping of the 2-dim incident vector $\vec{E}_{hv}^i(\vec{r})$ into the 2-dim scattered vector $\vec{E}_{hv}^s(\vec{r})$



Coherent Scattering Matrix

... also known as the Jones Matrix in the bistatic and Sinclair Matrix in the monostatic case

$$\begin{bmatrix} E_h^s \\ E_v^s \end{bmatrix} = \frac{\exp(i\kappa r)}{r} \begin{bmatrix} S_{HH} & S_{HV} \\ S_{VH} & S_{VV} \end{bmatrix} \begin{bmatrix} E_h^i \\ E_v^i \end{bmatrix}$$

Complex Scattering Amplitudes:
 $S_{IJ} = f(\text{Frequency, Scattering Geometry})$

[S] is independent on the polarisation of the incident wave !!!

and depends only on the physical and geometrical properties of the scatterer

Total Scattered Power: $TP = \text{Span} ([S]) = \text{Trace}([S][S]^+) = |S_{HH}|^2 + |S_{HV}|^2 + |S_{VH}|^2 + |S_{VV}|^2$

$$[S] = \frac{\exp(i\kappa r)}{r} \begin{bmatrix} |S_{HH}| \exp(i\phi_{HH}) & |S_{HV}| \exp(i\phi_{HV}) \\ |S_{VH}| \exp(i\phi_{VH}) & |S_{VV}| \exp(i\phi_{VV}) \end{bmatrix}$$

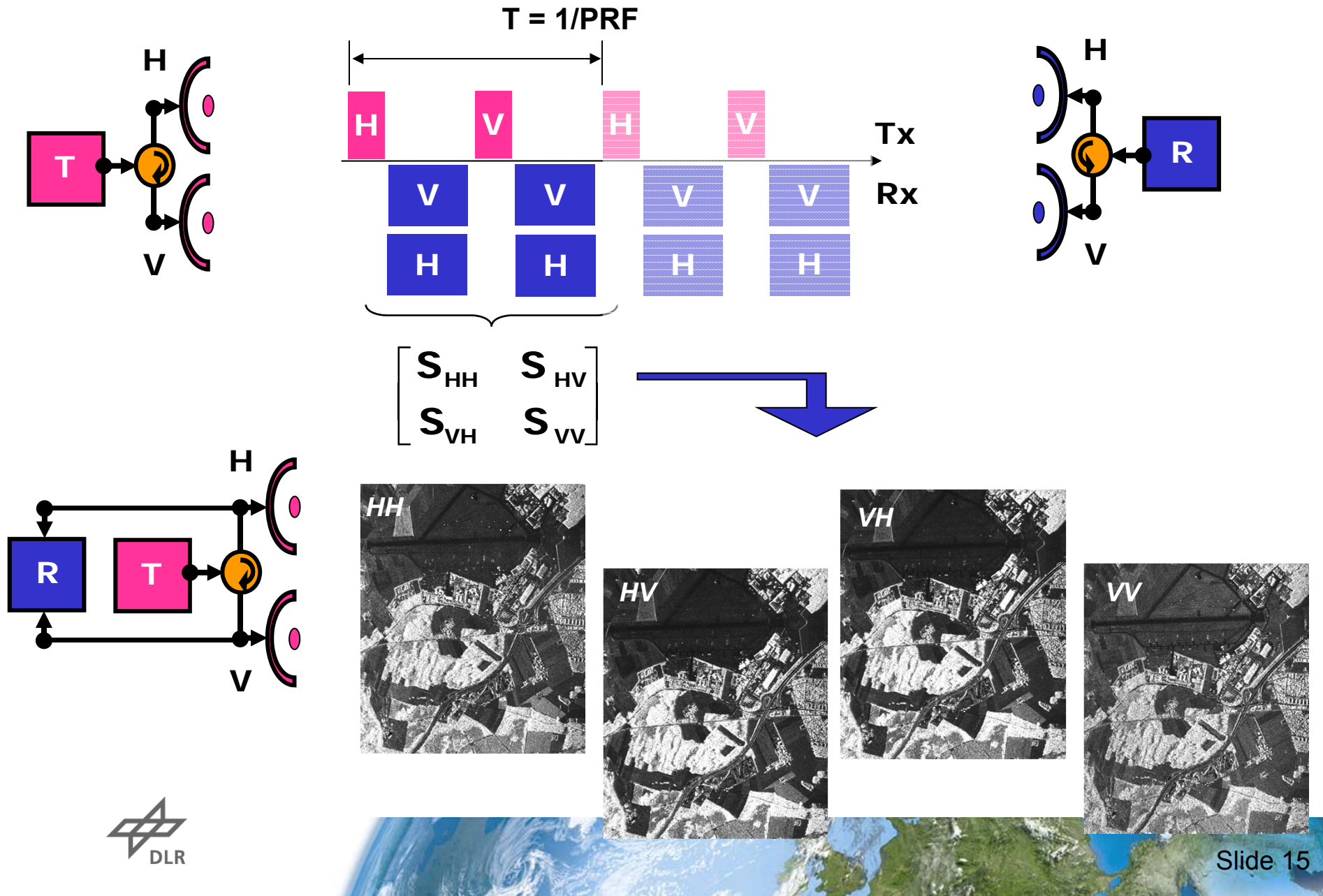
$$[S] = \frac{\exp(i\kappa r) \exp(i\phi_{VV})}{r} \begin{bmatrix} |S_{HH}| \exp(i(\phi_{HH} - \phi_{VV})) & |S_{HV}| \exp(i(\phi_{HV} - \phi_{VV})) \\ |S_{VH}| \exp(i(\phi_{VH} - \phi_{VV})) & |S_{VV}| \end{bmatrix}$$

Absolute Phase Factor

Seven Parameters: 4 Amplitudes & 3 Phases

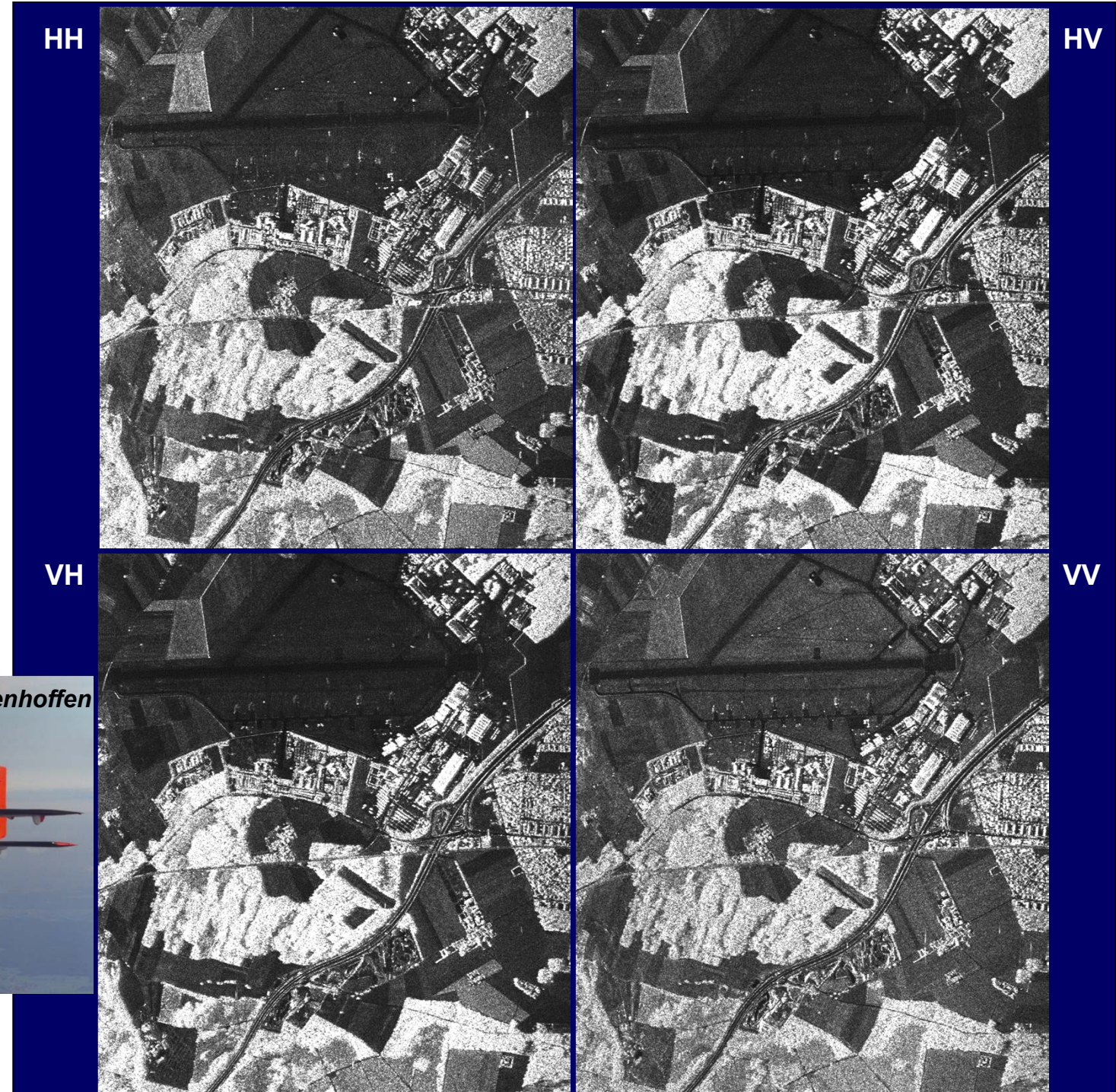


Bi- & Mono-Static Measurement of the Scattering Matrix



Scattering Amplitude Images

Azimuth
Range



Backscattering (FSA & BSA)

In the case of monostatic backscattering from reciprocal scatterers:

Reciprocity Theorem

$$S_{HV}^{BSA} = S_{VH}^{BSA} = S_{XX}^{BSA}$$

$$(S_{HV}^{FSA} = -S_{VH}^{FSA} = S_{XX}^{FSA})$$

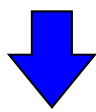


$$[S] = \begin{bmatrix} S_{HH} & S_{XX} \\ S_{XX} & S_{VV} \end{bmatrix} \rightarrow$$

$$[S] = \frac{\exp(i\kappa r) \exp(i\phi_{VV})}{r} \begin{bmatrix} |S_{HH}| \exp(i(\phi_{HH} - \phi_{VV})) & |S_{XX}| \exp(i(\phi_{XX} - \phi_{VV})) \\ |S_{XX}| \exp(i(\phi_{XX} - \phi_{VV})) & |S_{VV}| \end{bmatrix}$$

Absolute Phase Factor

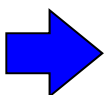
Five Parameters: 3 Amplitudes & 2 Phases



The scattering problem can be addressed in the 3-dim complex space:

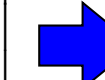
3-dim Lexicographic (L) and Pauli (P) Scattering Vectors:

$$\vec{k}_{4L} = \begin{bmatrix} S_{HH} \\ S_{XX} \\ S_{XX} \\ S_{VV} \end{bmatrix}$$



$$\vec{k}_{3L} = \begin{bmatrix} S_{HH} \\ \sqrt{2}S_{XX} \\ S_{VV} \end{bmatrix}$$

$$\vec{k}_{4P} = \frac{I}{\sqrt{2}} \begin{bmatrix} S_{HH} + S_{VV} \\ S_{HH} - S_{VV} \\ 2S_{XX} \\ 0 \end{bmatrix}$$



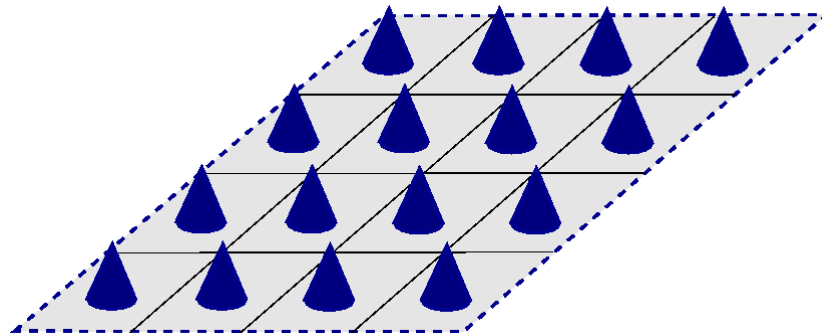
$$\vec{k}_{3P} = \frac{I}{\sqrt{2}} \begin{bmatrix} S_{HH} + S_{VV} \\ S_{HH} - S_{VV} \\ 2S_{XX} \end{bmatrix}$$

Note: The factor $\sqrt{2}$ is required to keep the vector norm of \vec{k}_{3L} invariant



Partial Scatterers

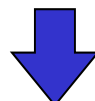
Deterministic Scatterers



Point Scatterers

- Change the polarisation state of the wave
- Do not change the degree of polarisation

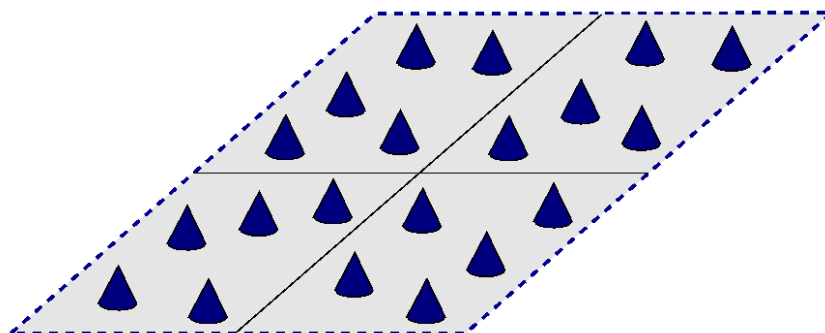
Monochromatic
Incident Wave



Completely described by [S]



Partial Scatterers

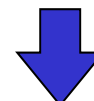


Scatterers with Space or Time Variability

- Change the polarisation state of the wave
and also change the degree of polarisation

Monochromatic
Scattered Wave

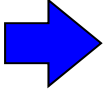
Depolarisation
described by second order statistics



Cannot be described by a single [S]

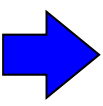


Covariance & Coherency Matrices in Backscattering

Lexicographic Scattering Vector: 

$$\vec{k}_{4L} = [S_{HH} \quad \sqrt{2}S_{xx} \quad S_{VV}]^T$$

$$[C_3] := \begin{bmatrix} \langle |S_{HH}|^2 \rangle & \sqrt{2} \langle S_{HH} S_{HV}^* \rangle & \langle S_{HH} S_{VV}^* \rangle \\ \sqrt{2} \langle S_{HV} S_{HH}^* \rangle & 2 \langle |S_{HV}|^2 \rangle & \sqrt{2} \langle S_{HV} S_{VV}^* \rangle \\ \langle S_{VV} S_{HH}^* \rangle & \sqrt{2} \langle S_{VV} S_{HV}^* \rangle & \langle |S_{VV}|^2 \rangle \end{bmatrix}$$

Pauli Scattering Vector: 

$$\vec{k}_{3P} = \frac{1}{\sqrt{2}} [S_{HH} + S_{VV} \quad S_{HH} - S_{VV} \quad 2S_{xx}]^T$$

$$[T_3] := \begin{bmatrix} \langle |(S_{HH} + S_{VV})|^2 \rangle & \langle (S_{HH} + S_{VV})(S_{HH} - S_{VV})^* \rangle & 2 \langle (S_{HH} + S_{VV}) S_{HV}^* \rangle \\ \langle (S_{HH} - S_{VV})(S_{HH} + S_{VV})^* \rangle & \langle |(S_{HH} - S_{VV})|^2 \rangle & 2 \langle (S_{HH} - S_{VV}) S_{HV}^* \rangle \\ 2 \langle S_{HV} (S_{HH} + S_{VV})^* \rangle & 2 \langle S_{HV} (S_{HH} - S_{VV})^* \rangle & 4 \langle |S_{HV}|^2 \rangle \end{bmatrix}$$

Covariance Matrix [C]:

$$[C_3] := \langle \vec{k}_{3L} \cdot \vec{k}_{3L}^+ \rangle$$

Coherency Matrix [T]:

$$[T_3] := \langle \vec{k}_{3P} \cdot \vec{k}_{3P}^+ \rangle$$

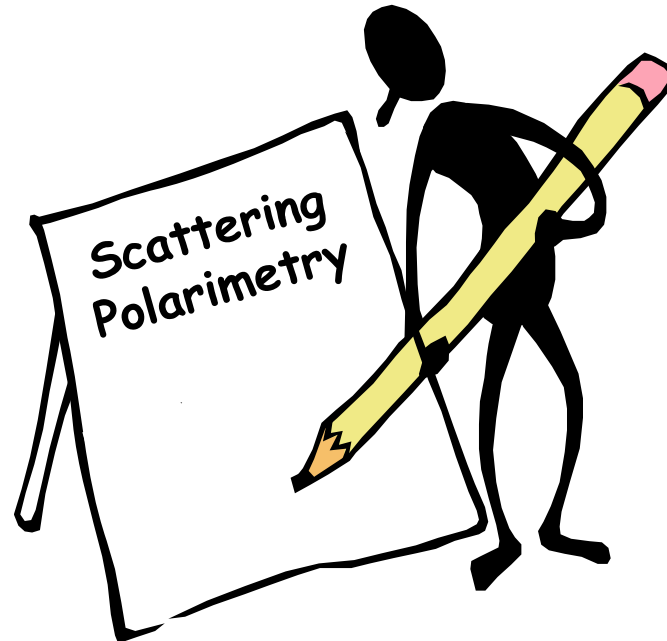
$[C_3]$ and $[T_3]$ are by definition 3x3 hermitian positive semi-definite matrices & contain in general 9 independent parameters



Scattering Polarimetry

INTERPRETATION OF SCATTERING MECHANISMS

- Directly from the Scattering Matrix
- Model based



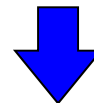
Interpretation of Scattering Mechanisms

Scattering Matrix:

$$[S] = \begin{bmatrix} S_{HH} & S_{HV} \\ S_{HV} & S_{VV} \end{bmatrix}$$

Scattering Vector:

$$\vec{k}_P = \frac{1}{\sqrt{2}} [S_{HH} + S_{VV} \quad S_{HH} - S_{VV} \quad 2S_{xx}]^T$$



Unitary Representation: $\vec{e} = \frac{1}{|\vec{k}_P|} \vec{k}_P$

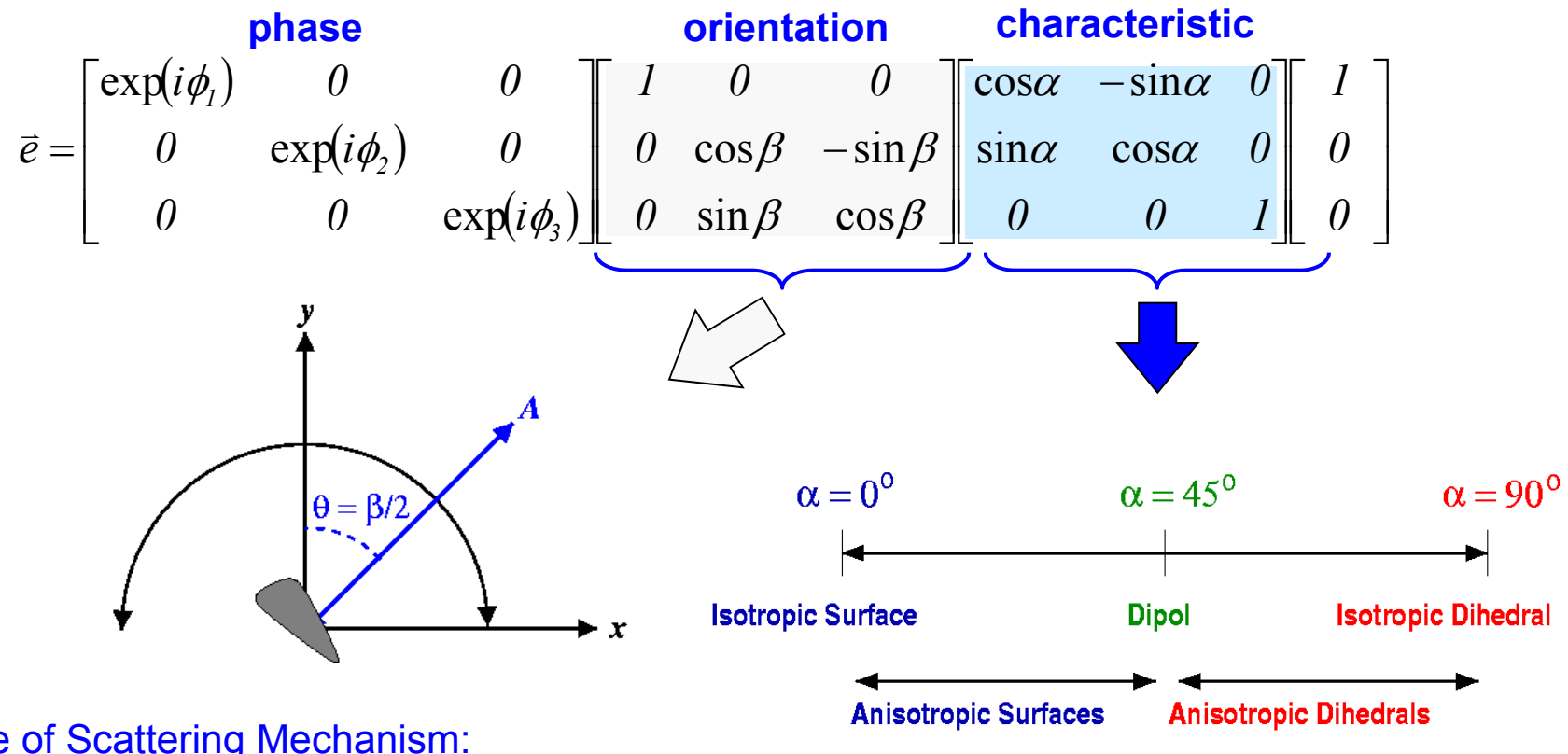
$$\vec{e} = \frac{1}{|\vec{k}_P|} \vec{k}_P = \begin{bmatrix} \cos\alpha \exp(i\phi_1) \\ \sin\alpha \cos\beta \exp(i\phi_2) \\ \sin\alpha \sin\beta \exp(i\phi_3) \end{bmatrix} = \frac{1}{\sqrt{2}|\vec{k}_P|} \begin{bmatrix} S_{HH} + S_{VV} \\ S_{HH} - S_{VV} \\ 2S_{xx} \end{bmatrix}$$

Parameterisation of \vec{e} in terms of five angles: $\alpha, \beta, \phi_1, \phi_2, \phi_3$



Interpretation of Scattering Mechanisms

Point Reduction Theorem:



Change of Scattering Mechanism:

$$\bar{e}' = \begin{bmatrix} I & 0 & 0 \\ 0 & \cos\Delta\beta & -\sin\Delta\beta \\ 0 & \sin\Delta\beta & \cos\Delta\beta \end{bmatrix} \bar{e}$$

$$\bar{e}' = \begin{bmatrix} \cos\Delta\alpha & -\sin\Delta\alpha & 0 \\ \sin\Delta\alpha & \cos\Delta\alpha & 0 \\ 0 & 0 & 1 \end{bmatrix} \bar{e}$$



Interpretation of Scattering Mechanisms

$$\vec{e}' = \begin{bmatrix} 1 & 0 & 0 \\ 0 & \cos\beta & -\sin\beta \\ 0 & \sin\beta & \cos\beta \end{bmatrix} \begin{bmatrix} \cos\alpha & -\sin\alpha & 0 \\ \sin\alpha & \cos\alpha & 0 \\ 0 & 0 & 1 \end{bmatrix} \begin{bmatrix} 1 \\ 0 \\ 0 \end{bmatrix} \quad \text{where} \quad \vec{e} = \begin{bmatrix} 1 \\ 0 \\ 0 \end{bmatrix} = \frac{I}{\sqrt{2}|\vec{k}_P|} \begin{bmatrix} S_{HH} + S_{VV} \\ S_{HH} - S_{VV} \\ 2S_{HV} \end{bmatrix}$$

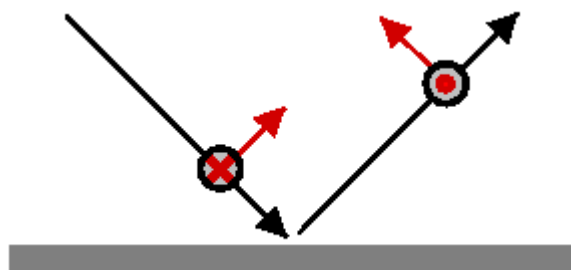
$\alpha=90^\circ$ and $\beta=0^\circ$ Dihedral Scatterer \rightarrow $\vec{e}' = \begin{bmatrix} 1 & 0 & 0 \\ 0 & 1 & 0 \\ 0 & 0 & 1 \end{bmatrix} \begin{bmatrix} 0 & 1 & 0 \\ 1 & 0 & 0 \\ 0 & 0 & 1 \end{bmatrix} \begin{bmatrix} 1 \\ 0 \\ 0 \end{bmatrix} = \begin{bmatrix} 0 \\ 1 \\ 0 \end{bmatrix}$ 

$\alpha=45^\circ$ and $\beta=0^\circ$ H-Dipol Scatterer \rightarrow $\vec{e}' = \begin{bmatrix} 1 & 0 & 0 \\ 0 & 1 & 0 \\ 0 & 0 & 1 \end{bmatrix} \begin{bmatrix} 1/\sqrt{2} & 1/\sqrt{2} & 0 \\ 1/\sqrt{2} & 1/\sqrt{2} & 0 \\ 0 & 0 & 1 \end{bmatrix} \begin{bmatrix} 1 \\ 0 \\ 0 \end{bmatrix} = \begin{bmatrix} 1/\sqrt{2} \\ 1/\sqrt{2} \\ 0 \end{bmatrix}$ 

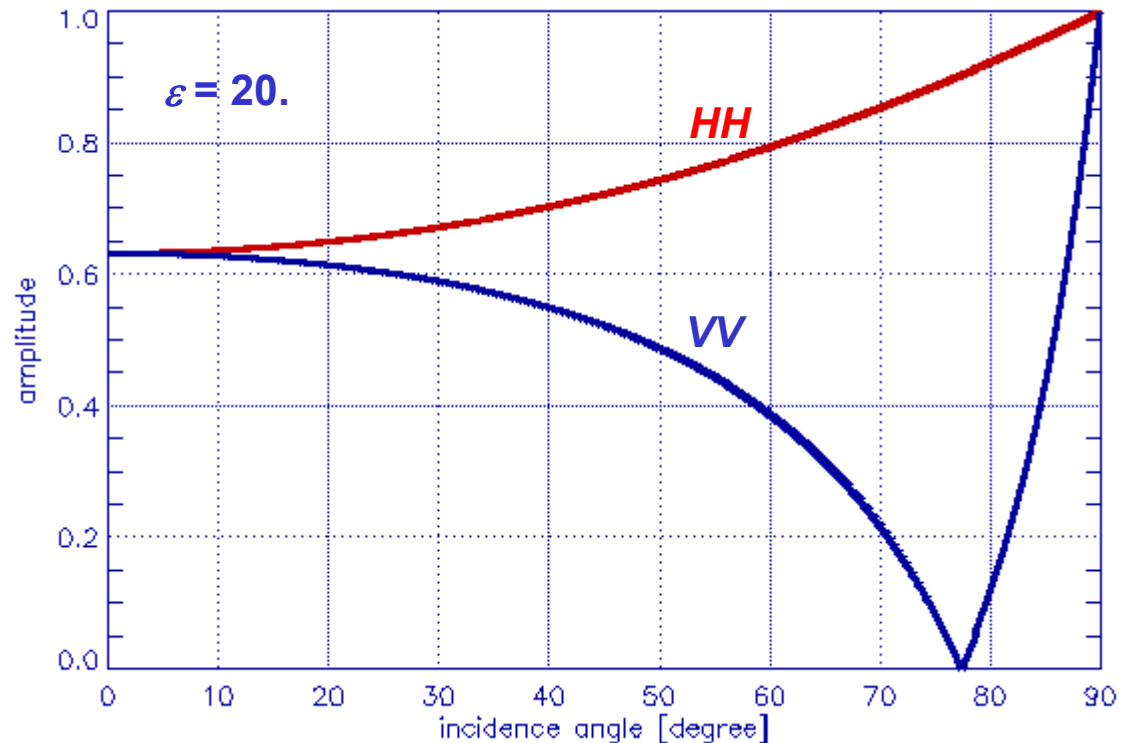
$\alpha=45^\circ$ and $\beta=180^\circ$ V-Dipol Scatterer \rightarrow $\vec{e}' = \begin{bmatrix} 1 & 0 & 0 \\ 0 & -1 & 0 \\ 0 & 0 & -1 \end{bmatrix} \begin{bmatrix} 1/\sqrt{2} & 1/\sqrt{2} & 0 \\ 1/\sqrt{2} & 1/\sqrt{2} & 0 \\ 0 & 0 & 1 \end{bmatrix} \begin{bmatrix} 1 \\ 0 \\ 0 \end{bmatrix} = \begin{bmatrix} 1/\sqrt{2} \\ -1/\sqrt{2} \\ 0 \end{bmatrix}$ 



Scattering Processes: Fresnel Scattering



Scattering Matrix: $[S] = \begin{bmatrix} R_H & 0 \\ 0 & R_V \end{bmatrix}$



Fresnel Reflection Coefficients:

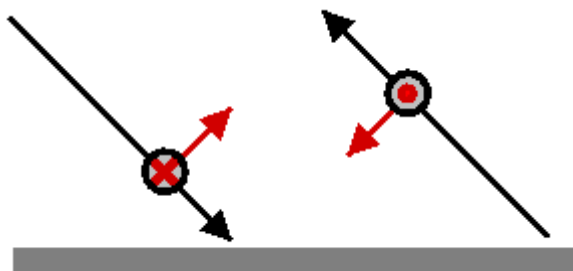
$$R_H = \frac{\cos\theta - \sqrt{\epsilon - \sin^2\theta}}{\cos\theta + \sqrt{\epsilon - \sin^2\theta}}$$

and

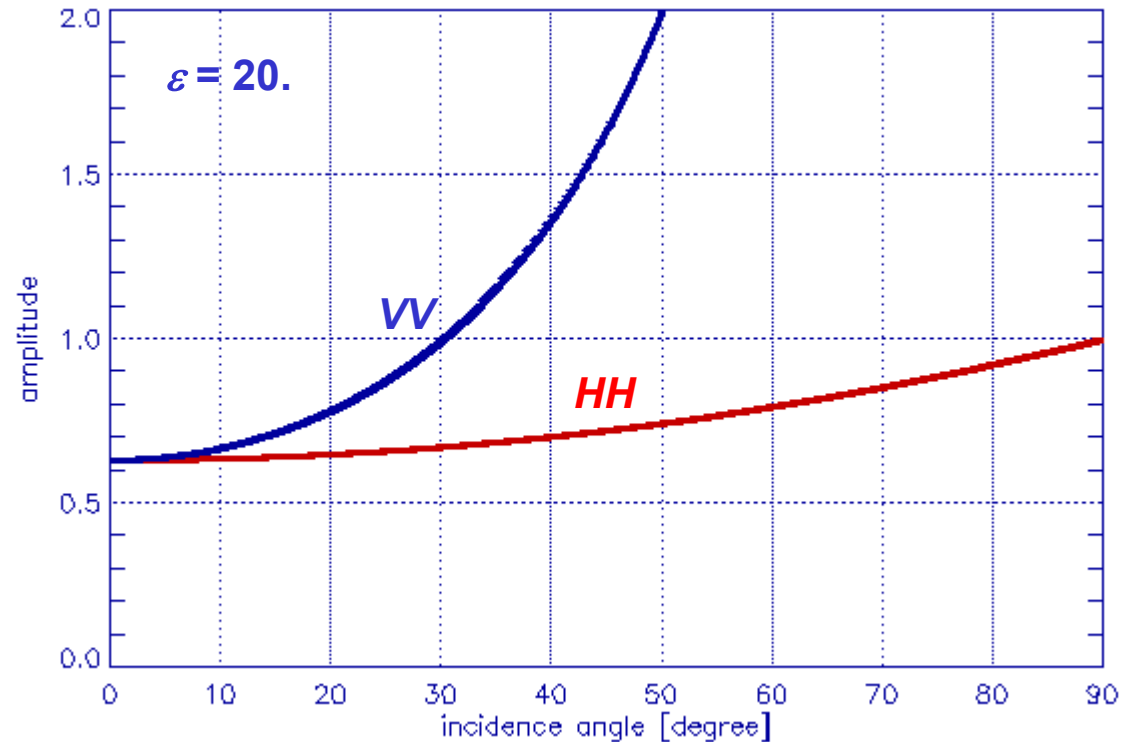
$$R_V = \frac{\epsilon \cos\theta - \sqrt{\epsilon - \sin^2\theta}}{\epsilon \cos\theta + \sqrt{\epsilon - \sin^2\theta}}$$

... where ϵ is the dielectric constant of the surface

Scattering Processes: Bragg Scattering



Scattering Matrix: $[S] = \begin{bmatrix} R_H & 0 \\ 0 & R_V \end{bmatrix}$



Bragg Scattering Coefficients:

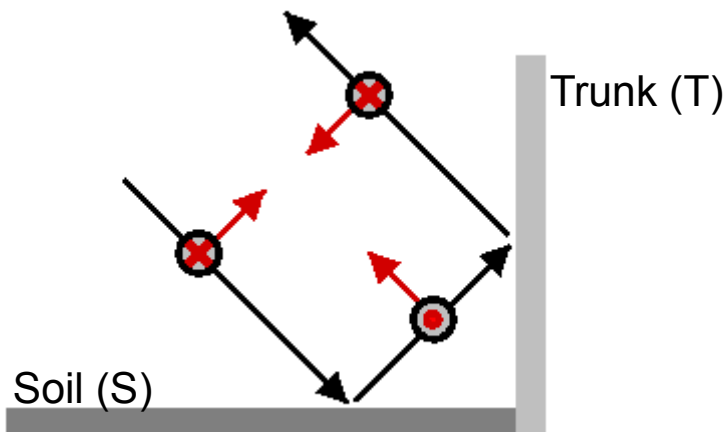
$$R_H = \frac{\cos\theta - \sqrt{\epsilon - \sin^2\theta}}{\cos\theta + \sqrt{\epsilon - \sin^2\theta}}$$

and

$$R_V = \frac{(\epsilon - 1)[\sin^2\theta - \epsilon(1 + \sin^2\theta)]}{\epsilon \cos\theta + \sqrt{\epsilon - \sin^2\theta}}$$

... where ϵ is the dielectric constant of the surface

Scattering Processes: Dihedral Scattering



Scattering Matrix:

$$[S] = \begin{bmatrix} 1 & 0 \\ 0 & -1 \end{bmatrix} \begin{bmatrix} 1 & 0 \\ 0 & e^{i\phi} \end{bmatrix} \begin{bmatrix} R_{HS} & 0 \\ 0 & R_{VS} \end{bmatrix} \begin{bmatrix} R_{HT} & 0 \\ 0 & R_{VT} \end{bmatrix} = \begin{bmatrix} R_{HS}R_{HT} & 0 \\ 0 & -R_{VS}R_{VT}e^{i\phi} \end{bmatrix}$$

Fresnel Coefficients:

$$R_{HS} = \frac{\cos\theta - \sqrt{\varepsilon_s - \sin^2\theta}}{\cos\theta + \sqrt{\varepsilon_s - \sin^2\theta}}$$

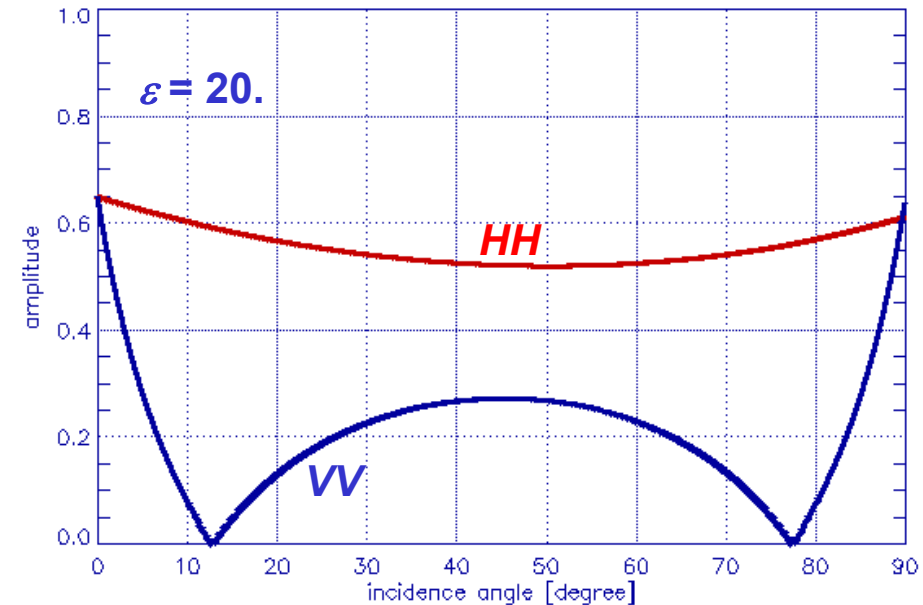
$$R_{HT} = \frac{\cos(90-\theta) - \sqrt{\varepsilon_T - \sin^2(90-\theta)}}{\cos(90-\theta) + \sqrt{\varepsilon_T - \sin^2(90-\theta)}}$$

and

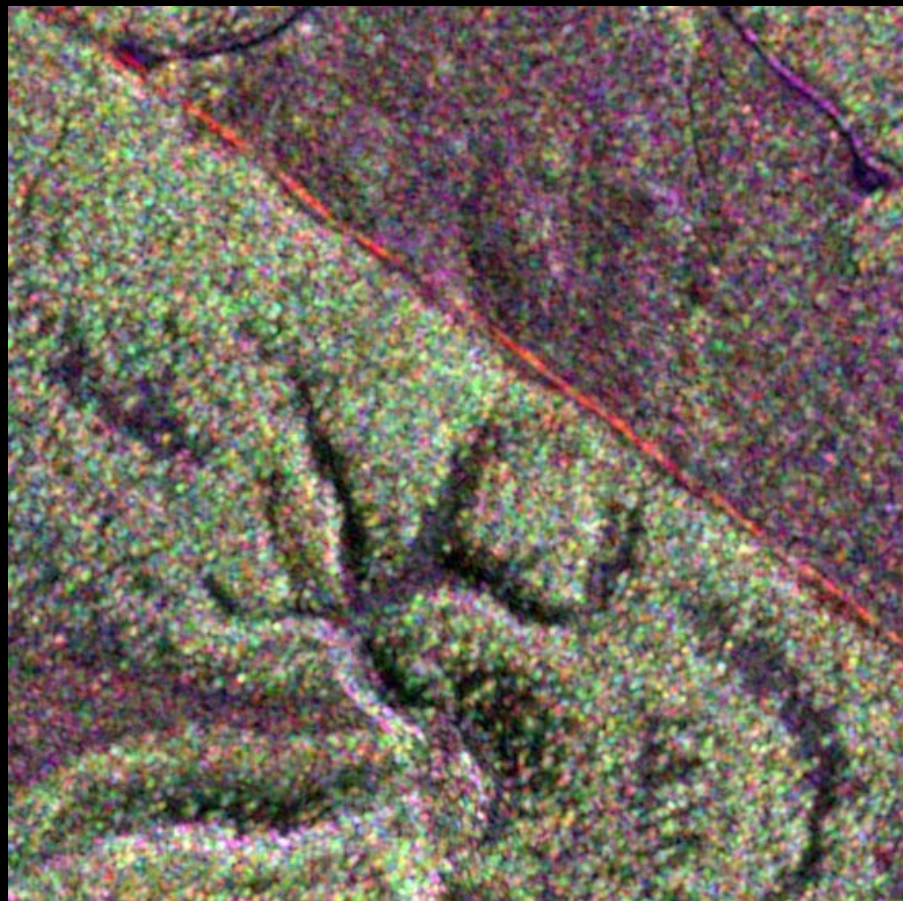
$$R_{VS} = \frac{\varepsilon_s \cos\theta - \sqrt{\varepsilon_s - \sin^2\theta}}{\varepsilon_s \cos\theta + \sqrt{\varepsilon_s - \sin^2\theta}}$$

and

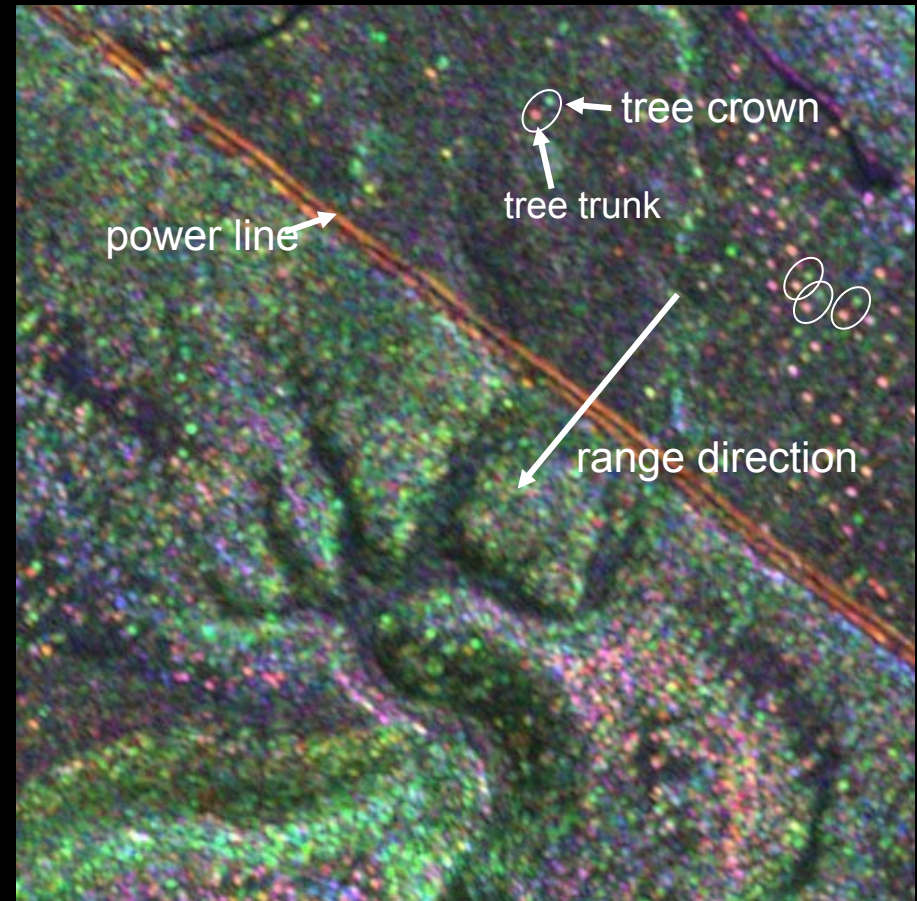
$$R_{VT} = \frac{\varepsilon_s \cos(90-\theta) - \sqrt{\varepsilon_s - \sin^2(90-\theta)}}{\varepsilon_s \cos(90-\theta) + \sqrt{\varepsilon_s - \sin^2(90-\theta)}}$$



Dihedral vs Volume Scattering (L- /P-Band E-SAR – Kryklan/Sweden)

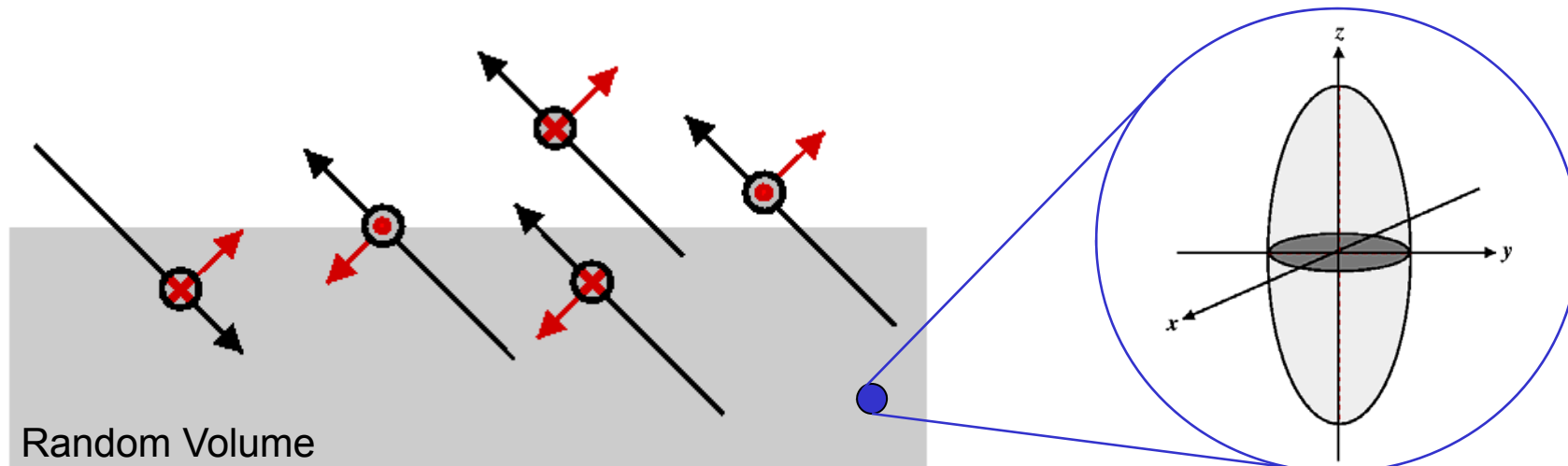


08biosar0201x1_t11 L-band, hh hv vv



08biosar0302x1_t12 P-band, hh hv vv

Scattering Processes: Volume Scattering



$$\vec{k}(\alpha, \beta, \gamma) = [R_3(\alpha)] [R_3(\beta)] [R_3(\gamma)] \vec{k}$$

←

$$[S] = \begin{bmatrix} a & b \\ b & d \end{bmatrix} \rightarrow \vec{k} = \frac{I}{\sqrt{2}} \begin{bmatrix} a+b \\ a-b \\ 2c \end{bmatrix}$$

Coherency Matrix: $[T] = \langle \vec{k}(\alpha, \beta, \gamma) \cdot \vec{k}^+(\alpha, \beta, \gamma) \rangle$

- $0 \leq \alpha \leq 2\pi$ Rotation about x-axis
- $0 \leq \beta \leq \pi$ Rotation about y-axis
- $0 \leq \gamma \leq 2\pi$ Rotation about z-axis

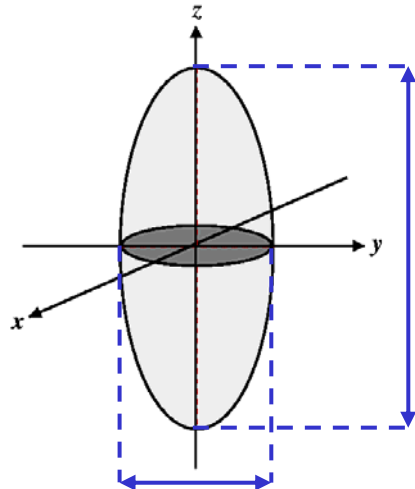
$$[R_3(\alpha)] := \begin{bmatrix} \cos\alpha & \sin\alpha & 0 \\ -\sin\alpha & \cos\alpha & 0 \\ 0 & 0 & 1 \end{bmatrix}$$

$$[R_3(\beta)] := \begin{bmatrix} \cos\beta & 0 & -\sin\beta \\ 0 & 1 & 0 \\ \sin\beta & 0 & \cos\beta \end{bmatrix}$$

$$[R_3(\gamma)] := \begin{bmatrix} \cos\gamma & \sin\gamma & 0 \\ -\sin\gamma & \cos\gamma & 0 \\ 0 & 0 & 1 \end{bmatrix}$$



Scattering Processes: Volume Scattering



Principal Polarisability Matrix:

$$[P] = \begin{bmatrix} \rho_x & 0 & 0 \\ 0 & \rho_y & 0 \\ 0 & 0 & \rho_z \end{bmatrix} \quad \text{with} \quad \rho_i = \frac{V}{4\pi(L_i + 1/(\epsilon_r - 1))}$$

where $V = \frac{3}{4}\pi \frac{l_x}{2} \frac{l_y}{2} \frac{l_z}{2}$ is the particle volume and

$$L_i = \int_0^{\infty} \frac{(l_x l_y l_z) / 8}{2(s + l_x/2)^{3/2} (s + l_y/2)^{3/2} (s + l_z/2)^{3/2}} ds$$

$$L_x : L_y : L_z = \frac{1}{l_x} : \frac{1}{l_y} : \frac{1}{l_z} \quad L_x + L_y + L_z = 1$$

Particle Anisotropy:

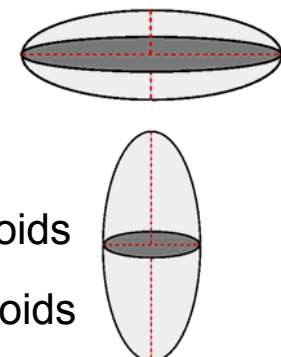
$$A_p := \frac{L_x(\epsilon_r - 1) + 1}{L_y(\epsilon_r - 1) + 1} = \frac{m\epsilon_r + 2}{m + \epsilon_r + 1}$$

Particle Shape Ratio:

$$m := \frac{L_x}{L_y} = \frac{l_y}{l_x} \quad 0 \leq m \leq \infty$$

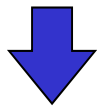
$m > 1$ oblate spheroids

$m < 1$ prolate spheroids



Scattering Processes: Volume Scattering

$$[P](\alpha, \beta, \gamma) = [R_3(\alpha)] [R_3(\beta)] [R_3(\gamma)] [P] [R_3(\gamma)]^T [R_3(\beta)]^T [R_3(\alpha)]^T$$

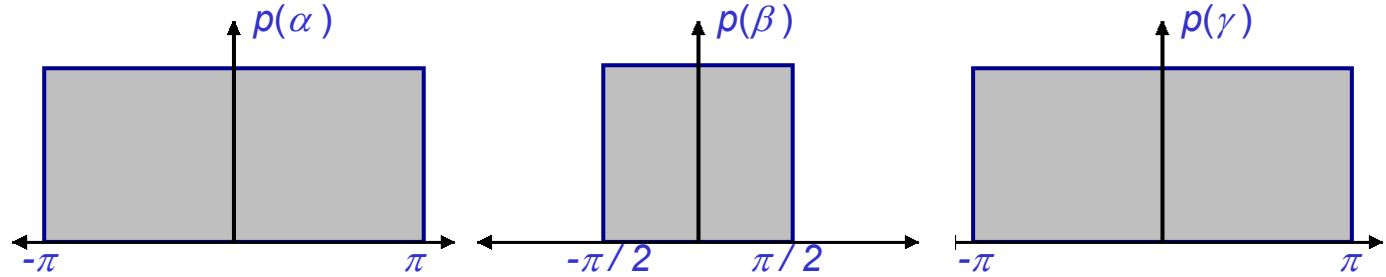


Coherency Matrix:

$$[T] = \int_{\alpha} \int_{\beta} \int_{\gamma} [P](\alpha, \beta, \gamma) p(\alpha) p(\beta) p(\gamma) d\alpha d\beta d\gamma$$

where $p(\alpha)$, $p(\beta)$, $p(\gamma)$ are the pdf's for the corresponding angle distributions

Special Case:
Random Volume



downward blue arrow

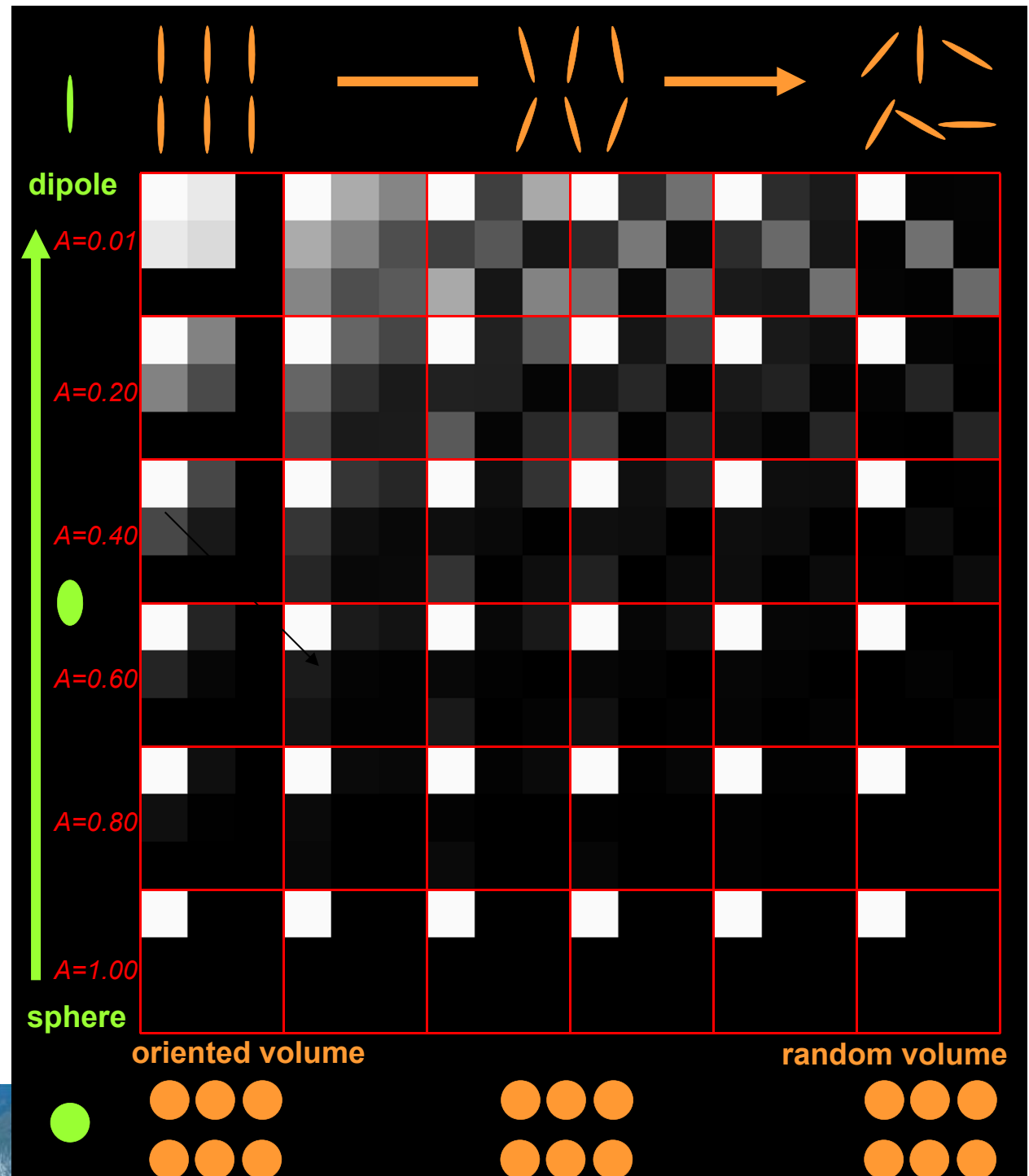
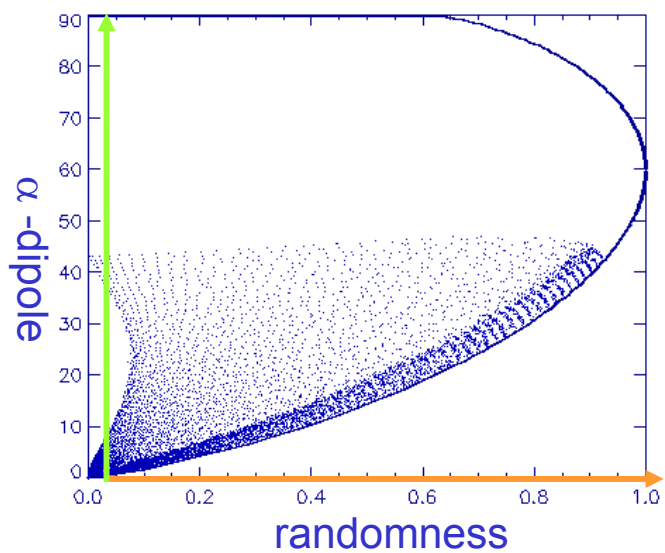
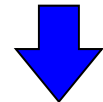
$$[T] = a \begin{bmatrix} 1 & 0 & 0 \\ 0 & b & 0 \\ 0 & 0 & b \end{bmatrix} \quad \text{where} \quad b = \frac{(A_p - I)^2}{2(2 + 6A_p + 7A_p^2)} \quad 0 \leq b \leq 0.5$$



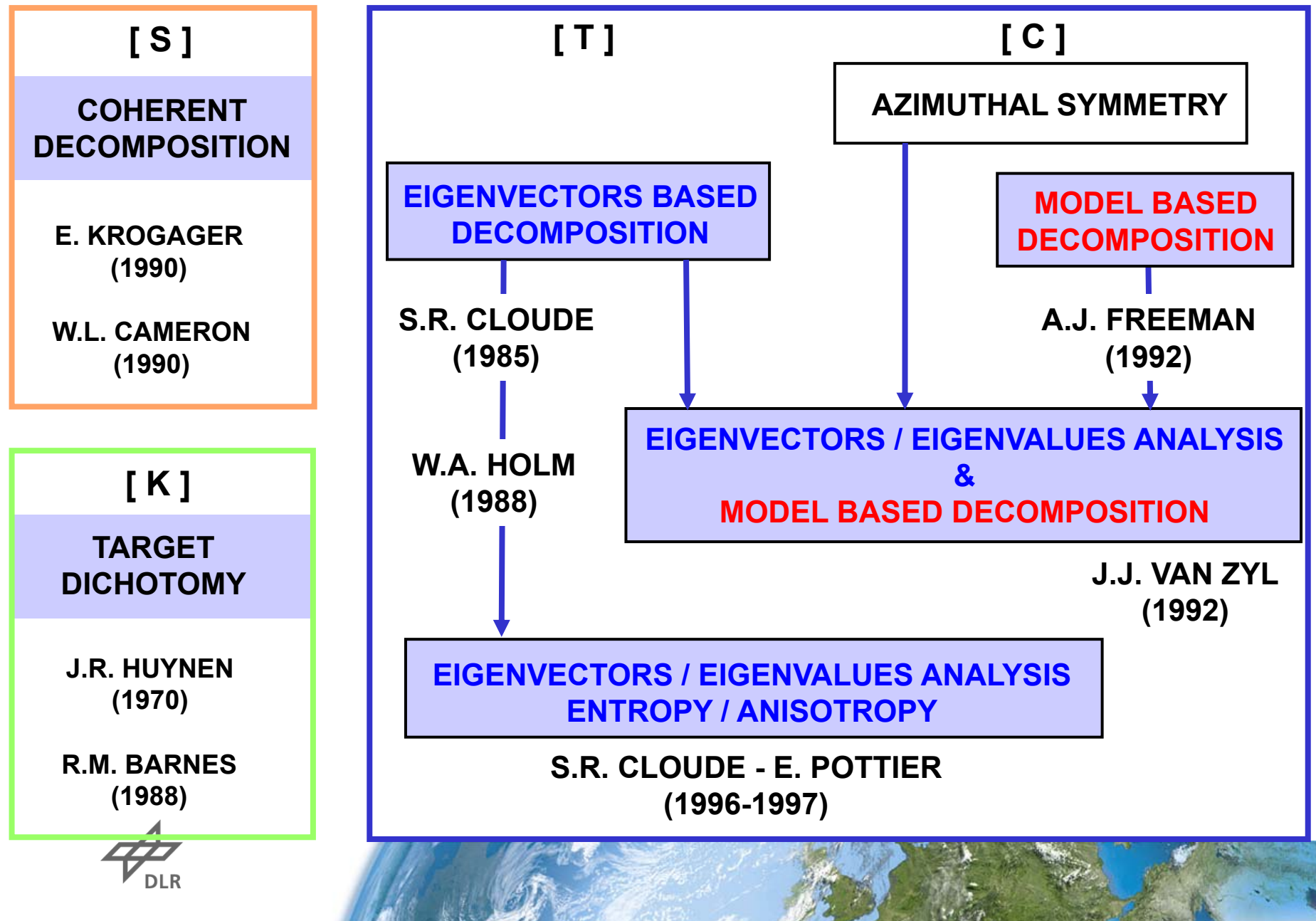
Scattering Processes: Volume Scattering

Prolate Particles

H/a Loci for varying particle
shape and width of distribution

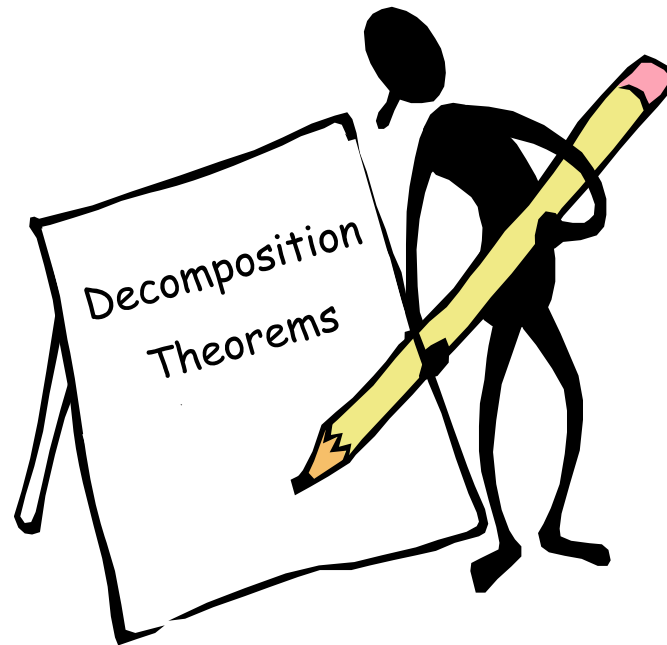


Decomposition Theorems



Decomposition Theorems

- Pauli Matrix Decomp.
- Model Based Decomp.
- Eigenvector Decomp.



Pauli Matrices Decomposition

$$[S] = \begin{bmatrix} S_{HH} & S_{HV} \\ S_{VH} & S_{VV} \end{bmatrix} = \begin{bmatrix} a+b & c-id \\ c+id & a-b \end{bmatrix} = a \begin{bmatrix} 1 & 0 \\ 0 & 1 \end{bmatrix} + b \begin{bmatrix} 1 & 0 \\ 0 & -1 \end{bmatrix} + c \begin{bmatrix} 0 & 1 \\ 1 & 0 \end{bmatrix} + d \begin{bmatrix} 0 & -i \\ i & 0 \end{bmatrix}$$

- $[S_a] = a \begin{bmatrix} 1 & 0 \\ 0 & 1 \end{bmatrix}$ Single Scattering: $S_{HH} = S_{VV}$
- $[S_b] = b \begin{bmatrix} 1 & 0 \\ 0 & -1 \end{bmatrix}$ Dihedral Scattering: $S_{HH} = -S_{VV}$
- $[S_c] = c \begin{bmatrix} 0 & 1 \\ 1 & 0 \end{bmatrix}$ Dihedral Scattering (... rotated by $\pi/2$ about the LOS)
- $[S_d] = d \begin{bmatrix} 0 & -i \\ i & 0 \end{bmatrix}$ Transforms all polarisation states into their orthogonal states (disappears in backscattering)



Azimuth
C-band
 λ 5 cm
Range

Scattering Amplitude Images



HH



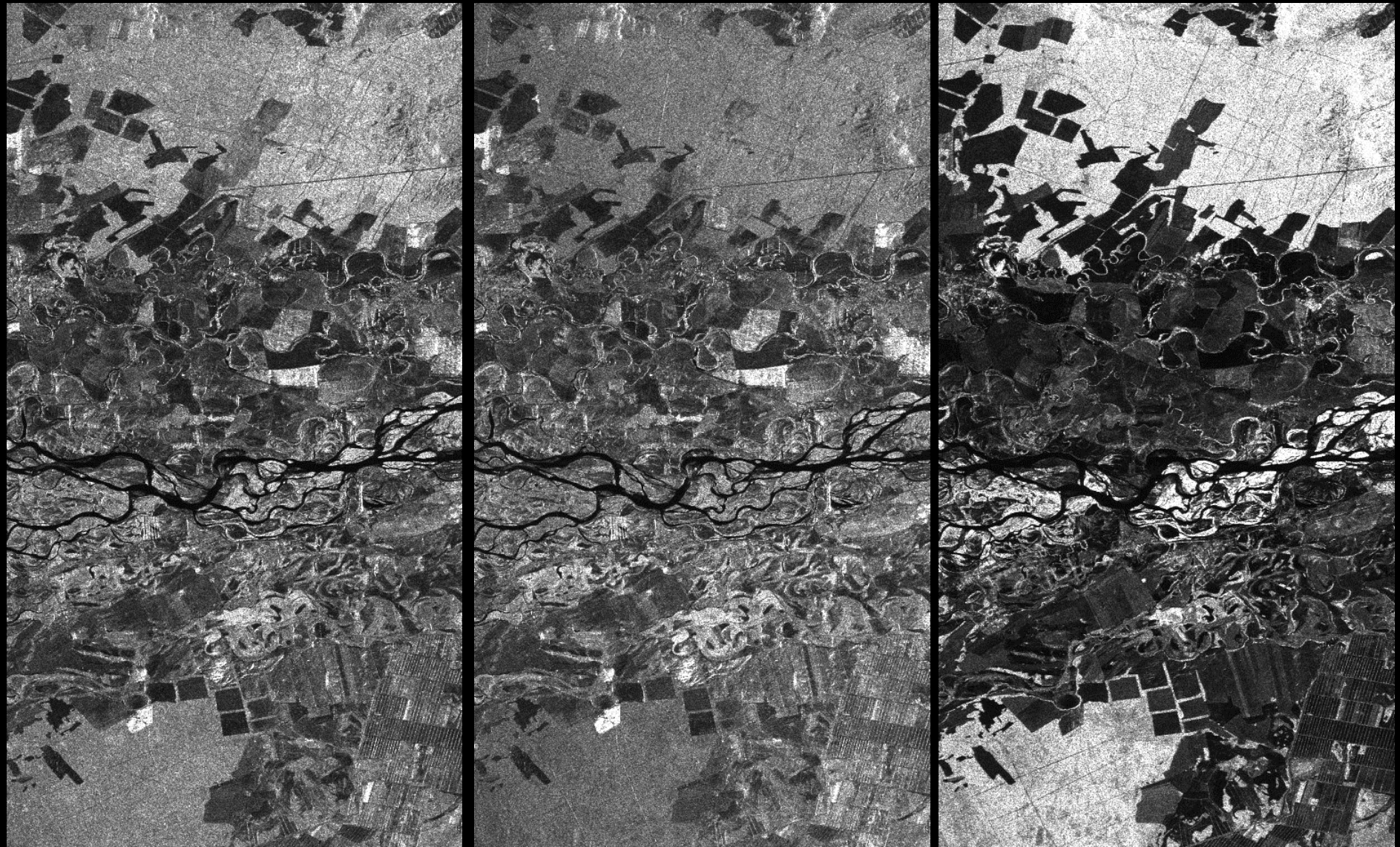
VV



HV

Azimuth
L-band
 λ 23 cm
Range

Scattering Amplitude Images



HH

VV

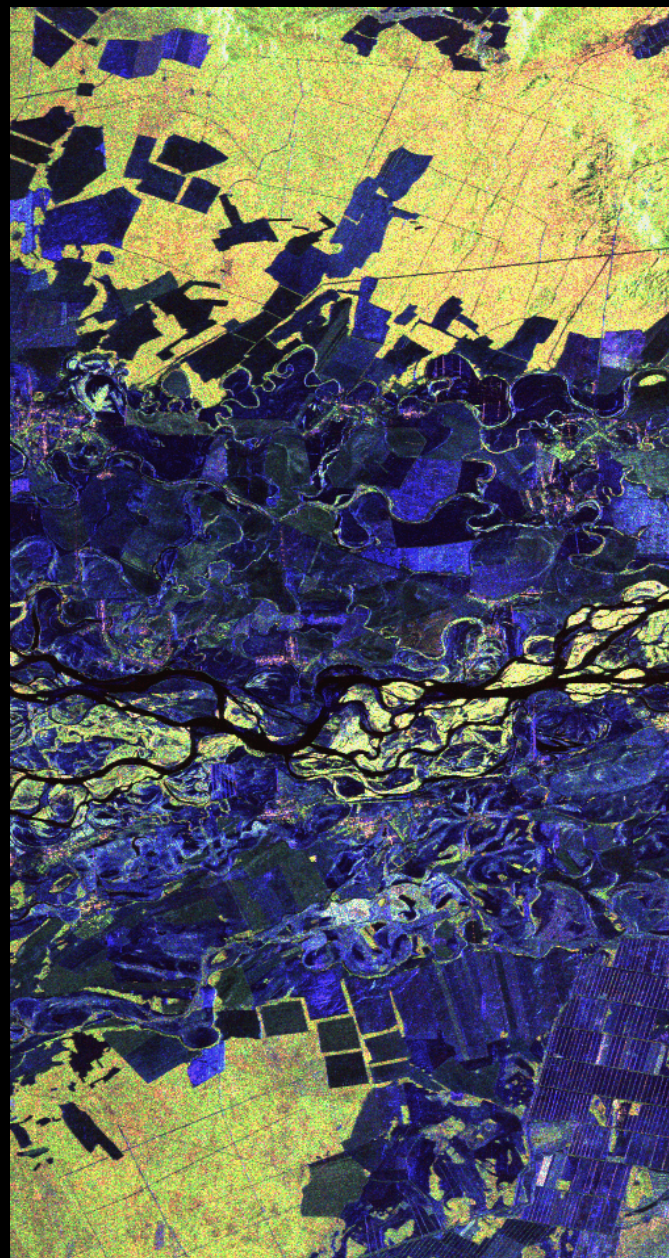
HV

Pauli Images

SIR-C / Test Site: Kudara, Russia



C-band

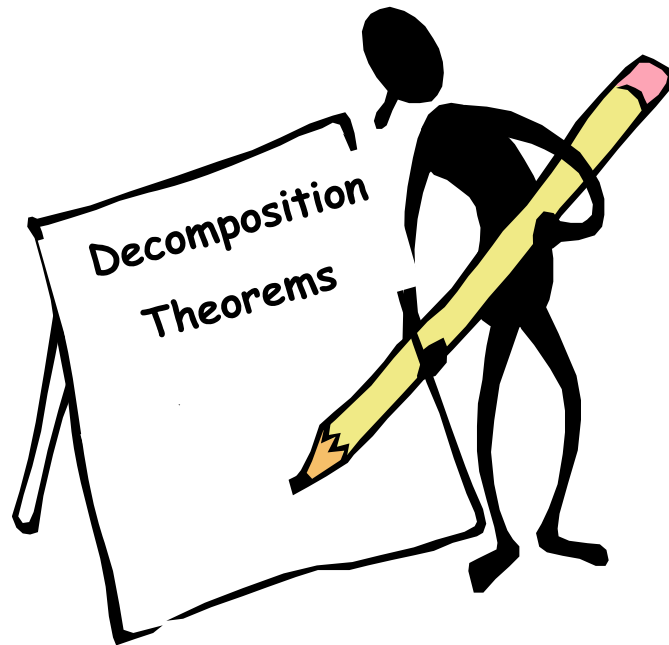


L-band

RGB-Coding:
HH-VV
2HV
HH+VV

Decomposition Theorems

- Pauli Matrice Decomp.
- **Eigenvector Decomp.**
- Model Based Decomp.



Eigenvector Decomposition

Coherence Matrix:

$$[T_3] := \langle \vec{k}_{3P} \cdot \vec{k}_{3P}^+ \rangle$$

Diagonalisation:

$$[T_3] = [U_3][\Lambda][U_3]^{-1}$$

$$[T_3] = \sum_{i=1}^3 \lambda_i (\vec{e}_i \cdot \vec{e}_i^+) = \lambda_1 (\vec{e}_1 \cdot \vec{e}_1^+) + \lambda_2 (\vec{e}_2 \cdot \vec{e}_2^+) + \lambda_3 (\vec{e}_3 \cdot \vec{e}_3^+) = [T_3^1] + [T_3^2] + [T_3^3]$$

$[S_1] \quad [S_2] \quad [S_3]$

- 3 real positive eigenvalues

$$\lambda_1 \geq \lambda_2 \geq \lambda_3 \geq 0$$

- 3 orthonormal eigenvectors

$$\vec{e}_1 = \begin{bmatrix} e_{11} \\ e_{21} \\ e_{31} \end{bmatrix} \quad \vec{e}_2 = \begin{bmatrix} e_{12} \\ e_{22} \\ e_{32} \end{bmatrix} \quad \vec{e}_3 = \begin{bmatrix} e_{13} \\ e_{23} \\ e_{33} \end{bmatrix}$$

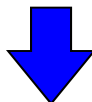
where: $[\Lambda] = \begin{bmatrix} \lambda_1 & 0 & 0 \\ 0 & \lambda_2 & 0 \\ 0 & 0 & \lambda_3 \end{bmatrix}$ $[U_3] = \begin{bmatrix} e_{11} & e_{12} & e_{13} \\ e_{21} & e_{22} & e_{23} \\ e_{31} & e_{32} & e_{33} \end{bmatrix}$ $[U_3]^{-1} = [U_3]^+ = \begin{bmatrix} e_{11}^* & e_{21}^* & e_{31}^* \\ e_{12}^* & e_{22}^* & e_{32}^* \\ e_{13}^* & e_{23}^* & e_{33}^* \end{bmatrix}$



Scattering Entropy / Anisotropy

Coherency Matrix Diagonalisation:

$$[T_3] = \sum_{i=1}^3 \lambda_i (\vec{e}_i \cdot \vec{e}_i^+) = \lambda_1 (\vec{e}_1 \cdot \vec{e}_1^+) + \lambda_2 (\vec{e}_2 \cdot \vec{e}_2^+) + \lambda_3 (\vec{e}_3 \cdot \vec{e}_3^+) = [T_3^1] + [T_3^2] + [T_3^3]$$



Scattering Entropy: $H := \sum_{i=1}^3 P_i \log_3 P_i$ with: $P_i := \frac{\lambda_i}{\lambda_1 + \lambda_2 + \lambda_3}$

$$0 \leq H \leq 1 \quad \text{where:}$$

- $H = 0 \rightarrow$ Totally Polarised Scatterer
- $H = 1 \rightarrow$ Totally Unpolarised Scatterer

Scattering Anisotropy:

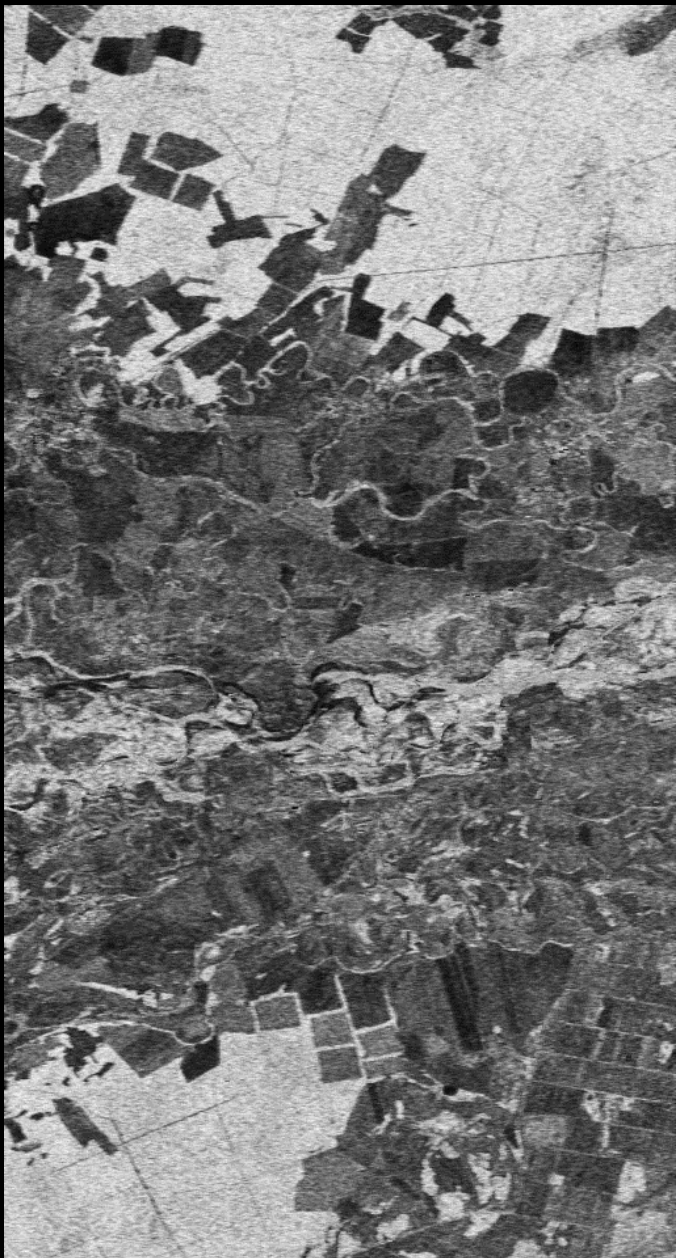
$$A := \frac{\lambda_2 - \lambda_3}{\lambda_2 + \lambda_3} = \frac{P_2 - P_3}{P_2 + P_3}$$

$$0 \leq A \leq 1 \quad \text{where:}$$

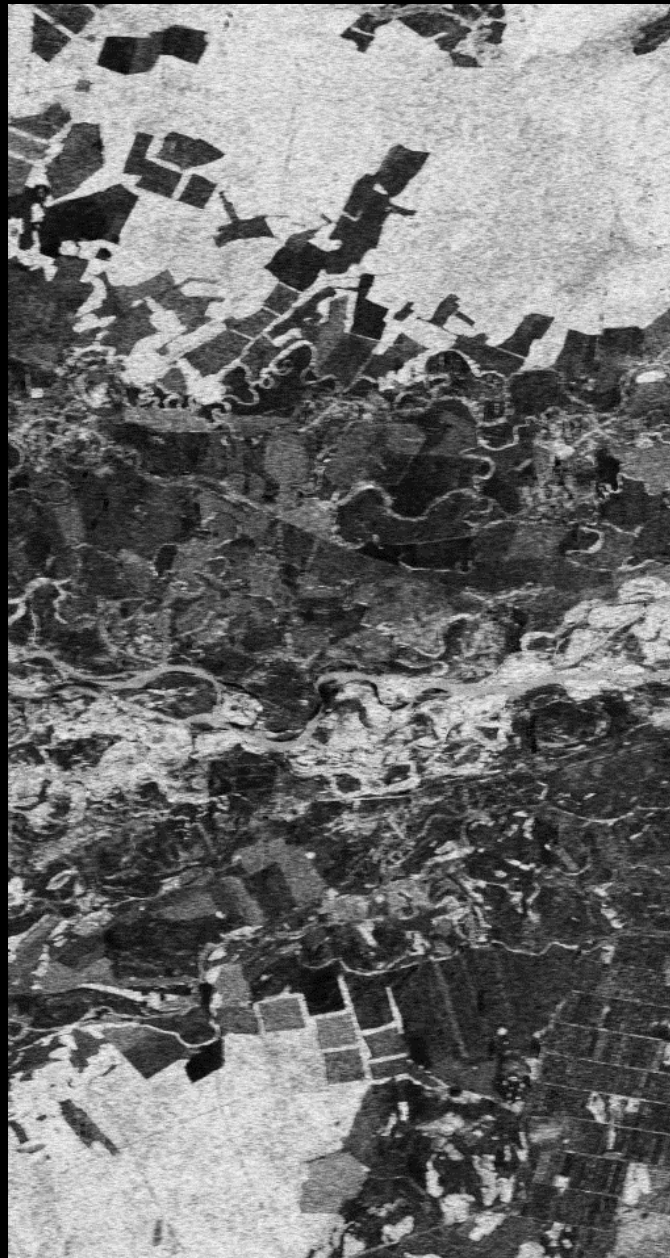
- $A = 0 \rightarrow$ 2 Equal Secondary Scattering Processes
- $A = 1 \rightarrow$ Only 1 Secondary Scattering Process



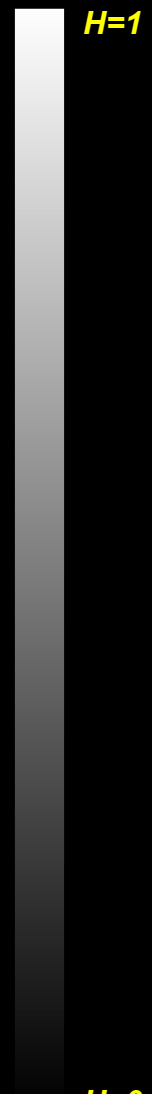
Scattering Entropy Images



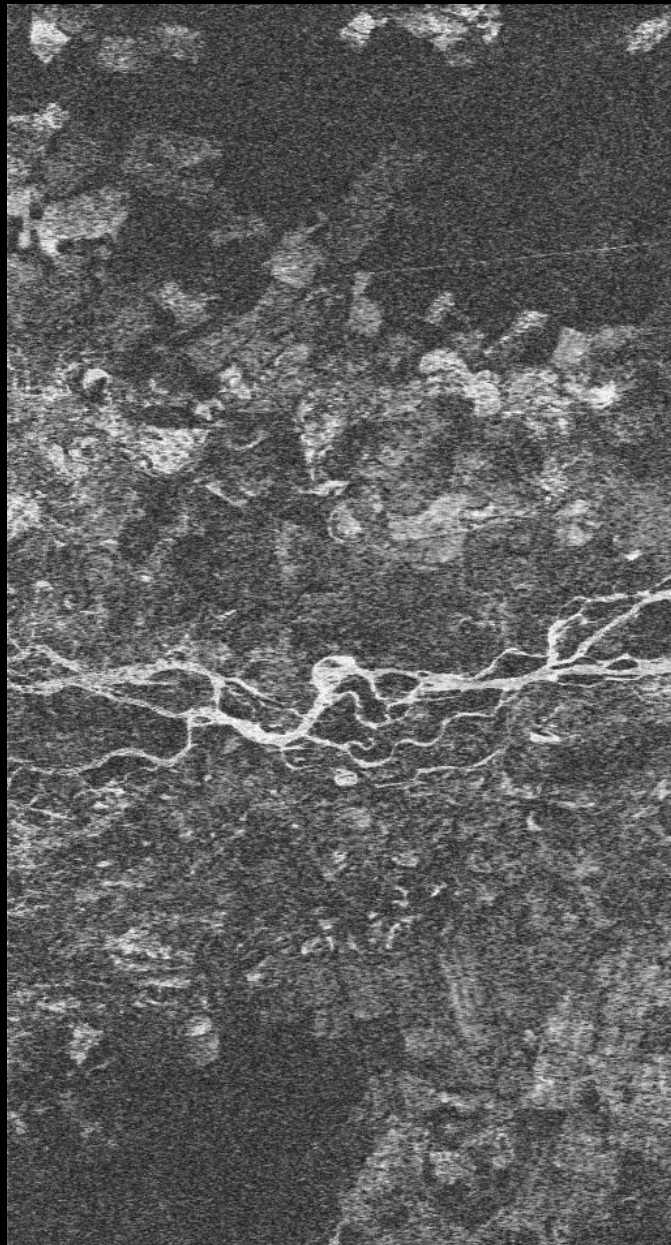
C-band



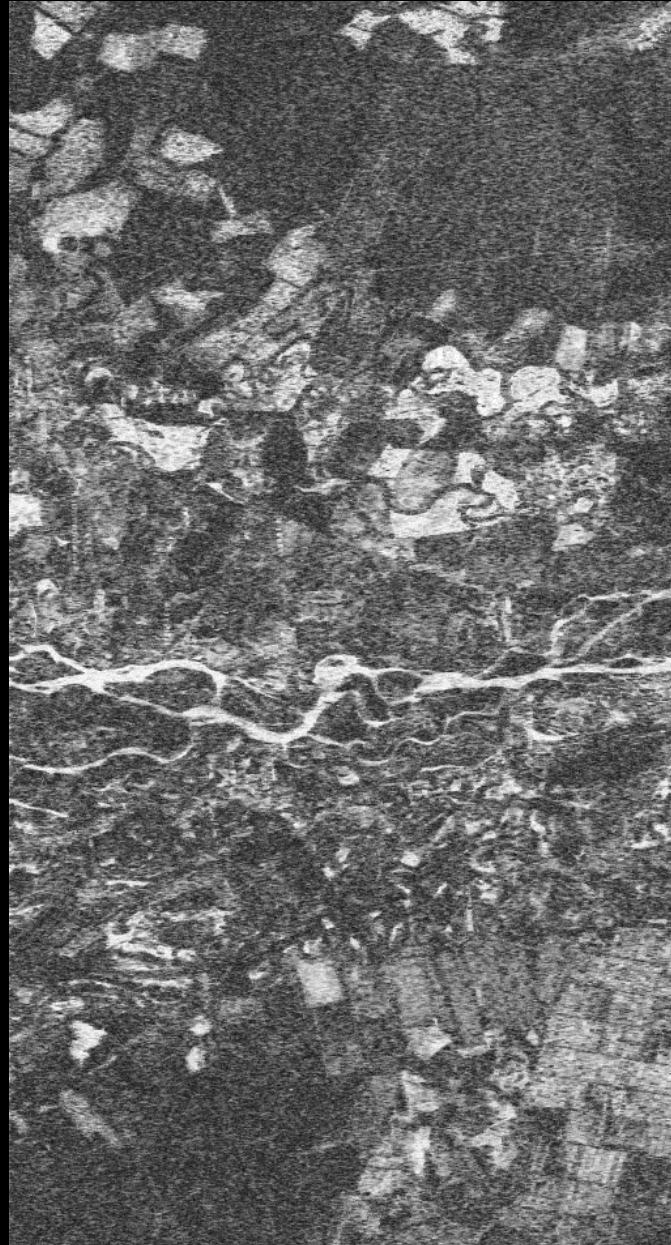
L-band



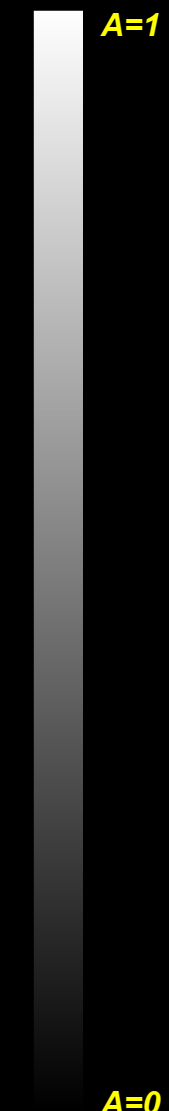
Scattering Anisotropy Images



C-band



L-band



Mean Scattering Parameters: Eigenvector

Coherency Matrix Diagonalisation:

$$[T_3] = \lambda_1(\vec{e}_1 \cdot \vec{e}_1^+) + \lambda_2(\vec{e}_2 \cdot \vec{e}_2^+) + \lambda_3(\vec{e}_3 \cdot \vec{e}_3^+)$$

Eigenvectors $\vec{e}_i = \begin{bmatrix} \cos(\alpha_i) \exp(i\gamma_i) \\ \sin(\alpha_i) \cos(\beta_i) \exp(i\delta_i) \\ \sin(\alpha_i) \sin(\beta_i) \exp(i\varepsilon_i) \end{bmatrix}$

Appearance Probabilities: $P_i := \frac{\lambda_i}{\lambda_1 + \lambda_2 + \lambda_3}$

Mean α -Angle: $\alpha = P_1 \alpha_1 + P_2 \alpha_2 + P_3 \alpha_3$

Mean β -Angle: $\beta = P_1 \beta_1 + P_2 \beta_2 + P_3 \beta_3$

Mean γ -Angle: $\gamma = P_1 \gamma_1 + P_2 \gamma_2 + P_3 \gamma_3$

Mean δ -Angle: $\delta = P_1 \delta_1 + P_2 \delta_2 + P_3 \delta_3$

Mean ε -Angle: $\varepsilon = P_1 \varepsilon_1 + P_2 \varepsilon_2 + P_3 \varepsilon_3$

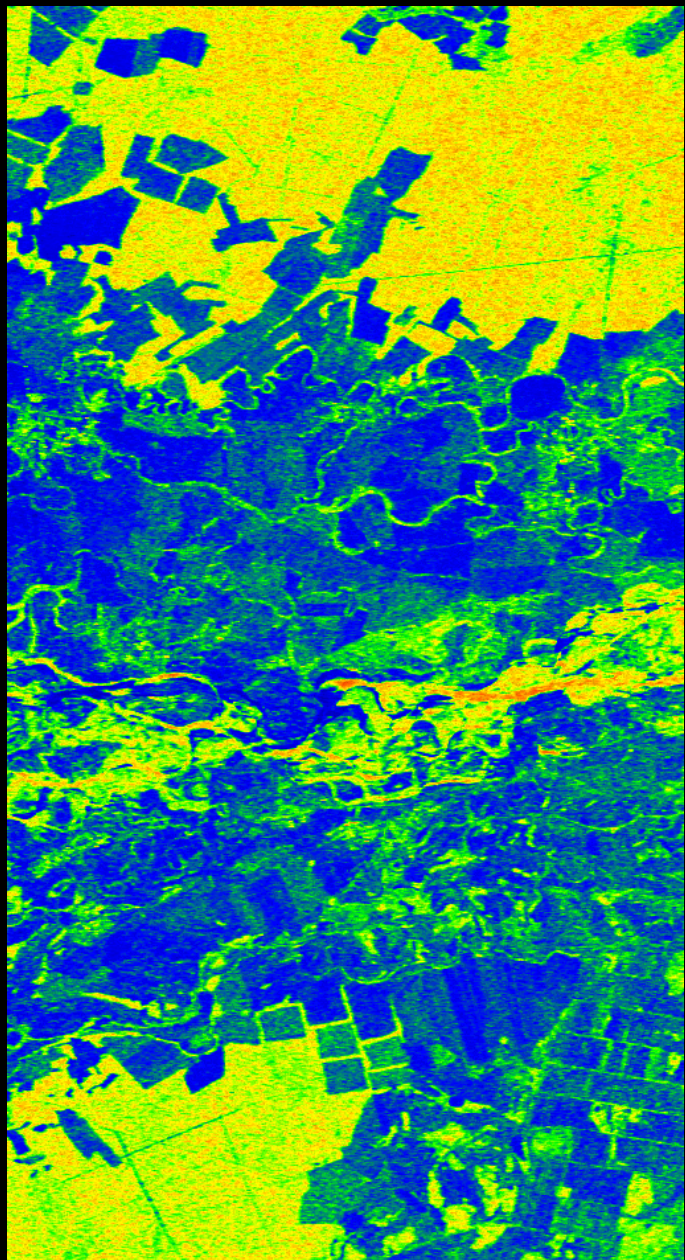
Mean Scattering Mechanism

$$\vec{e} = \begin{bmatrix} \cos(\alpha) \exp(i\gamma) \\ \sin(\alpha) \cos(\beta) \exp(i\delta) \\ \sin(\alpha) \sin(\beta) \exp(i\varepsilon) \end{bmatrix}$$

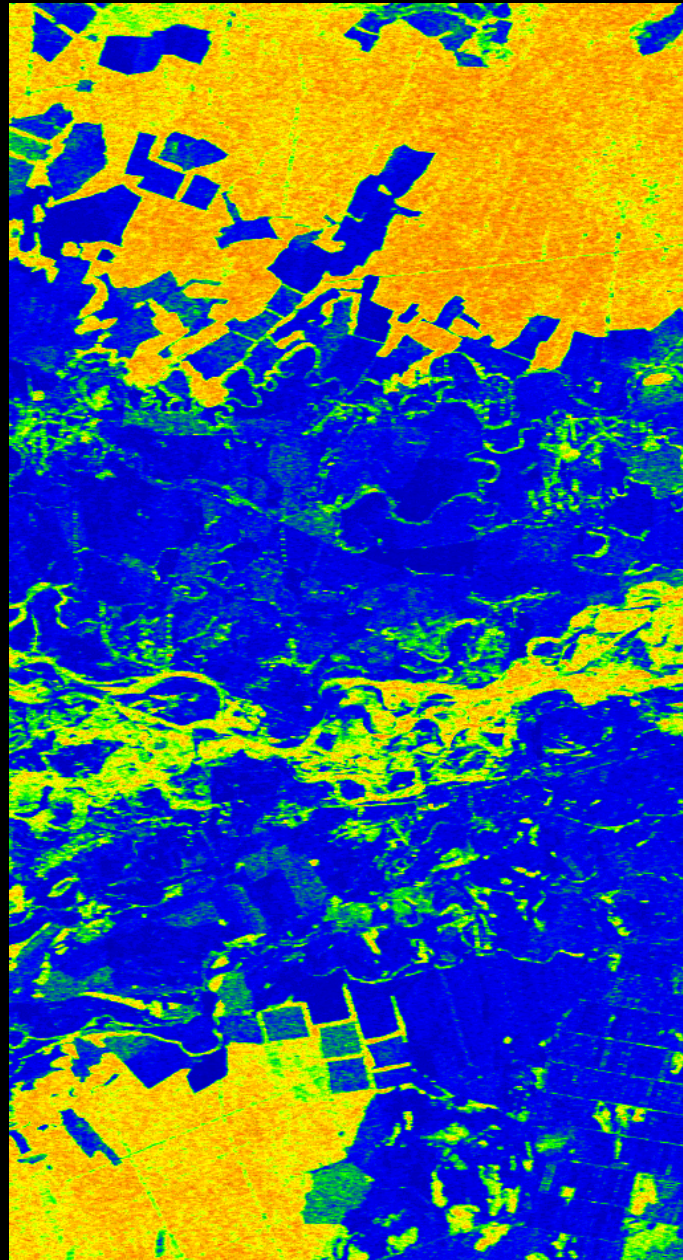


α -Angle Images

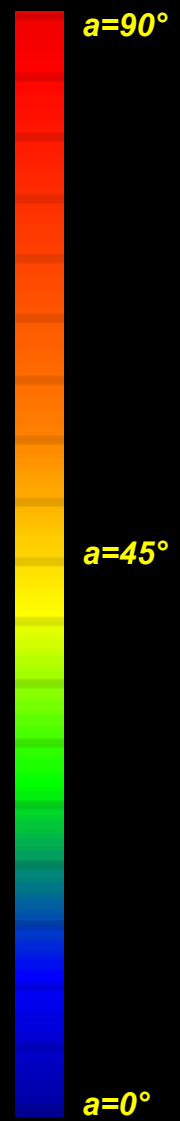
SIR-C / Test Site: Kudara, Russia



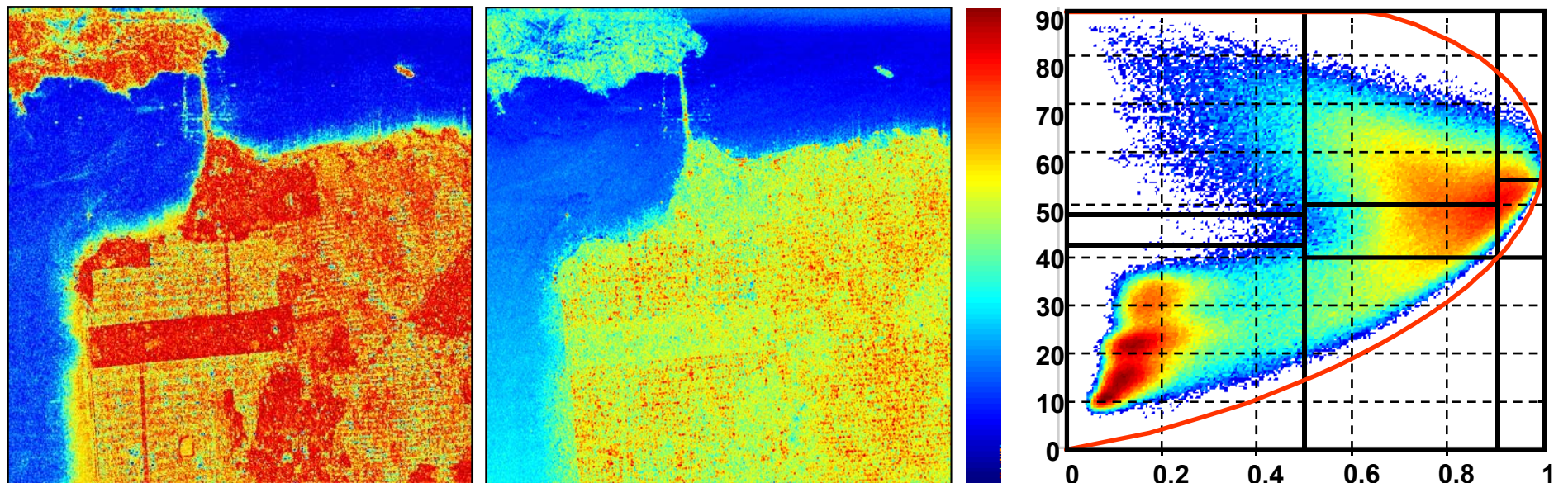
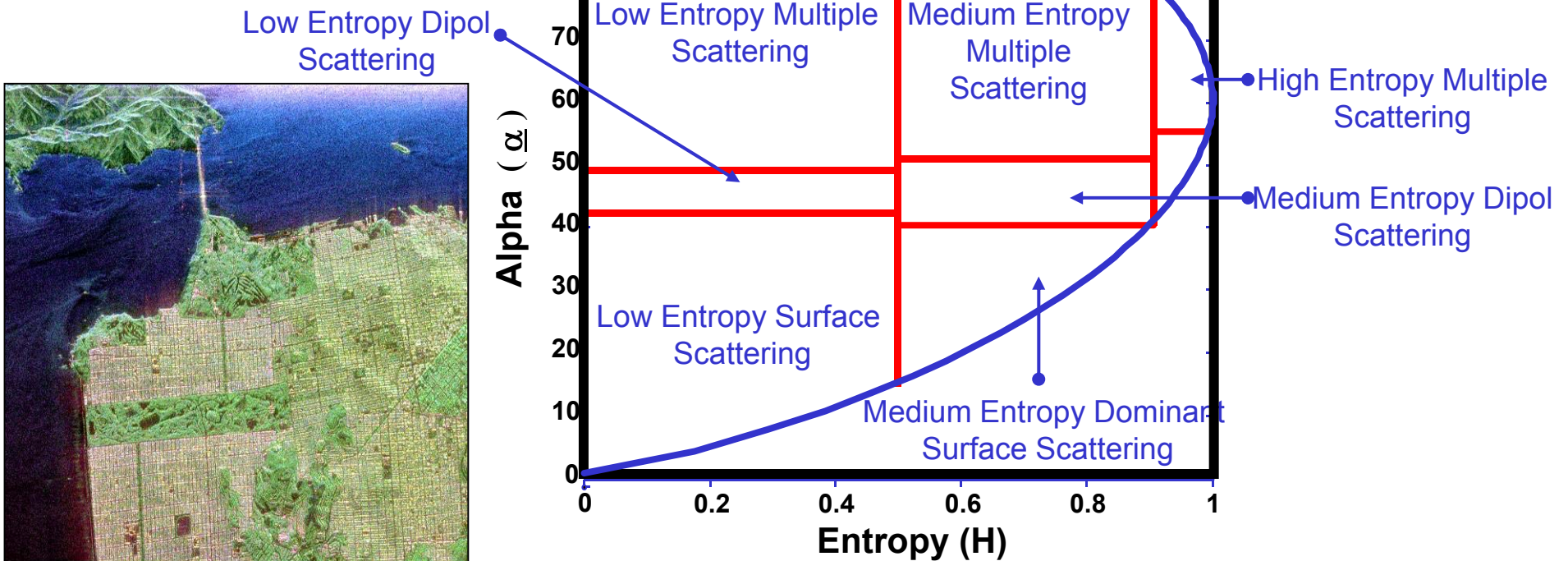
C-band



L-band

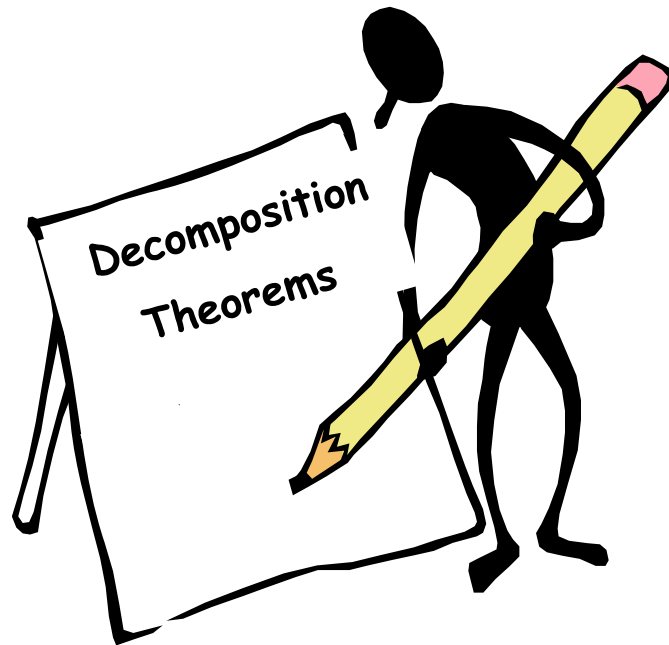


2D H- α Angle Plane



Decomposition Theorems

- Pauli Matrice Decomp.
- Eigenvector Decomp.
- **Model Based Decomp.**



Freeman 3 Component Decomposition

Vegetation Scattering : Bragg-Scattering + Dihedral Scattering + Random Volume of Dipols

$$[T] = [T_S] + [T_D] + [T_V]$$

where $[T_S] = f_S \begin{bmatrix} \beta^2 & \beta & 0 \\ \beta & 1 & 0 \\ 0 & 0 & 0 \end{bmatrix}$ $[T_D] = f_D \begin{bmatrix} \alpha^2 & -\alpha & 0 \\ -\alpha & 1 & 0 \\ 0 & 0 & 0 \end{bmatrix}$ and $[T_V] = f_V \begin{bmatrix} 2 & 0 & 0 \\ 0 & 1 & 0 \\ 0 & 0 & 1 \end{bmatrix}$

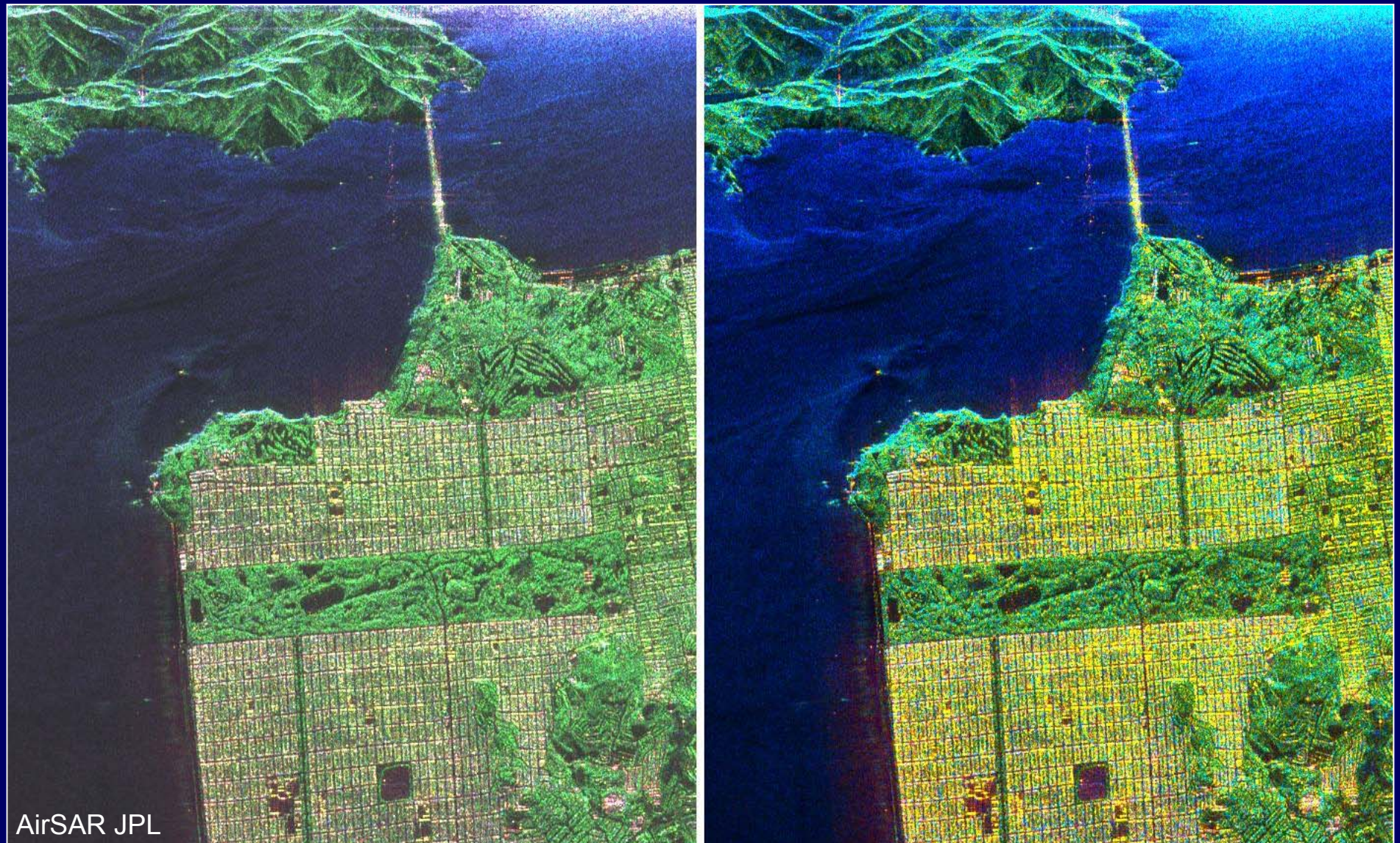
$$[T] = \begin{bmatrix} f_S \beta^2 + f_D \alpha^2 + 2f_V & f_S \beta - f_D \alpha & 0 \\ f_S \beta - f_D \alpha & f_S + f_D + f_V & 0 \\ 0 & 0 & f_V \end{bmatrix}$$

4 Equations
for
5 Unknowns

- $\text{Re(HHVV)} - fv/3 > 0 \rightarrow \text{Single bounce is dominant} \rightarrow \alpha = 1$
- $\text{Re(HHVV)} - fv/3 < 0 \rightarrow \text{Double bounce is dominant} \rightarrow \beta = 1$



3 Component Freeman Decomposition (San Francisco)



Freeman 2 Component Decomposition

$$[T] = [T_{S/D}] + [T_V]$$
$$\begin{bmatrix} T_{11} & T_{12} & 0 \\ T_{12}^* & T_{22} & 0 \\ 0 & 0 & T_{33} \end{bmatrix} = f_G \begin{bmatrix} |\alpha|^2 & \alpha & 0 \\ \alpha^* & 1 & 0 \\ 0 & 0 & 0 \end{bmatrix} + f_V \begin{bmatrix} 1+\rho & 0 & 0 \\ 0 & 1-\rho & 0 \\ 0 & 0 & 1-\rho \end{bmatrix}$$

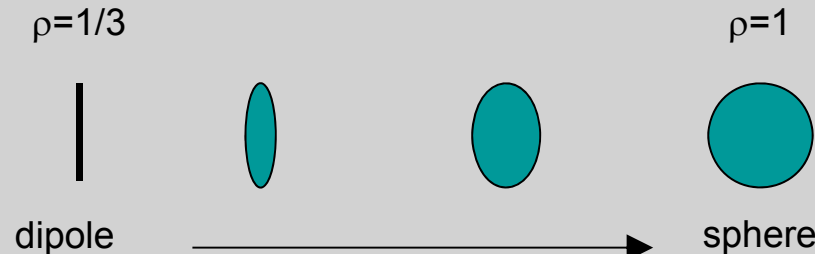
Scattering Power Components:

$$P_G = f_G(1 + |\alpha|^2) \quad P_V = f_V(3 - \rho)$$

Distinction between dihedral and surface of the ground component:

$|\alpha| < 1$ dihedral
 $|\alpha| \geq 1$ surface

Volume shape parameter ρ of a randomly oriented volume:



Summary: Polarimetric Parameters / Scattering Matrix

$$[S] = \begin{bmatrix} S_{HH} & S_{XX} \\ S_{XX} & S_{VV} \end{bmatrix} \rightarrow [S] = \frac{\exp(i\kappa r) \exp(i\varphi_V)}{r} \begin{bmatrix} |S_{HH}| \exp i(\varphi_{HH} - \varphi_V) & |S_{XX}| \exp i(\varphi_{XX} - \varphi_V) \\ |S_{XX}| \exp i(\varphi_{XX} - \varphi_V) & |S_{VV}| \end{bmatrix}$$

Absolute Phase Factor Five Parameters: 3 Amplitudes & 2 Phases

- Scattering Amplitudes $\sigma_{HH}^0 := |S_{HH} S_{HH}^*|_N$ $\sigma_{XX}^0 := |S_{XX} S_{XX}^*|_N$ $\sigma_{VV}^0 := |S_{VV} S_{VV}^*|_N$
- Total Power $TP := |S_{VV}|^2 + 4 |S_{XX}|^2 + |S_{VV}|^2$
- Amplitude Ratios $\sigma_{HH}^0 / \sigma_{VV}^0$ $\sigma_{XX}^0 / \sigma_{VV}^0$ $\sigma_{XX}^0 / (\sigma_{HH}^0 + \sigma_{VV}^0)$
- Pol Phase Differences $\varphi_{HHVV} := \varphi_{HH} - \varphi_V$
- Helicity $Hel := |S_{LL}| - |S_{RR}|$



Summary: Second Order Polarimetric Parameters

$\vec{k}_3 = \begin{bmatrix} A \\ B \\ C \end{bmatrix}$  $[X_3] := \vec{k}_3 \cdot \vec{k}_3^+ = \begin{bmatrix} \langle AA^* \rangle & \langle AB^* \rangle & \langle AC^* \rangle \\ \langle BA^* \rangle & \langle BB^* \rangle & \langle BC^* \rangle \\ \langle CA^* \rangle & \langle CB^* \rangle & \langle CC^* \rangle \end{bmatrix}$ <u>Nine Parameters: 3 Real & 3 Complex Elements</u>	Pauli Scat. Vector $A := \frac{1}{\sqrt{2}}(S_{HH} + S_W)$ $B := \frac{1}{\sqrt{2}}(S_{HH} - S_W)$ $C := \sqrt{2} S_{xx}$	Lexico. Scat. Vector $A := S_{HH}$ $B := \sqrt{2}S_{xx}$ $C := S_W$
--	--	--

• Correlation Coefficients	$\gamma_{HHVV} := \frac{ \langle S_{HH} S_{VV}^* \rangle }{\sqrt{ \langle S_{HH} S_{HH}^* \rangle \langle S_{VV} S_{VV}^* \rangle }}$	$\gamma_{LLRR} := \frac{ \langle S_{LL} S_{RR}^* \rangle }{\sqrt{ \langle S_{LL} S_{LL}^* \rangle \langle S_{RR} S_{RR}^* \rangle }}$
• Scattering Entropy	$H := \sum_{i=1}^3 P_i \log_3 P_i$	$P_i := \frac{\lambda_i}{\lambda_1 + \lambda_2 + \lambda_3}$
• Scattering Anisotropy	$A := \frac{\lambda_2 - \lambda_3}{\lambda_2 + \lambda_3} = \frac{P_2 - P_3}{P_2 + P_3}$	
• Polarimetric Alpha Angle	$\alpha := P_1 \alpha_1 + P_2 \alpha_2 + P_3 \alpha_3$	
• Polarimetric Beta Angle	$\beta := P_1 \beta_1 + P_2 \beta_2 + P_3 \beta_3$	



Applications of Radar Polarimetry

Agriculture/Land-Use

Crop Classification/Moisture Content Estimation
Urban Area mapping
Urban Topography for Mobilecomms

Forestry

Biomass Estimation: (Saturates For High Biomass)

C-band saturation at 50 tons/hectare
L-band saturation at 100 tons/hectare
P band saturation at 200 tons/hectare

Deforestation
Forest Canopy Height Estimation
Tree Species Discrimination
Forest Re-growth Monitoring

Geology

Playas :Smooth Natural Surfaces(rms = 1cm)
Alluvial fans, Sand Dunes, Moraines
Sedimentary Rock formations
Lava Flows (extreme in surface roughness)
Weathering Erosion Studies
Surface Roughness Estimates



Hydrology

Flood mapping/Forest Inundation
Snow Hydrology
Soil Moisture

Sea Ice/Oceanography

Ice Roughness/Thickness Studies
Polar Ice Cap Studies
Extra-Terrestrial Ice/Water Studies

Meteorology

Rain rate estimation
Water/Ice particle studies
Severe Storm/Flood warning

Topography/Cartography

Direct Surface Slope Estimation
Accurate DEM Generation
Difference of DEMS for Vegetation mapping

Humanitarian Demining

Surface Penetrating Radar (SPR)
SAR for Mine Field Detection

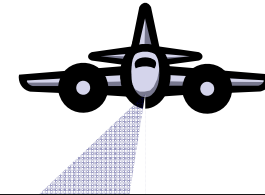


Soil Moisture Estimation

- Surface characterisation
- mv estimation over bare surface
- mv estimation under the vegetation



Surface Characterisation



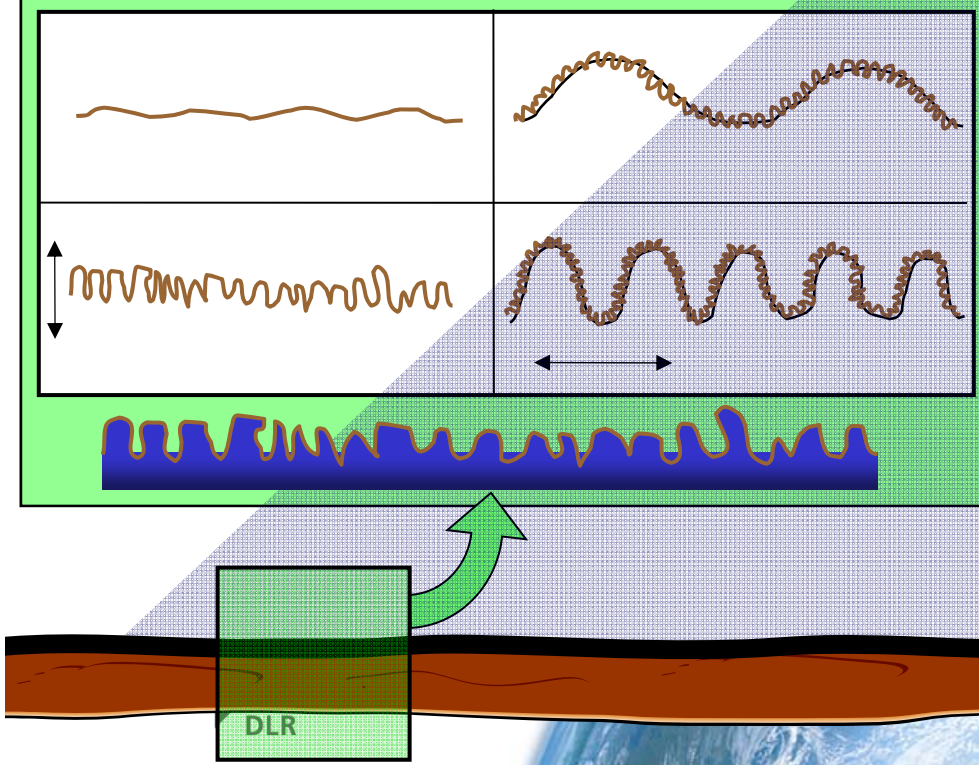
VOLUMETRIC MOISTURE CONTENT

m_v [vol. %]

SURFACE ROUGHNESS

rms - height
 σ [cm]

autocorrelation length
 l [cm]



The Backscattered signal depends on the moisture, and roughness of the surface.

Single channel SAR cannot resolve unambiguously the bare surface scattering problem.

Models for the Estimation of Bare Surface

Modeling and Inversion

THEORETICAL MODELS

Geometrical-Optic 1963

Physical-Optic 1963

Small Perturbation 1988

Integral Equation 1992

- very complex
- inversion is restricted possible

Shi Model 1997

EMPIRICAL EXTENSIONS

Oh Model 1992

Dubois Model 1995

- inversion with dual pol observables
- based on regressions coefficients of a specific test site

MODEL BASED EXTENSIONS

X-Bragg 1999

- simple model extension
- based on SPM (1st order) with an roughness extension

Time



Models for the Estimation of Vegetated Surface

Modeling and Inversion

THEORETICAL MODELS

Vegetation Models
(Stiles 2000)

- very complex scat. models
- inversion is not possible

SCATTERING DECOMPOSITION APPROACHES

Eigen-Decomposition
Model based-Decomposition

Hajnsek 2009
Jagdhuber 2012

- simple canonical scat. models
- inversion possible

SEMI-MODEL BASED EXTENSIONS

Optimisation
(physical and numerical)

Ari 2010
Neumann 2010

- extended scat. models
- inversion with higher computation time

Time



Small Perturbation Model



$$[S] = \begin{bmatrix} S_{HH} & S_{HV} \\ S_{VH} & S_{VV} \end{bmatrix} = j2k \cos(\theta) Z \begin{bmatrix} R_s(\theta, \epsilon_r) & 0 \\ 0 & R_p(\theta, \epsilon_r) \end{bmatrix}$$

Exact solution of Maxwell Equation for $s \rightarrow 0$

$$R_s = \frac{\cos\theta - \sqrt{\epsilon_r - \sin^2\theta}}{\cos\theta + \sqrt{\epsilon_r - \sin^2\theta}}$$

$$R_p = \frac{(\epsilon_r - 1)(\sin^2\theta - \epsilon_r(1 + \sin^2\theta))}{(\epsilon_r \cos\theta + \sqrt{\epsilon_r - \sin^2\theta})^2}$$

$$Z = F.T.(E(x, y))$$

θ = Incidence angle and $k = 2\pi/\lambda$

Roughness:



Depolarises the incident wave introducing (depolarised) HV and decreasing polarimetric coherence.

Ambiguity: Terrain Slopes introduce also a HV component but this is co-related to HH and VV.

Moisture content:

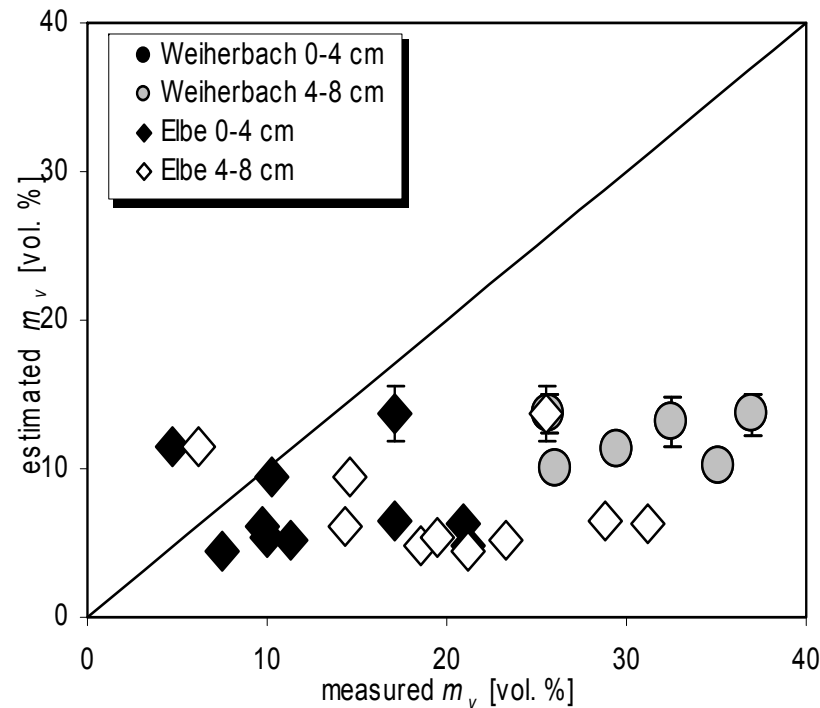
Effects the scattering amplitude of all polarisations. For “smooth” (with respect to wavelength) surfaces the co-polarimetric ratio (HH/VV) becomes independent of roughness

$$\frac{S_{HH}}{S_{VV}} = \frac{R_s}{R_p} \quad \text{is independent of roughness}$$

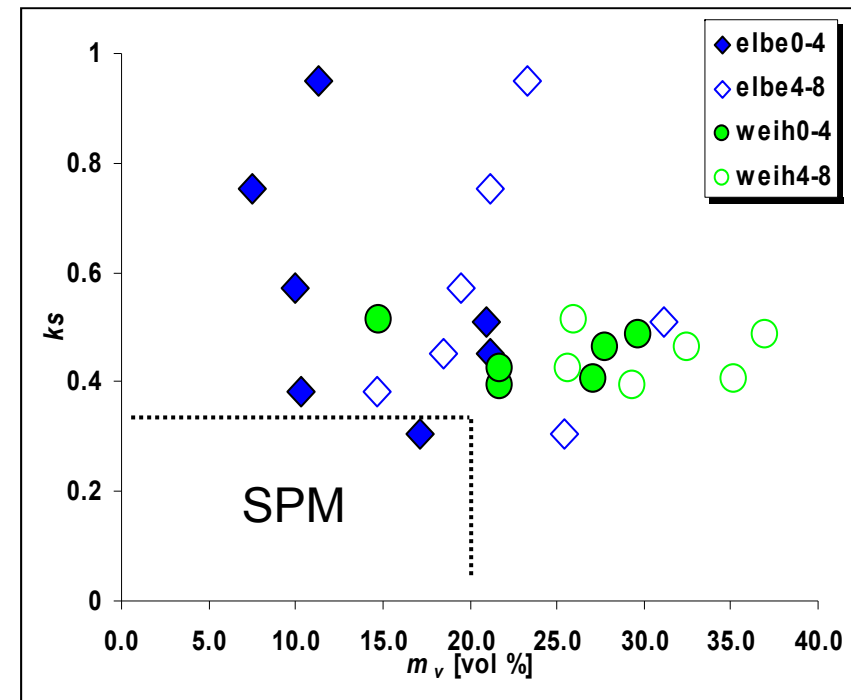
Polarimetry provides an observation space that allows to separate roughness from moisture effects.



Small Perturbation Model (Bragg-Model)



Measured versus estimated volumetric moisture content m_v [vol. %] using SPM



Validity range of the SPM for the ground measurements - surface roughness against volumetric soil moisture

Semi-Empirical Models

Oh-Model

Y. Oh, K. Sarabandi and F.T. Ulaby, "An Empirical Model and an Inversion Technique for Radar Scattering from Bare Soil Surfaces", IEEE Transactions on Geoscience and Remote Sensing, vol. 30, no. 2, pp. 370-381, 1992.

Cross-Pol Amplitude Relation

$$p = \frac{\sigma_{hh}^0}{\sigma_{vv}^0} = \left(1 - \left(\frac{20}{\pi} \right)^{\frac{1}{3\Gamma_0}} e^{-ks} \right)^2$$

$$q = \frac{\sigma_{hv}^0}{\sigma_{vv}^0} = 0.23 \sqrt{\Gamma_0} (1 - e^{-ks})$$

s_{xx}^0 : backscattering coefficient for different polarisations

q : incidence angle in radians

ϵ_r : real part of the dielectric constant

s : RMS height

k : wavenumber ($2\pi/l$)

G_0 : Fresnel reflectivity of the surface at nadir



Dubois-Model

P. C. Dubois, J. J. van Zyl and J. Engman, "Measuring Soil Moisture with Imaging Radar", IEEE Transactions on Geoscience and Remote Sensing, vol. 33, no. 4, pp. 915-926, 1995.

Co-Pol Amplitude Relation

$$\sigma_{hh}^0 = 10^{-2.75} \frac{\cos^{1.5} \theta}{\sin \theta^5} 10^{0.028 \epsilon \tan \theta} (k s \sin \theta)^{1.4} \lambda^{0.7}$$

$$\sigma_{vv}^0 = 10^{-2.35} \frac{\cos^3 \theta}{\sin^3 \theta} 10^{0.046 \epsilon \tan \theta} (k s \sin \theta)^{1.1} \lambda^{0.7}$$

q : incidence angle in radians

ϵ_r : real part of the dielectric constant

s : RMS height

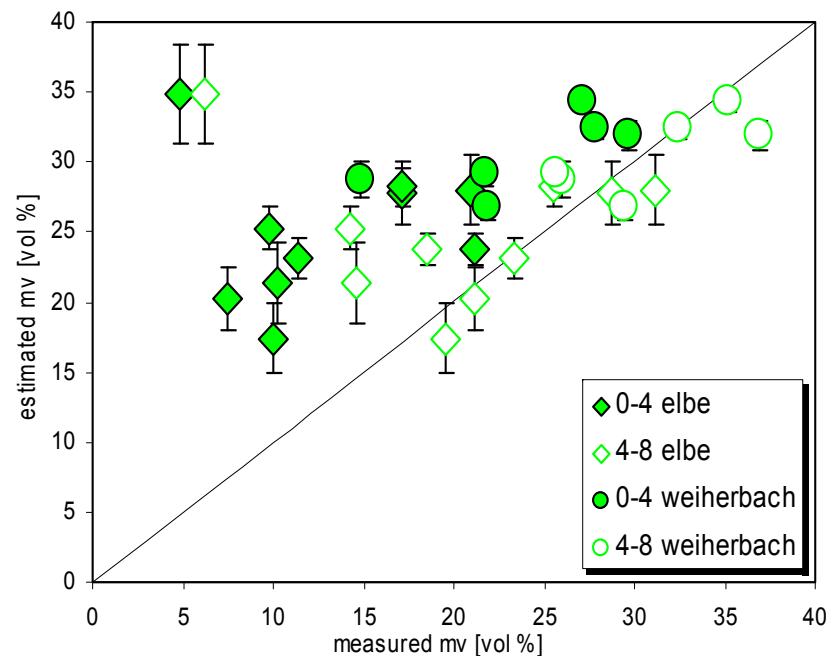
k : wave number ($2\pi/l$)

l : wavelength [cm]

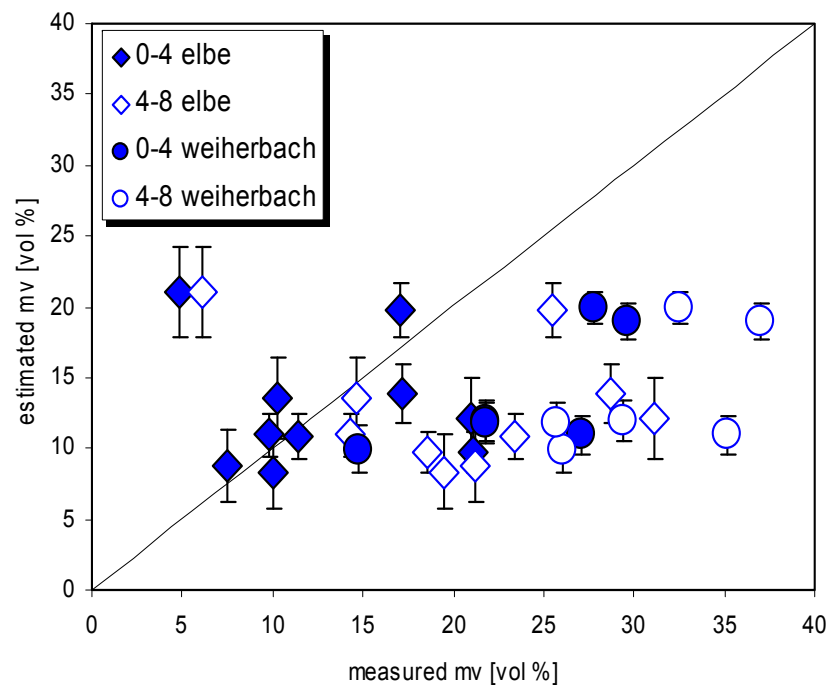


Quantitative Estimation of Volumetric Moisture m_v [vol %]

Dubois



Oh

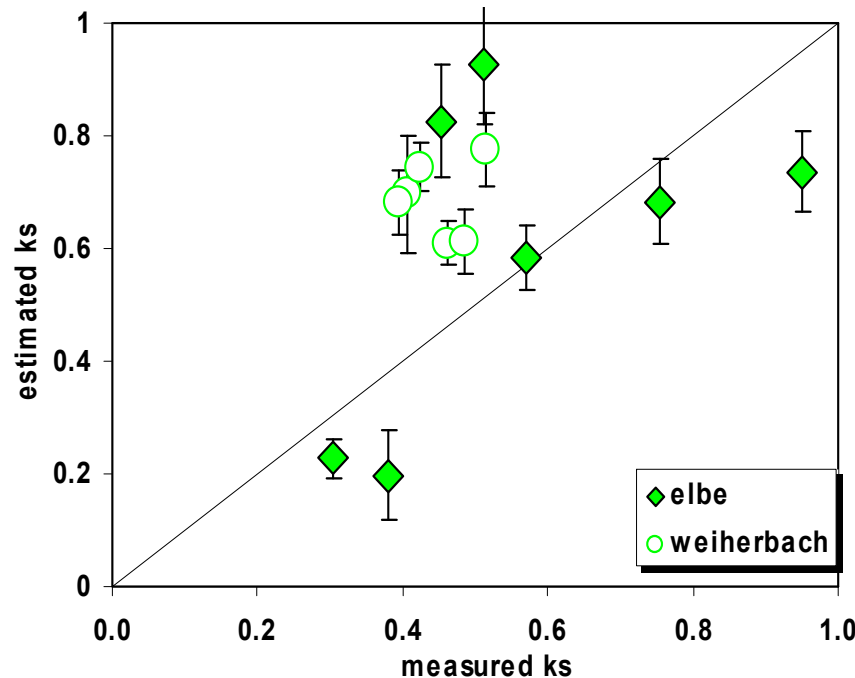


	0-4 cm	4-8 cm	corr.
Elbe RMS _{error}	14	10	-/-
Weih RMS _{error}	11	17	0.2/0.4

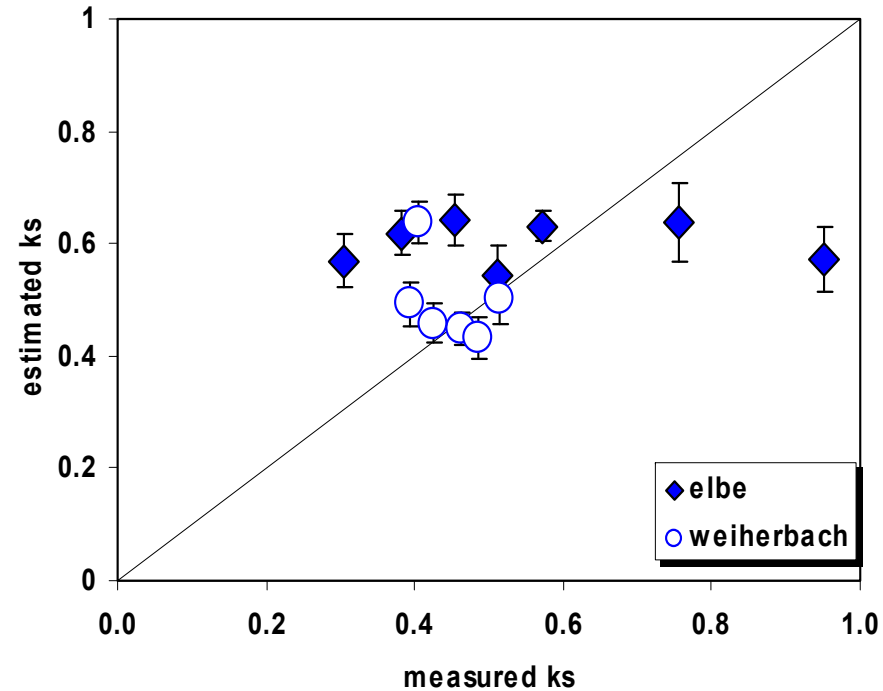
	0-4 cm	4-8 cm	corr.
Elbe RMS _{error}	7	12	-/-
Weih RMS _{error}	18	25	0.5/0.6

Quantitative Estimation of Surface Roughness ks

Dubois



Oh



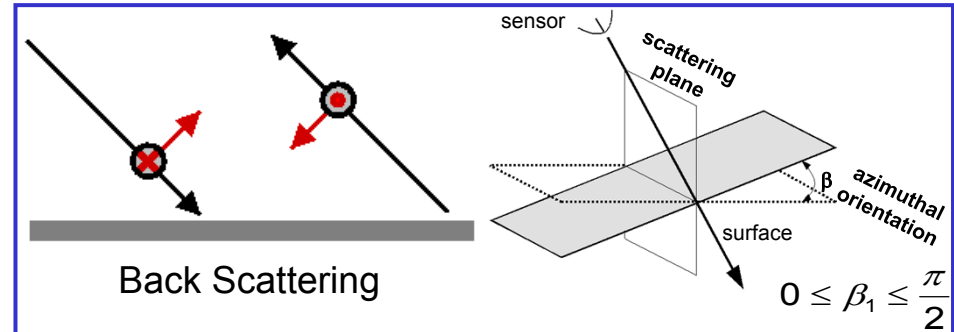
	ks	corr.
Elbe RMS _{error}	0.24	-
Weih RMS _{error}	0.19	-0.7

	ks	corr.
Elbe RMS _{error}	0.21	0.6
Weih RMS _{error}	0.19	-0.6



Surface Parameter @ X-Bragg

Surface scattering model for the estimation of soil moisture content & surface roughness



Bragg Surface

$$[T] = \begin{bmatrix} \langle |R_s + R_p|^2 \rangle & \langle (R_s - R_p)(R_s + R_p)^* \rangle & 0 \\ \langle (R_s + R_p)(R_s - R_p)^* \rangle & \langle |R_s - R_p|^2 \rangle & 0 \\ 0 & 0 & 0 \end{bmatrix}$$

Advantage:

- Simple model with direct relation to soil moisture content

Disadvantage:

- not realistic enough for natural surfaces

extension

X-Bragg Surface

$$[T] = \begin{bmatrix} C_1 & C_2 \operatorname{sinc}(2\beta_1) & 0 \\ C_2 * \operatorname{sinc}(2\beta_1) & C_3(1 + \operatorname{sinc}(4\beta_1)) & 0 \\ 0 & 0 & C_3(1 - \operatorname{sinc}(4\beta_1)) \end{bmatrix}$$

Advantage:

- Integration of a roughness & decorrelation term provides natural surface statistics

Disadvantage:

- very sensitive to vegetation cover

$$R_s = \frac{\cos \theta - \sqrt{\varepsilon_r - \sin^2 \theta}}{\cos \theta + \sqrt{\varepsilon_r - \sin^2 \theta}}$$

$$R_p = \frac{(\varepsilon_r - 1)(\sin^2 \theta - \varepsilon_r(1 + \sin^2 \theta))}{(\varepsilon_r \cos \theta + \sqrt{\varepsilon_r - \sin^2 \theta})^2}$$

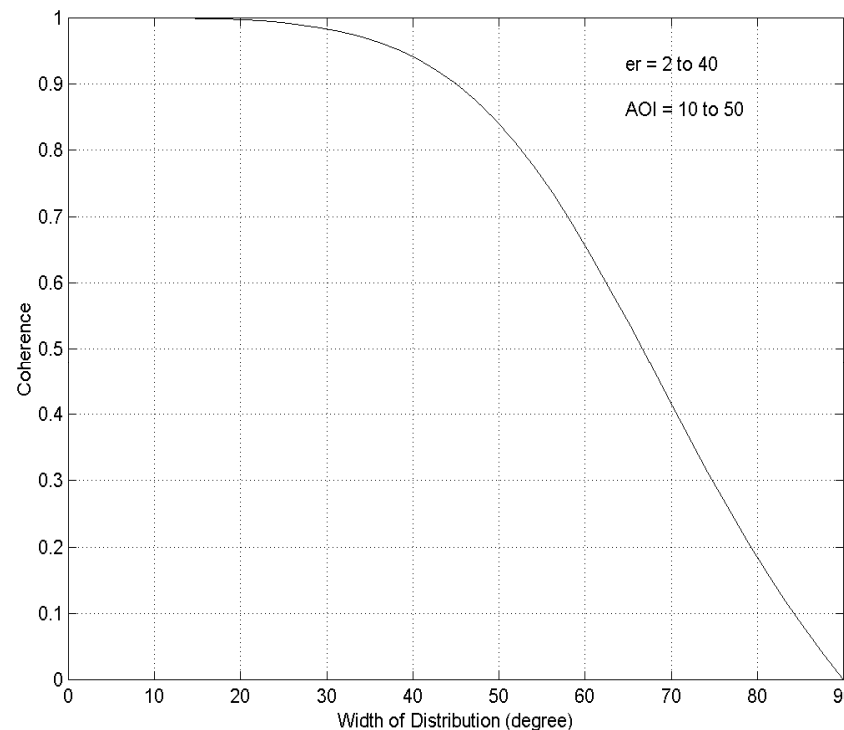
$$C_1 = |R_s + R_p|^2 \quad C_2 = (R_s + R_p)(R_s^* - R_p^*) \quad C_3 = \frac{1}{2}|R_s - R_p|^2$$

I. Hajnsek, E. Pottier, S. Cloude, Surface Parameter Estimation using Polarimetric SAR,
IEEE TGARS, 2003, vol. 41, no. 4, pp. 727-745

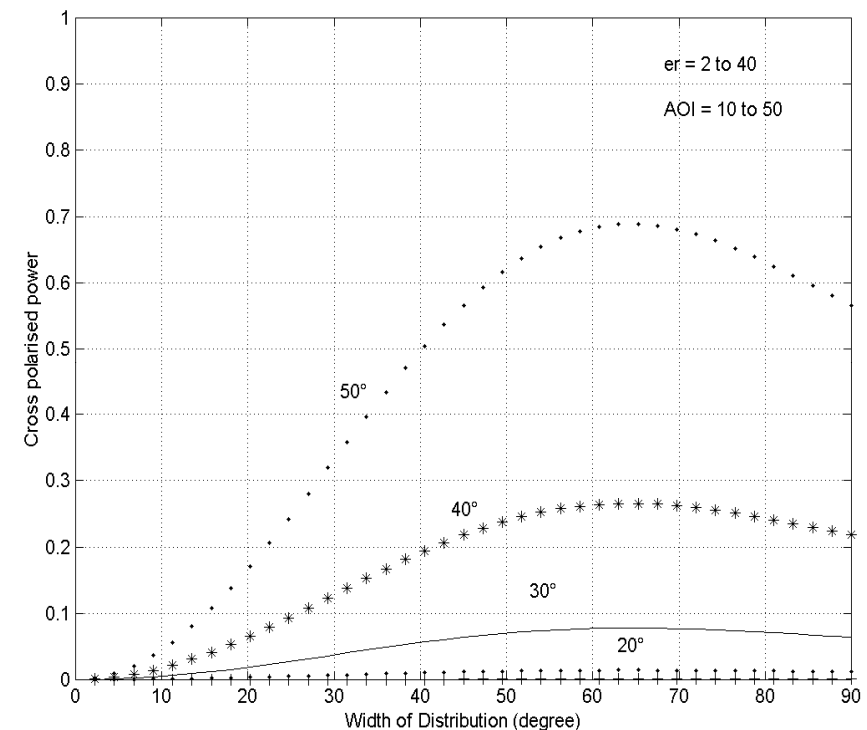


Prediction of the X-Bragg Model I

(HH+VV)(HH-VV) coherence versus b_1
for different local incidence angles

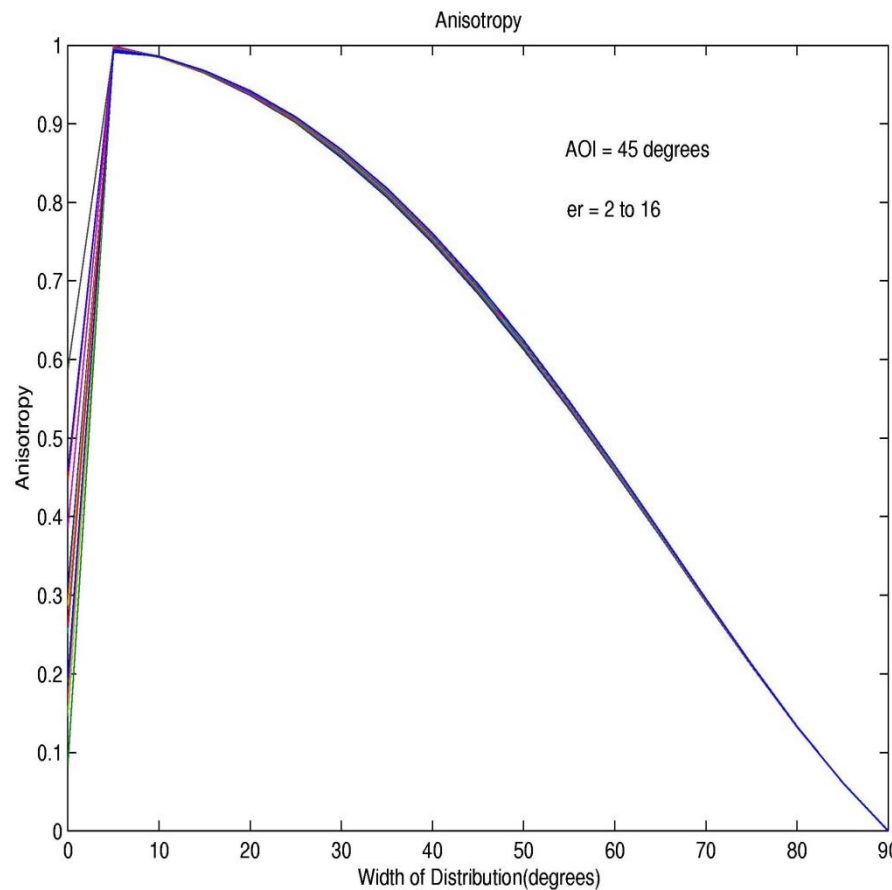


Cross polarised power versus b_1 for
different local incidence angles

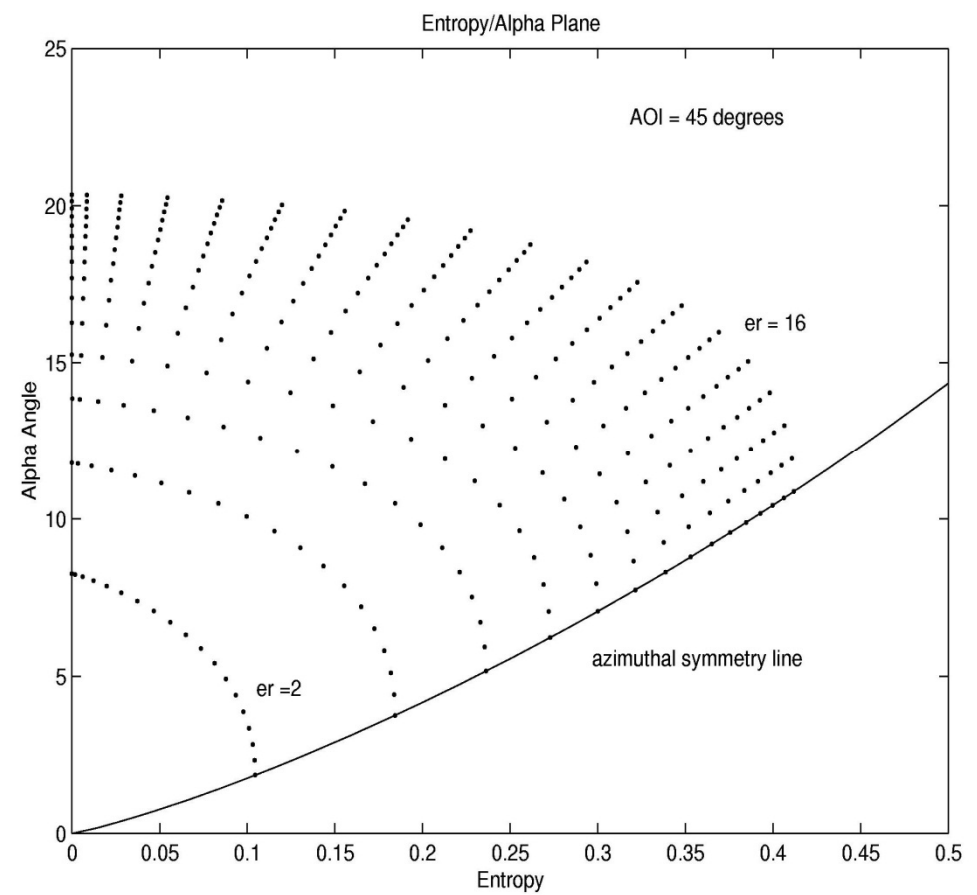


Prediction of the X-Bragg Model II

Variation of Anisotropy
with Roughness (Model Parameter β_1)

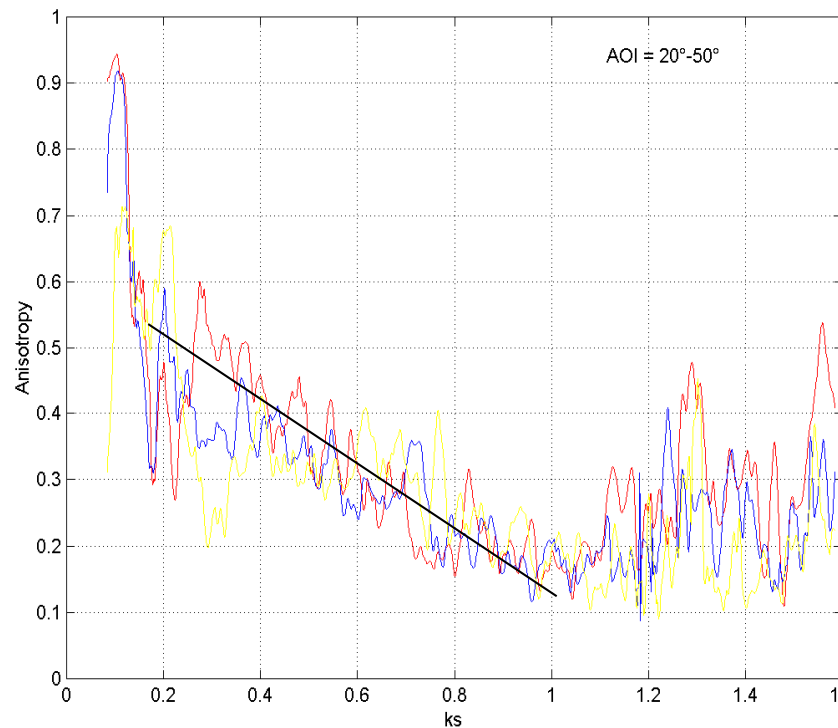


Variation of Entropy/Alpha values with
Dielectric Constant (45 degrees AOI)

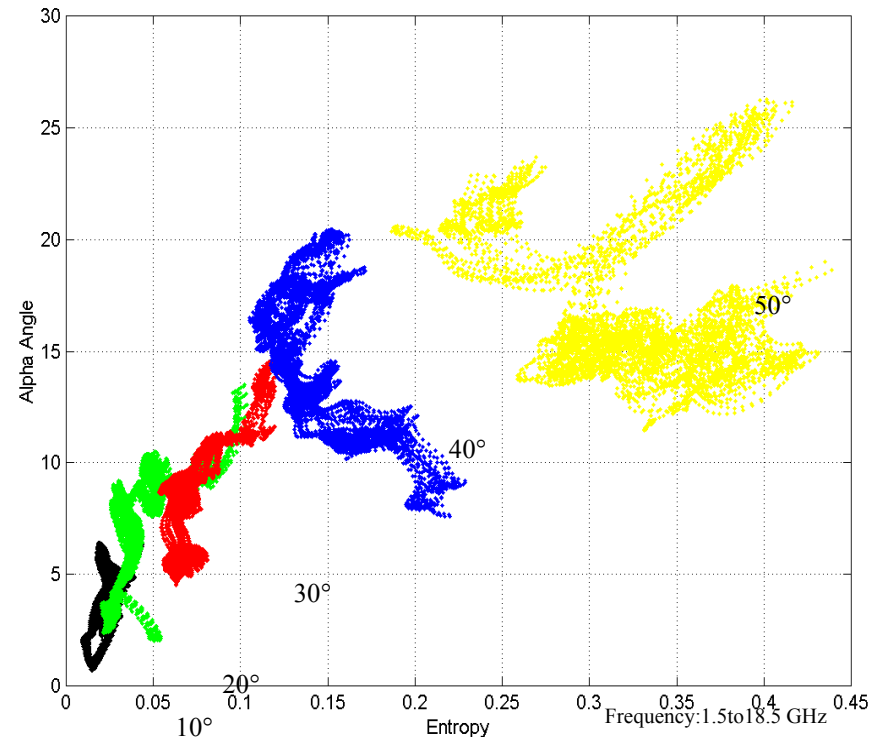


Experimental Data from Anechoic Chamber (JRC - Ispra)

Collected in European Mircowave Signature Laboratory (EMSL)
quad-pol scattering matrix(HH,VV,HV,VH); $s = 0.4$ cm; surface correlation lenght $l = 6$;
dielectric constant $\epsilon' = 8$; frequency range = 1.5-18.5



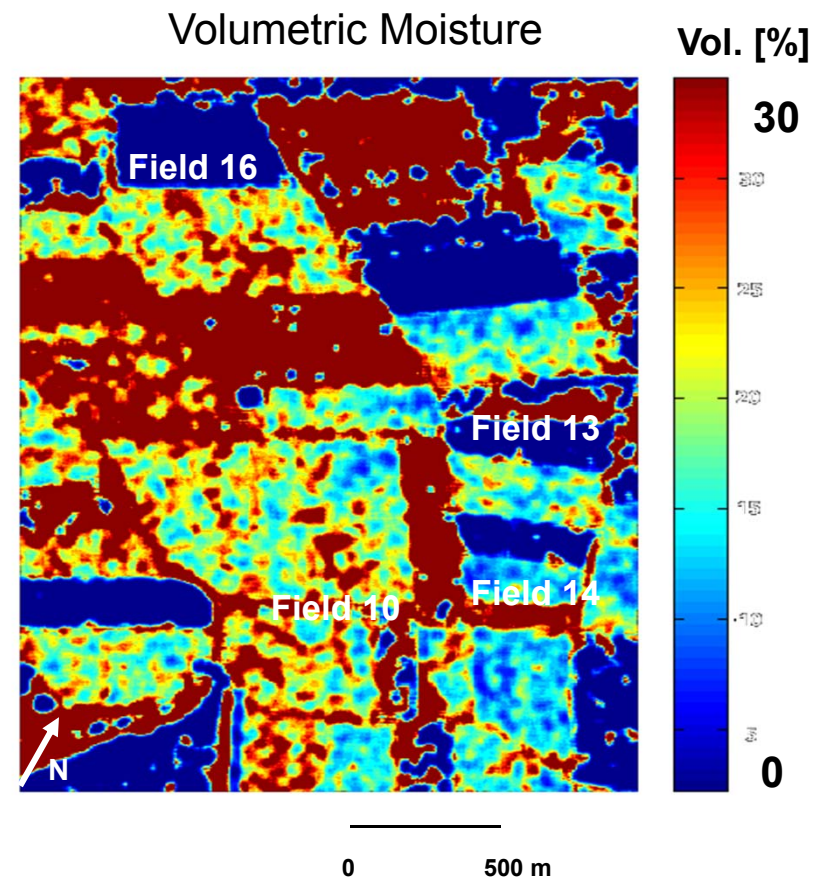
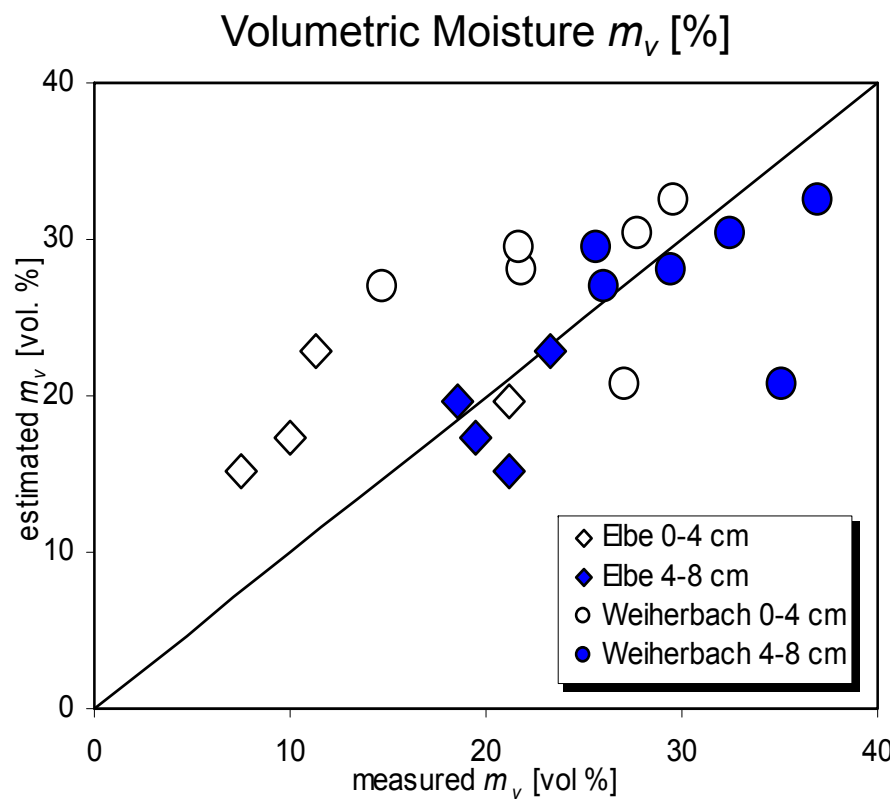
Anisotropy versus frequency plot for
the EMSL data



Entropy/alpha angle plot for the
EMSL data

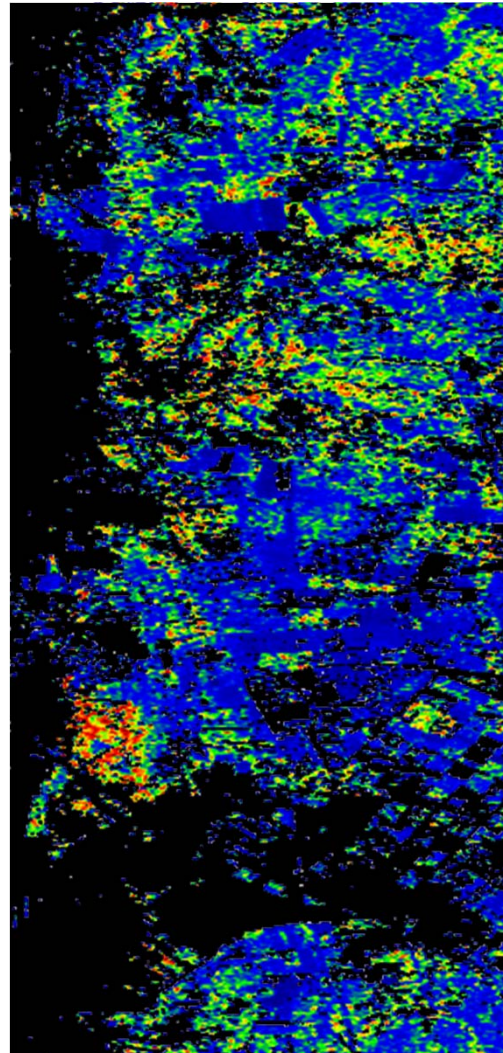
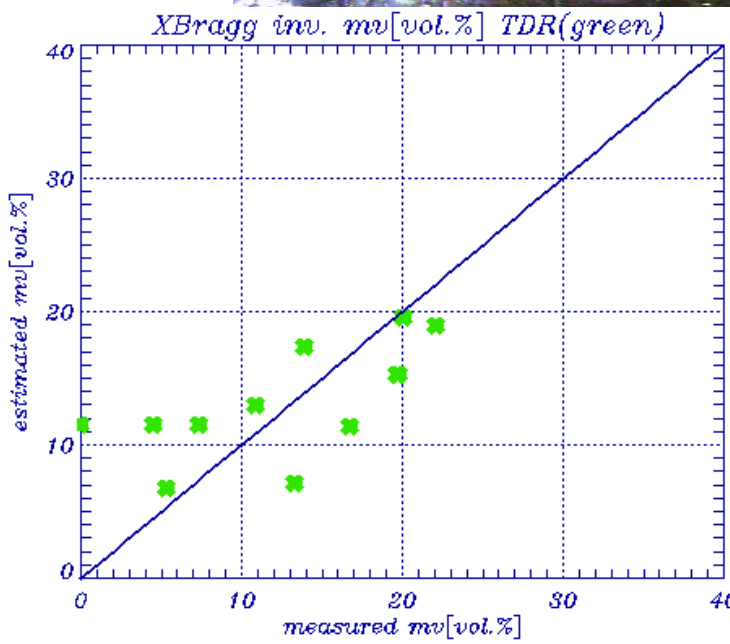
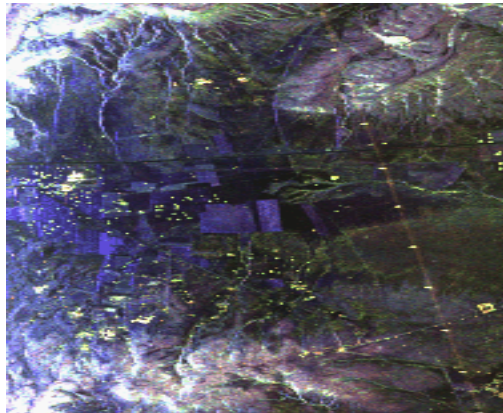


Inversion Results @ X-Bragg – Early Example on ELBE 2000

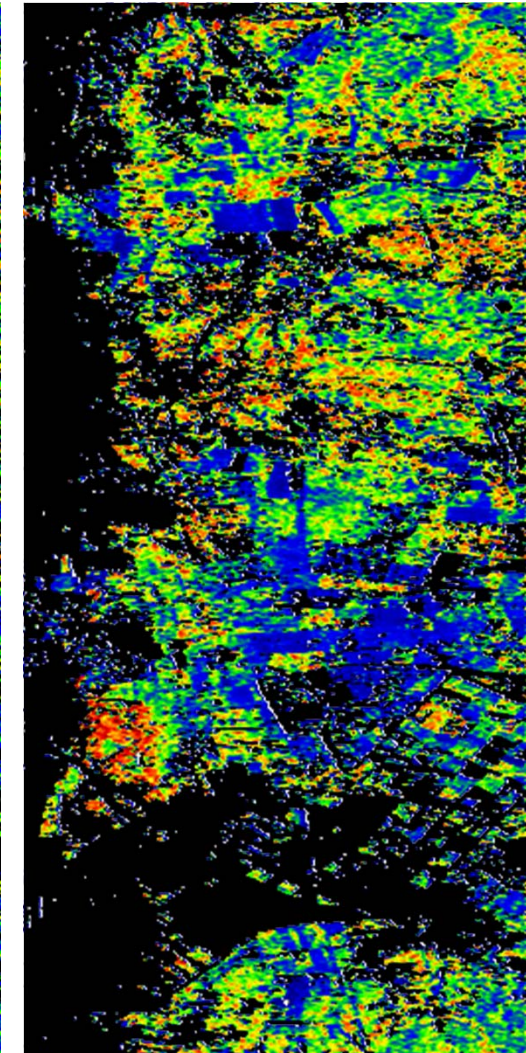


Bare Surfaces: Soil Moisture Estimation @ AQUIFEREX 05

E-SAR / Test Site: Aquiferex, Tunisia



Dielectric Constant



Vol. Soil Moisture



L-band / Pauli RGB

Soil Moisture Estimation

- Surface Characterisation
- mv estimation over bare surface
- **mv estimation under the vegetation**
 - **3 component model decomp.**
 - **improvement of the 3 component model decomp.**
 - **multi-angle approach combined with 3 comp. model decomp.**
 - **hybrid decomposition**



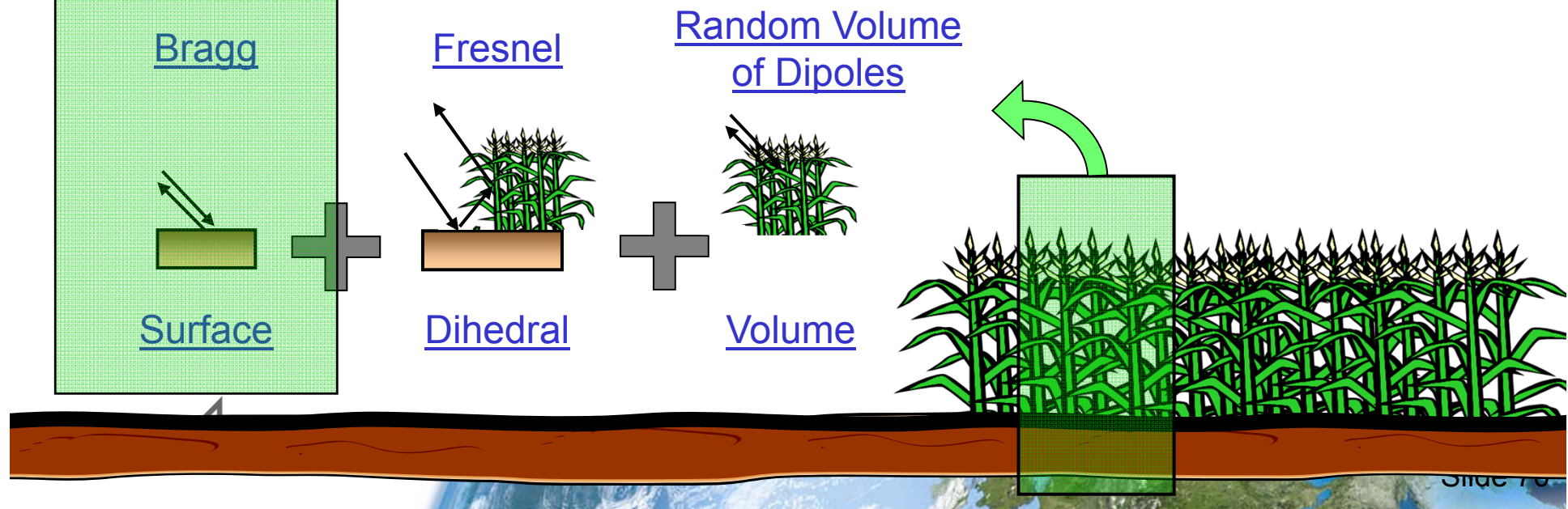
3 Component Freeman Decomposition

$$[T_{\text{Bragg}}] = f_S \begin{bmatrix} 1 & \beta^* & 0 \\ \beta & |\beta|^2 & 0 \\ 0 & 0 & 0 \end{bmatrix} \quad \beta = \frac{R_H - R_V}{R_H + R_V}$$

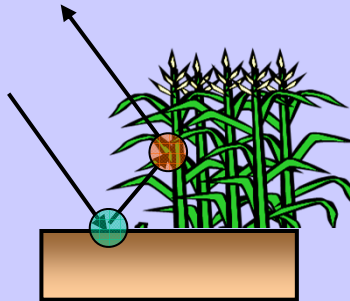
$$R_H = \frac{\cos\theta - \sqrt{\epsilon_r - \sin^2\theta}}{\cos\theta + \sqrt{\epsilon_r - \sin^2\theta}}$$

$$R_V = \frac{(\epsilon_r - 1)(\sin^2\theta - \epsilon_r(1 + \sin^2\theta))}{(\epsilon_r \cos\theta + \sqrt{\epsilon_r - \sin^2\theta})^2}$$

$$f_S \begin{bmatrix} 1 & \beta^* & 0 \\ \beta & |\beta|^2 & 0 \\ 0 & 0 & 0 \end{bmatrix} + f_D \begin{bmatrix} |\alpha|^2 & \alpha & 0 \\ \alpha^* & 1 & 0 \\ 0 & 0 & 0 \end{bmatrix} + \frac{f_V}{4} \begin{bmatrix} 2 & 0 & 0 \\ 0 & 1 & 0 \\ 0 & 0 & 1 \end{bmatrix} = \begin{bmatrix} T_{11} & T_{12} & 0 \\ T_{12}^* & T_{22} & 0 \\ 0 & 0 & T_{33} \end{bmatrix}$$



$$[S] = \begin{bmatrix} 1 & 0 \\ 0 & -1 \end{bmatrix} \begin{bmatrix} R_{SS} & 0 \\ 0 & R_{PS} \end{bmatrix} \begin{bmatrix} R_{ST} & 0 \\ 0 & R_{PT} \end{bmatrix} = \begin{bmatrix} R_{SS}R_{ST} & 0 \\ 0 & -R_{PS}R_{PT}e^i \end{bmatrix}$$

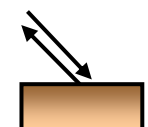


$$R_{S(S/T)} = \frac{\cos\theta - \sqrt{\epsilon_{S/T} - \sin^2\theta}}{\cos\theta + \sqrt{\epsilon_{S/T} - \sin^2\theta}}$$

$$R_{P(S/T)} = \frac{\epsilon_{S/T} \cos\theta - \sqrt{\epsilon_{S/T} - \sin^2\theta}}{\epsilon_{S/T} \cos\theta + \sqrt{\epsilon_{S/T} - \sin^2\theta}}$$

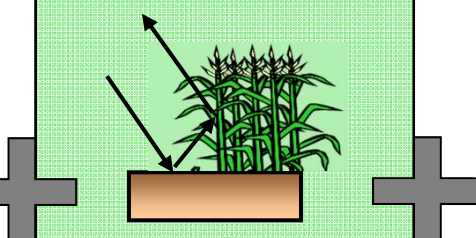
$$f_S \begin{bmatrix} 1 & \beta^* & 0 \\ \beta & |\beta|^2 & 0 \\ 0 & 0 & 0 \end{bmatrix} + f_D \begin{bmatrix} |\alpha|^2 & \alpha & 0 \\ \alpha^* & 1 & 0 \\ 0 & 0 & 0 \end{bmatrix} + \frac{f_V}{4} \begin{bmatrix} 2 & 0 & 0 \\ 0 & 1 & 0 \\ 0 & 0 & 1 \end{bmatrix} = \begin{bmatrix} T_{11} & T_{12} & 0 \\ T_{12}^* & T_{22} & 0 \\ 0 & 0 & T_{33} \end{bmatrix}$$

Bragg



Surface

Fresnel

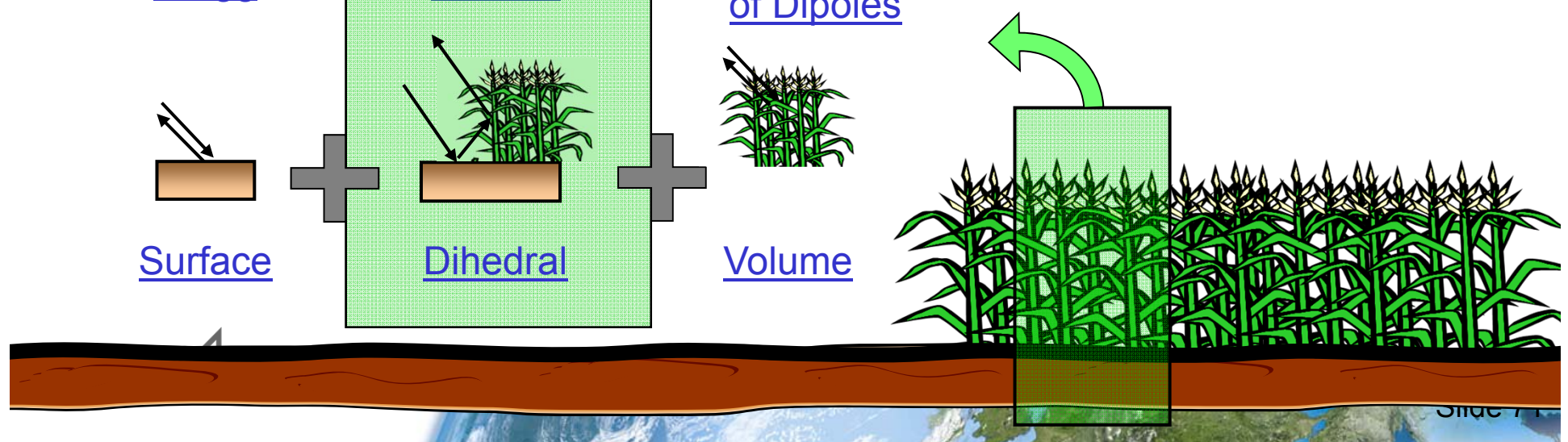


Dihedral

Random Volume
of Dipoles

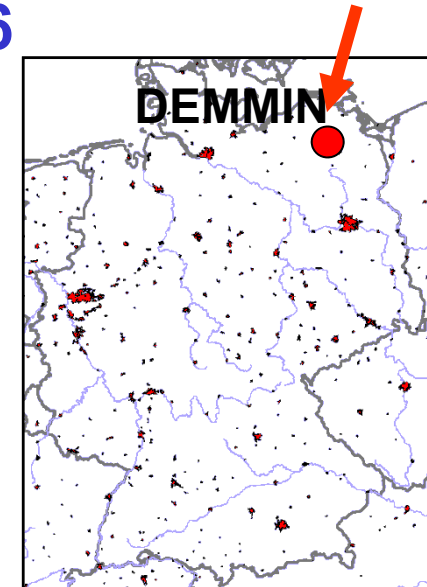


Volume

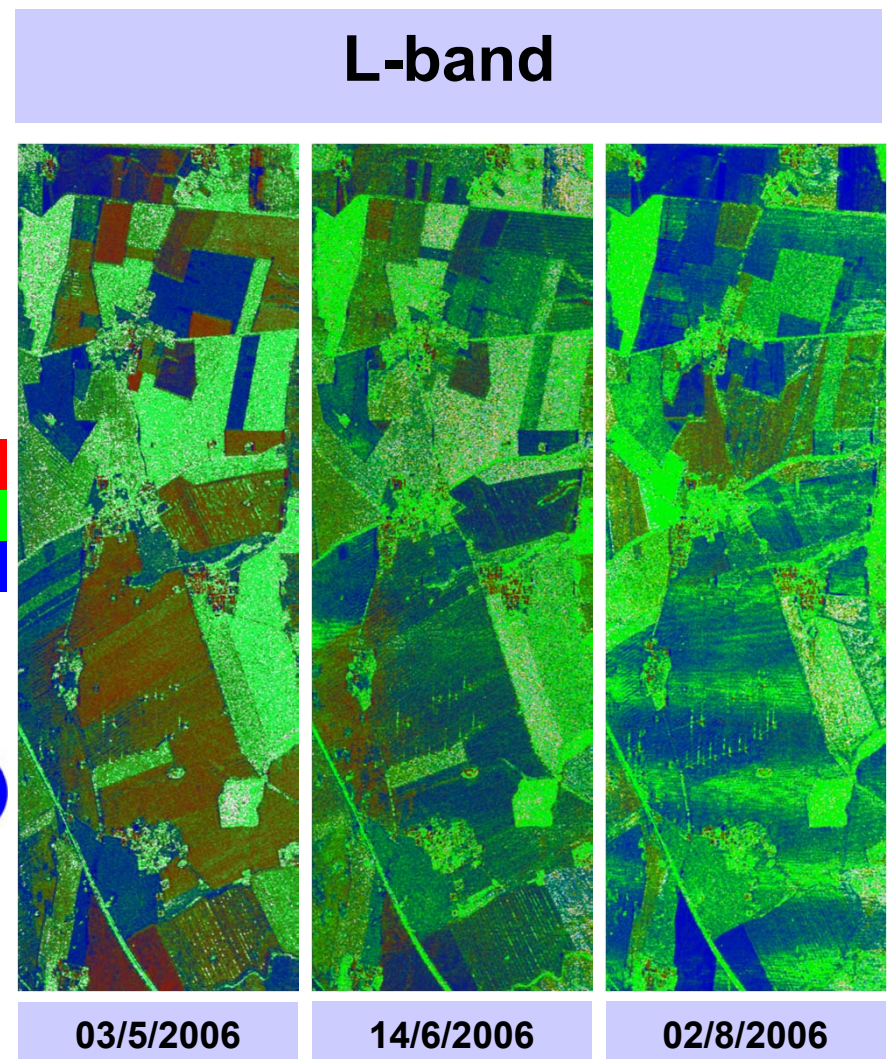
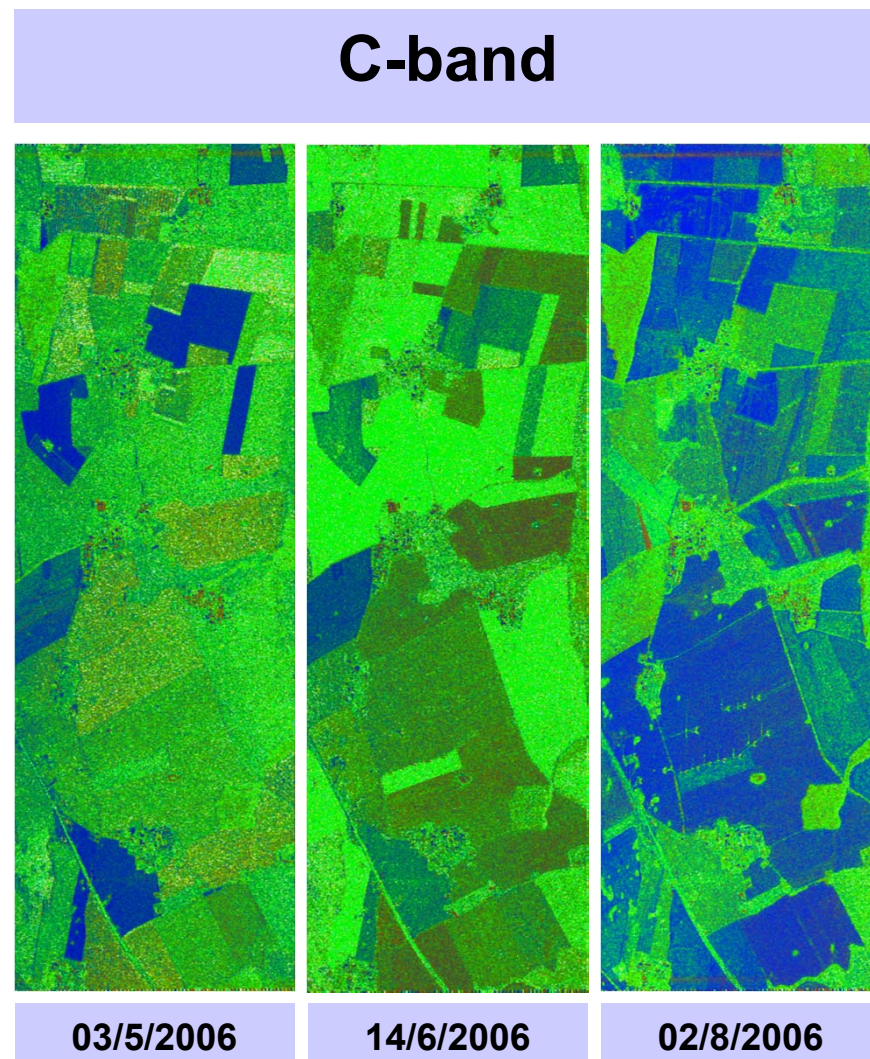


AGRISAR Campaign in Northern Germany 2006

1. Agricultural data base over a whole vegetation growth period - April - August 2006
2. 16 data acquisitions (DLR's E-SAR) & ground measurements
3. Support by ESA for the space segment - Sentinel Program



Freeman-Durden 3-Component Decomposition (AGRISAR 2006)

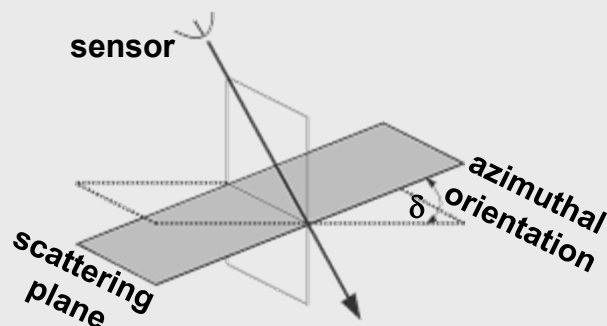


3 Component Decomposition and Modifications

	Surface	Dihedral	Volume
Decision rule	$\text{Re}\langle S_{HH} S_{VV}^* \rangle > 0$ $\alpha = 0$	or	$\text{Re}\langle S_{HH} S_{VV}^* \rangle < 0$ $\beta = 0$

Surface modification (X-Bragg) (ε_s , θ , δ):

$$[T_{XB}] = f_s \begin{bmatrix} 1 & \beta^* \text{sinc}(2\delta) & 0 \\ \beta \text{sinc}(2\delta) & \frac{1}{2} |\beta|^2 (1 + \text{sinc}(4\delta)) & 0 \\ 0 & 0 & \frac{1}{2} |\beta|^2 (1 - \text{sinc}(4\delta)) \end{bmatrix}$$



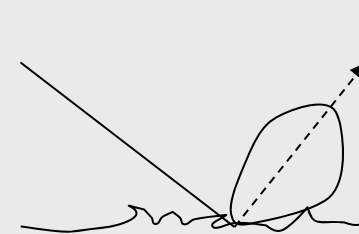
- Incorporation of a roughness and HV-decorrelation term (δ)

[Hajnsek et al., 2001]

Dihedral modification (modified Fresnel coefficients) (ε_s , ε_t , θ , ϕ , L_S):

$$[T_{moD}] = f_D \cdot |L_S|^2 \cdot \begin{bmatrix} |\alpha|^2 & \alpha & 0 \\ \alpha^* & 1 & 0 \\ 0 & 0 & 0 \end{bmatrix} \quad 0 < L_S \leq 1$$

$$L_S = \exp(-2 \cdot (ks)^2 \cdot \cos(\theta)^2) \quad ks = 1 - A$$



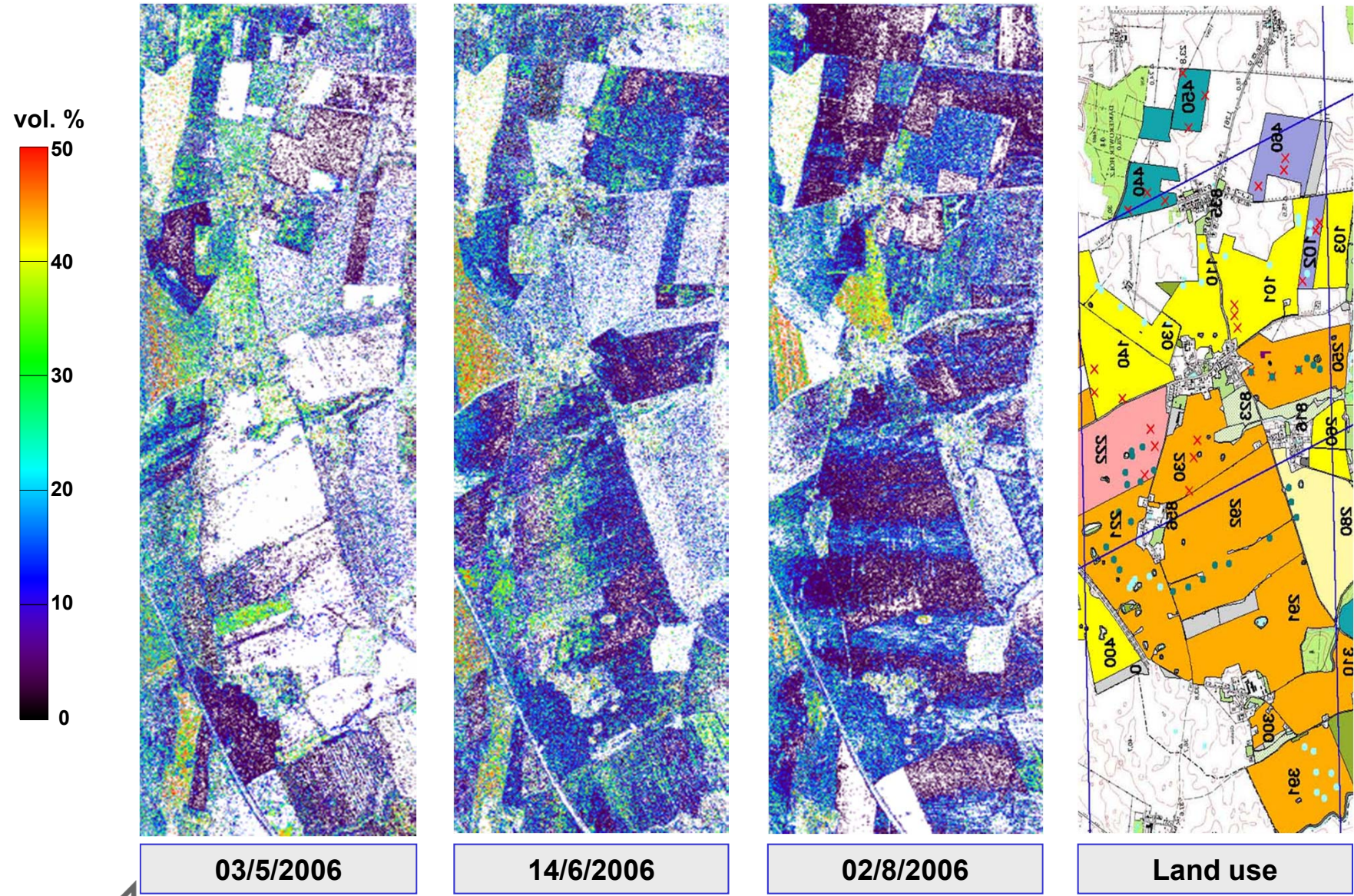
- Incorporation of a surface scattering loss L_S

[Lee et al., 2005]

[Freeman & Durden, 1998, Yamaguchi et al., 2006]

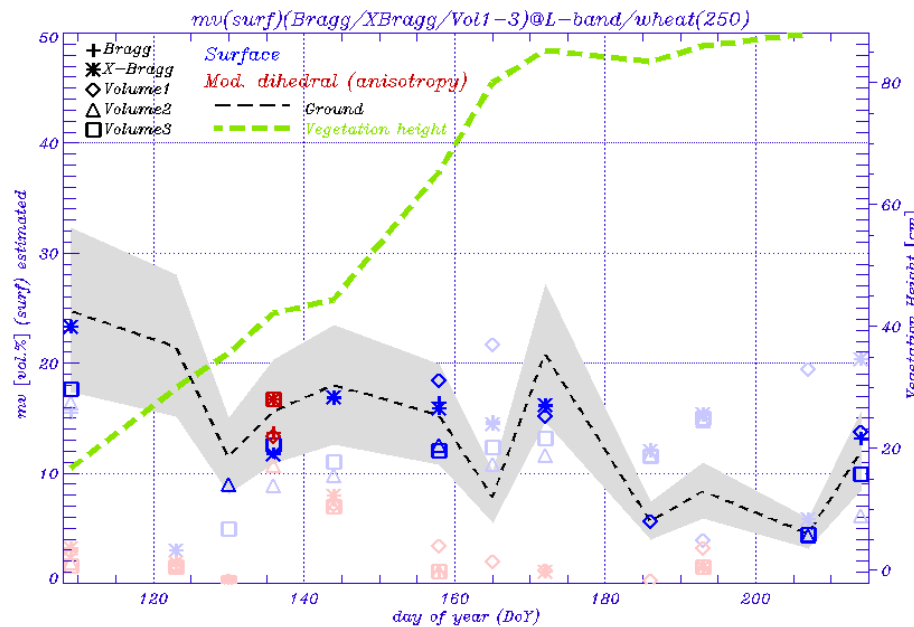


Inverted Soil Moisture @ L-band Volume 2 (surface) and modified Dihedral (dihedral)

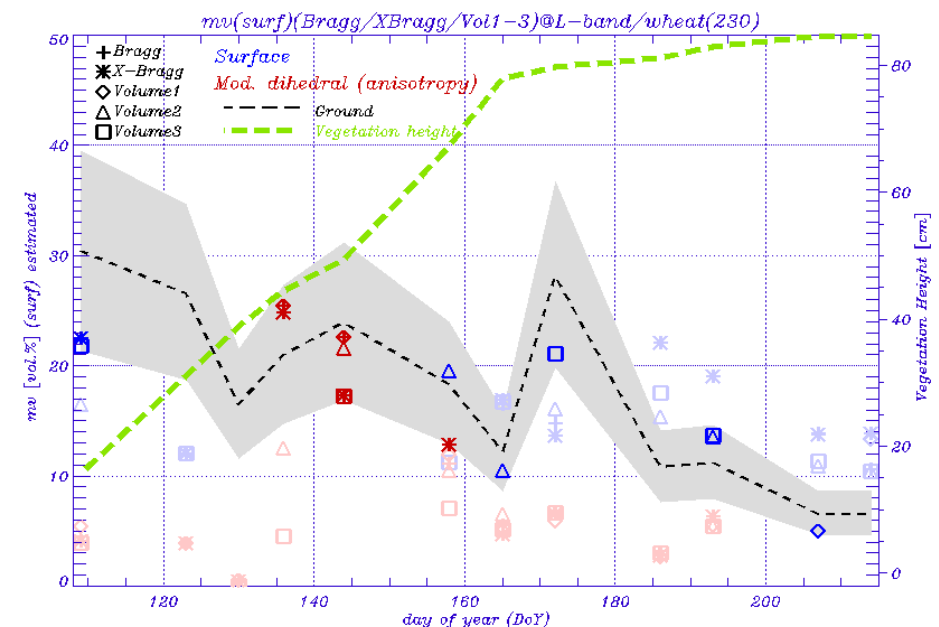


Time Series of Inverted Soil Moisture @ L-band

Wheat field (No. 250)



Wheat field (No. 230)



+ Bragg * X-Bragg ◆ Volume 1 △ Volume 2 □ Volume 3

Surface

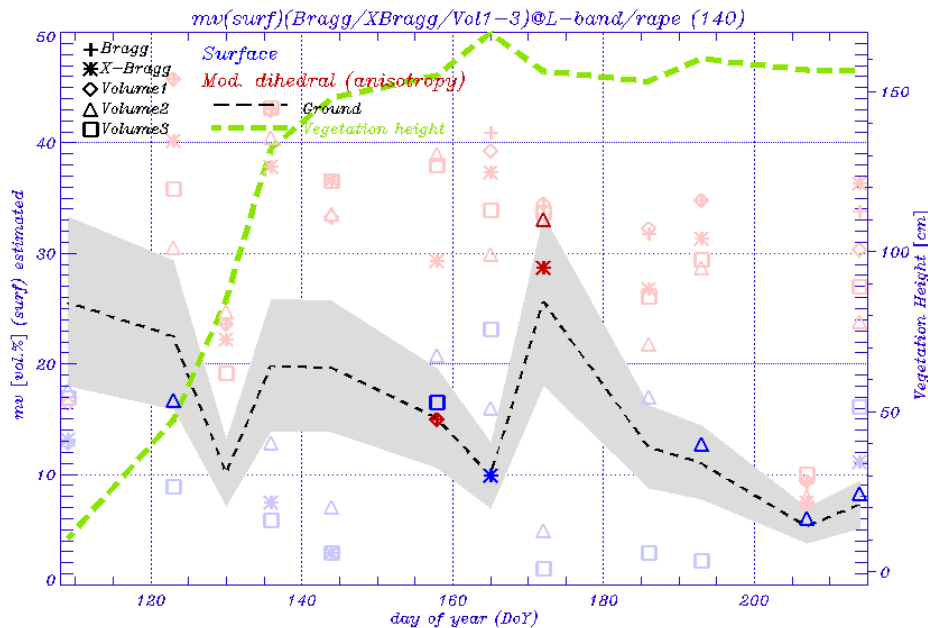
Dihedral

--- ±30% Intervall

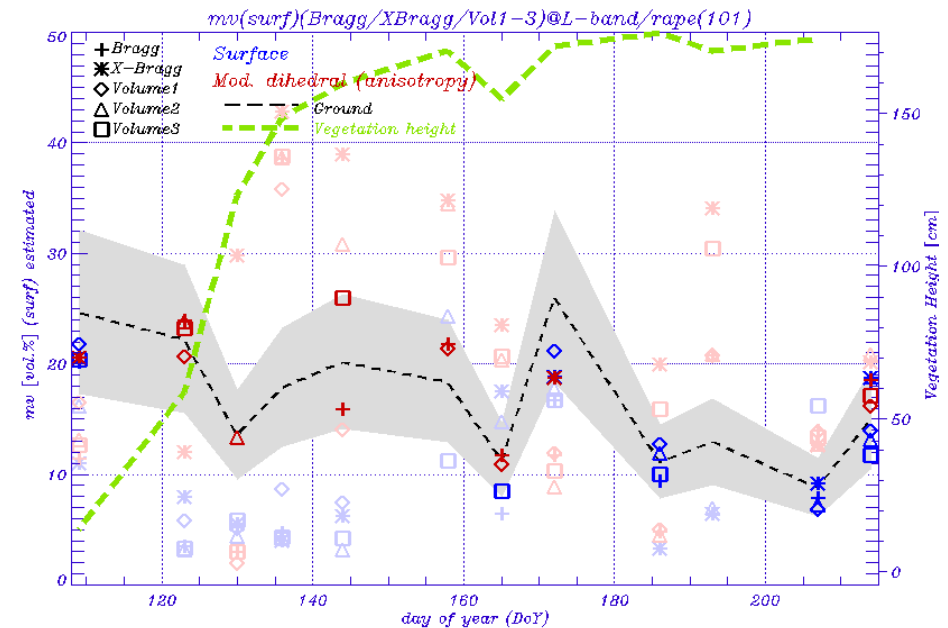


Time Series of Inverted Soil Moisture @ L-band

Rape field (No. 140)



Rape field (No. 101)



+ Bragg	* X-Bragg	◊ Volume 1	△ Volume 2	□ Volume 3
				
Surface	Dihedral	--- ±30% Intervall		

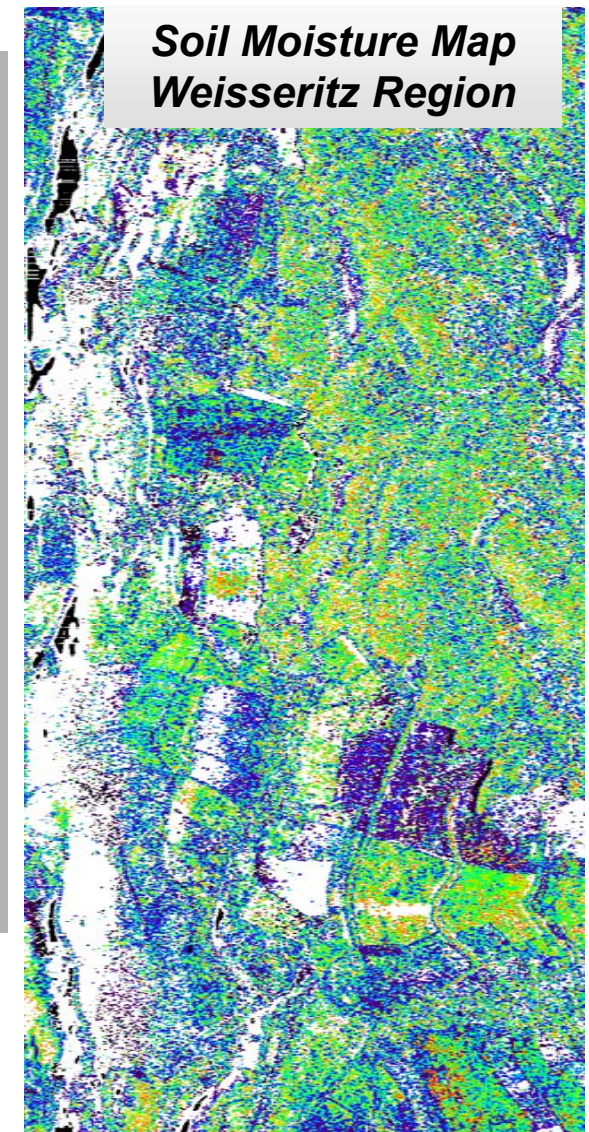
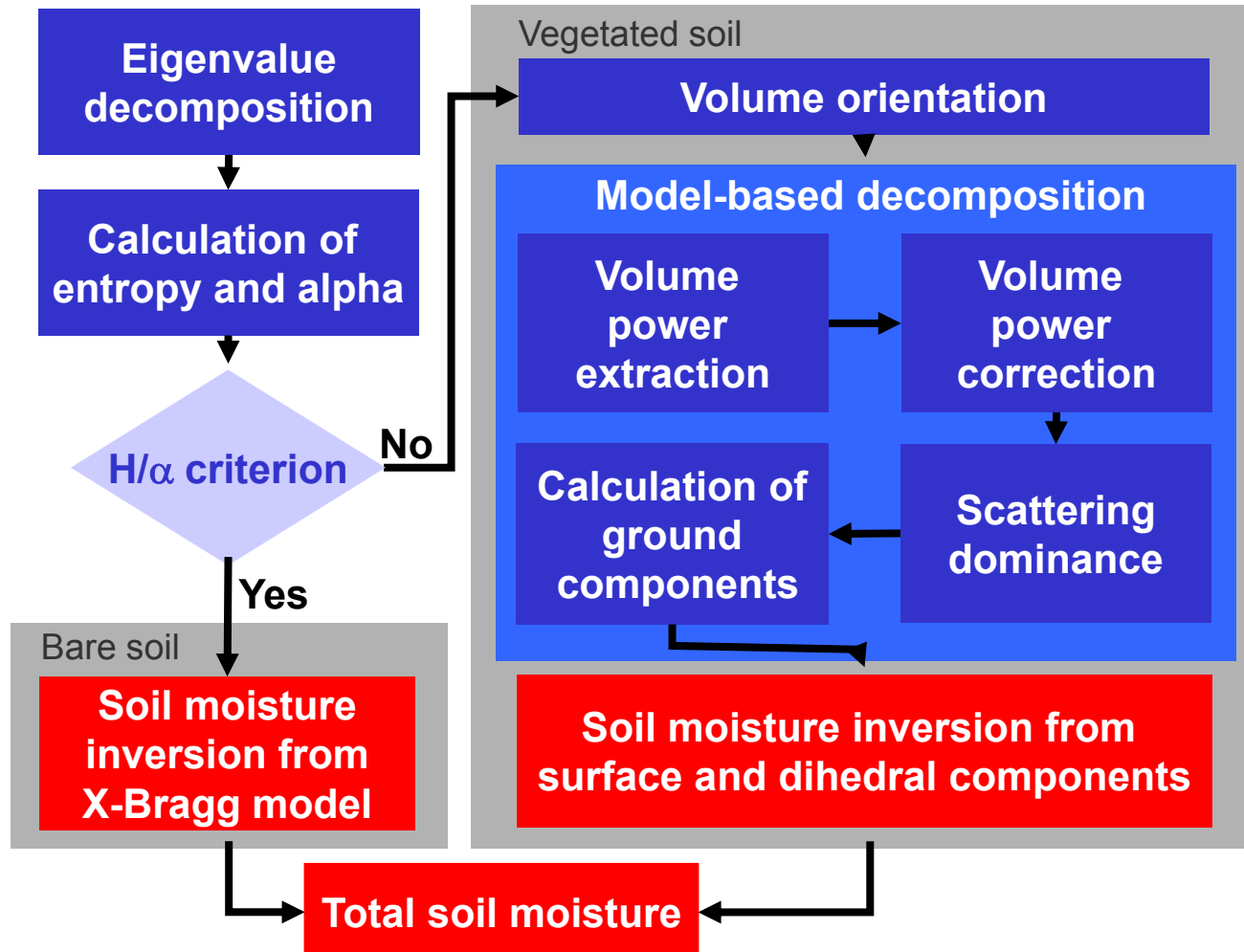


Soil Moisture Estimation

- Surface Characterisation
- mv estimation over bare surface
- **mv estimation under the vegetation**
 - 3 component model decomp.
 - **improvement of the 3 component model decomp.**
 - multi-angle approach combined with 3 comp. model decomp.
 - hybrid decomposition

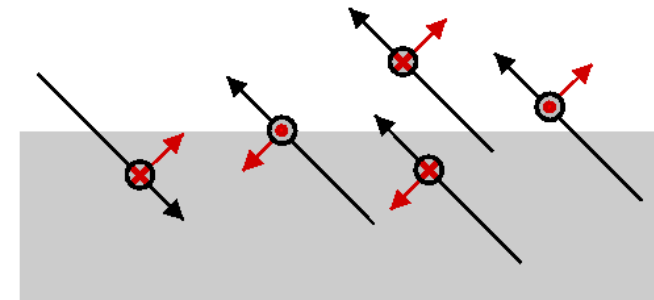


Polarimetric Decomposition Techniques & Inversion Scheme



Modeling of Volume Orientation

Volume modelling of a cloud of uniformly **shaped** (ρ) particles with an **orientation** (τ) in azimuthal direction



Selection of volume orientation by **polarisation power ratio** P_r :

$$P_r = 10 \cdot \log \frac{\langle |S_{vv}|^2 \rangle}{\langle |S_{HH}|^2 \rangle}$$

General Case	Vertical dipoles [$P_r < -2\text{dB}$]	Random dipoles [-2dB < $P_r < 2\text{dB}$]	Horizontal dipoles [$P_r > 2\text{dB}$]
	$pdf(\tau) = \frac{1}{2} \cdot \sin(\tau)$ $0 < \tau \leq \pi$	$pdf(\tau) = \frac{1}{2\pi}$ $0 < \tau \leq 2\pi$	$pdf(\tau) = \frac{1}{2} \cdot \cos(\tau)$ $-\pi/2 < \tau \leq \pi/2$
$[T_v] = f_v \begin{bmatrix} C1 & C4 & 0 \\ C4 & C2 & 0 \\ 0 & 0 & C3 \end{bmatrix}$	$[T_v] = \frac{f_v}{30} \begin{bmatrix} 15 & 5 & 0 \\ 5 & 7 & 0 \\ 0 & 0 & 8 \end{bmatrix}$	$[T_v] = \frac{f_v}{4} \begin{bmatrix} 2 & 0 & 0 \\ 0 & 1 & 0 \\ 0 & 0 & 1 \end{bmatrix}$	$[T_v] = \frac{f_v}{30} \begin{bmatrix} 15 & -5 & 0 \\ -5 & 7 & 0 \\ 0 & 0 & 8 \end{bmatrix}$



[Yamaguchi et al., 2005]

Slide 83

Correction of Volume Intensity f_v with Eigen-based analysis

$$\begin{bmatrix} T_{11} & T_{12} & 0 \\ T_{12}^* & T_{22} & 0 \\ 0 & 0 & T_{33} \end{bmatrix} - f_v \cdot \begin{bmatrix} C_1 & C_4 & 0 \\ C_4 & C_2 & 0 \\ 0 & 0 & C_3 \end{bmatrix} = \underbrace{\begin{bmatrix} \text{Ground} \\ [T_{\text{Surface}}] + [T_{\text{Dihedral}}] \end{bmatrix}}_{\downarrow}$$

Eigenanalysis of Ground Components

Set Eigenvalues to zero (lower calculus limit)

Solutions for f_v :

$$f_{v_1} = 4T_{33}$$

$$f_{v_{2,3}} = T_{11} + 2T_{22}$$

$$\pm \sqrt{T_{11}^2 + 8T_{12} \cdot T_{12}^* - 4T_{11} \cdot T_{22} + 4T_{22}^2}$$

Solution

Negative Powers

=

Too Strong Volume Subtraction!

Find Minimum

Decomposition with Corrected Volume Intensity
 f_{vcorr}

[van Zyl et al., 2008]



OPAQUE – Campaign

May 2007

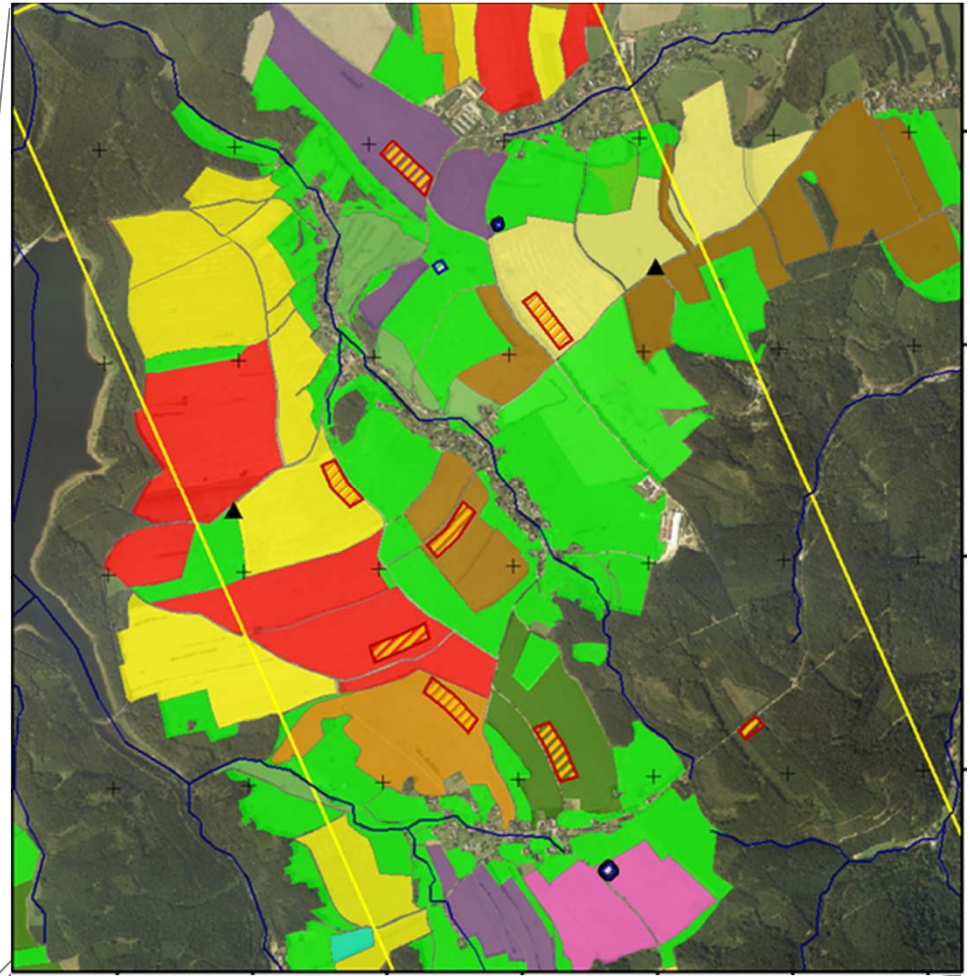
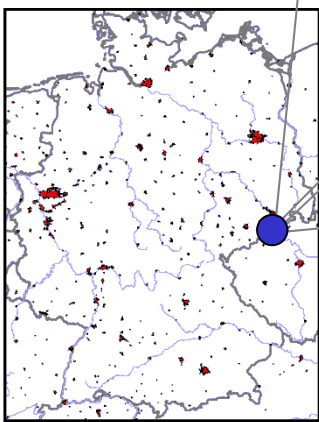
1. Soil moisture estimation under different land cover with measurement approaches at different scales

2 Radar data acquisition flights

(single pol X-, dual-pol C- and quad-pol L- and P-band)

Ground measurements (soil moisture, soil roughness, biomass,...)

2. Goal: Support flood forecasting by identification of critical catchment states

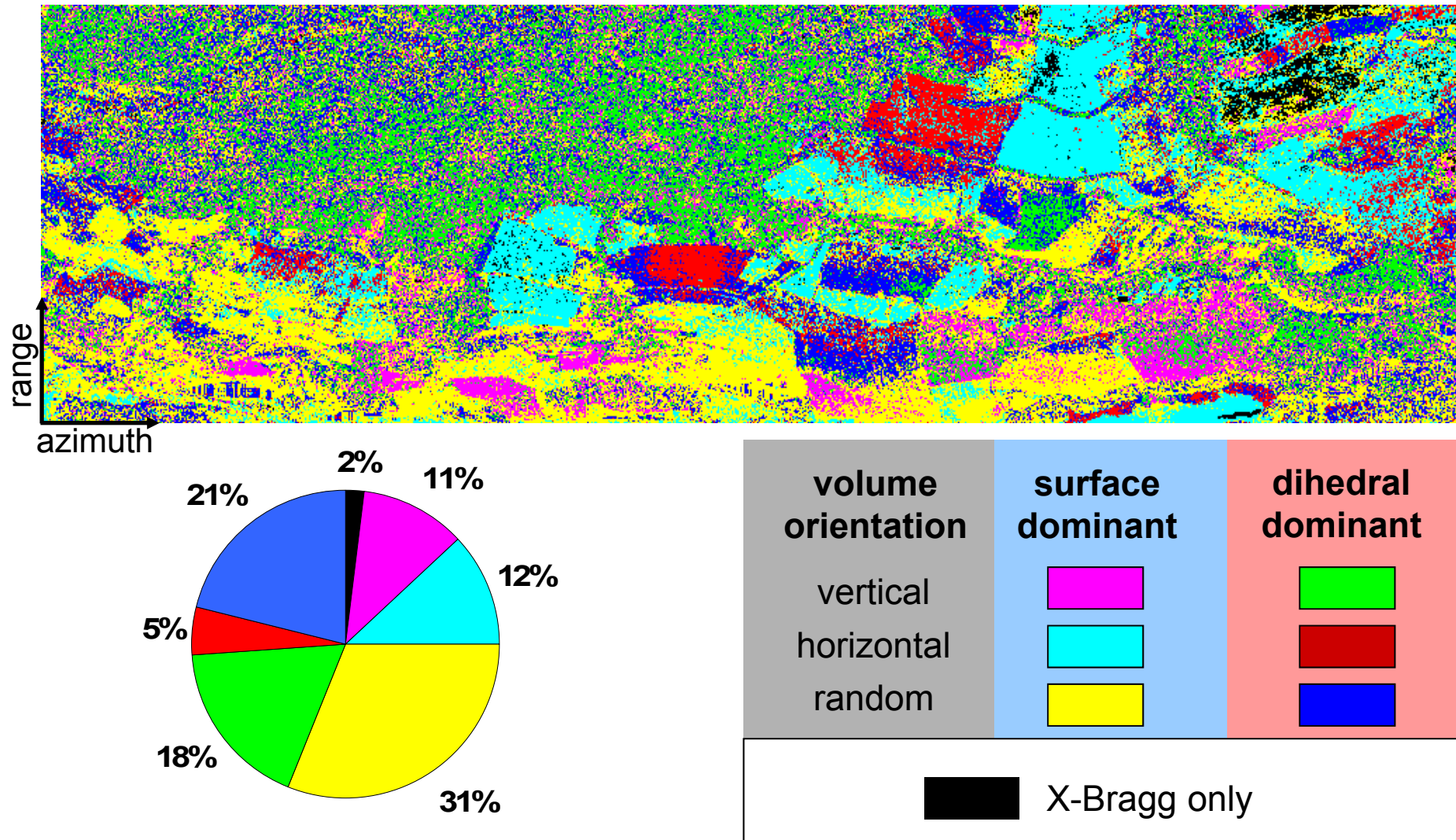


▲ Corner-reflector
— Weißenitz
— Flight strip
■ Test site

■ Winter triticale
■ Winter wheat
■ Summer barley
■ Winter barley
■ Grass land
■ Winter rape
■ Summer corn
■ Bare soil

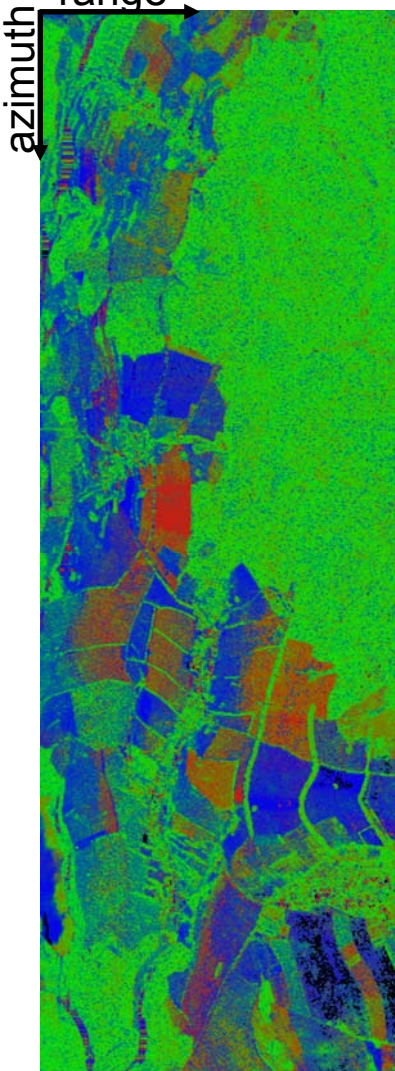


Volume Orientation and Scattering Dominance @ L-band

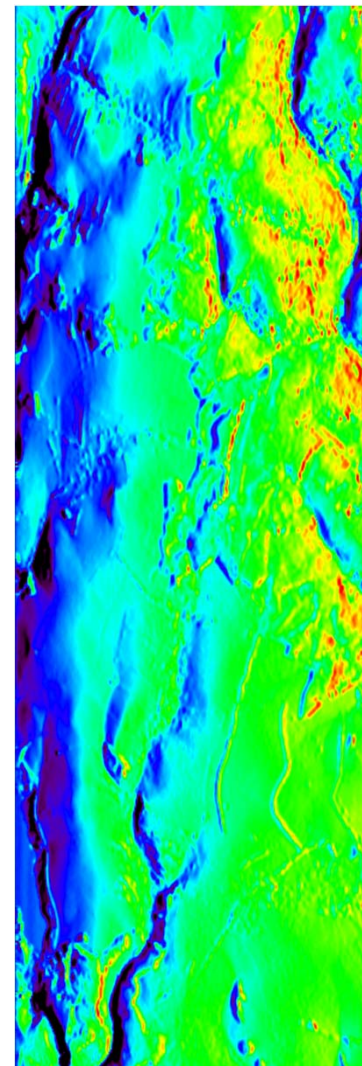
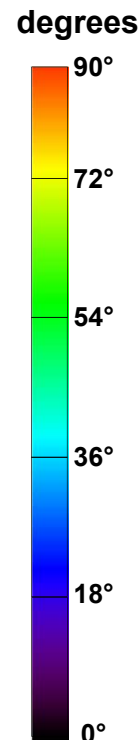


Model-based Decomposition @ L-band

range
azimuth

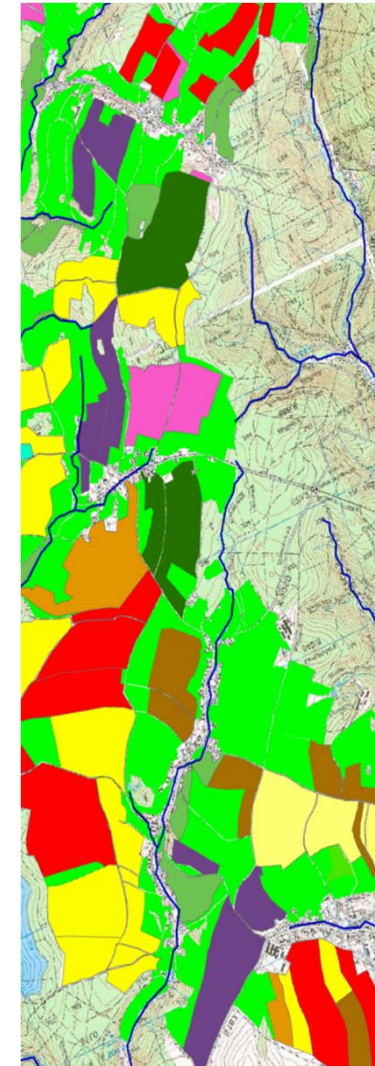


L-Band



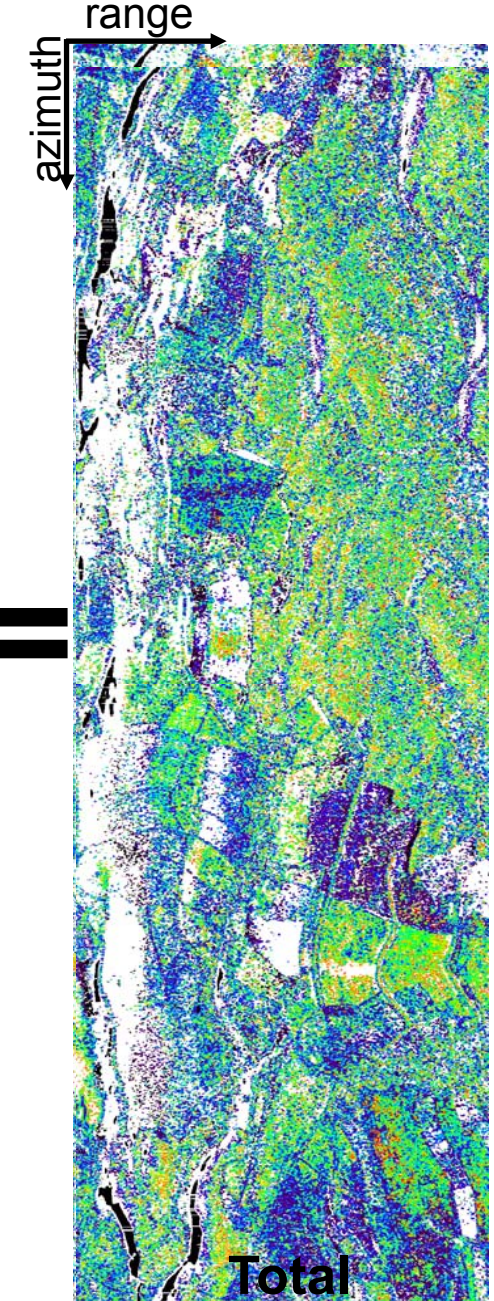
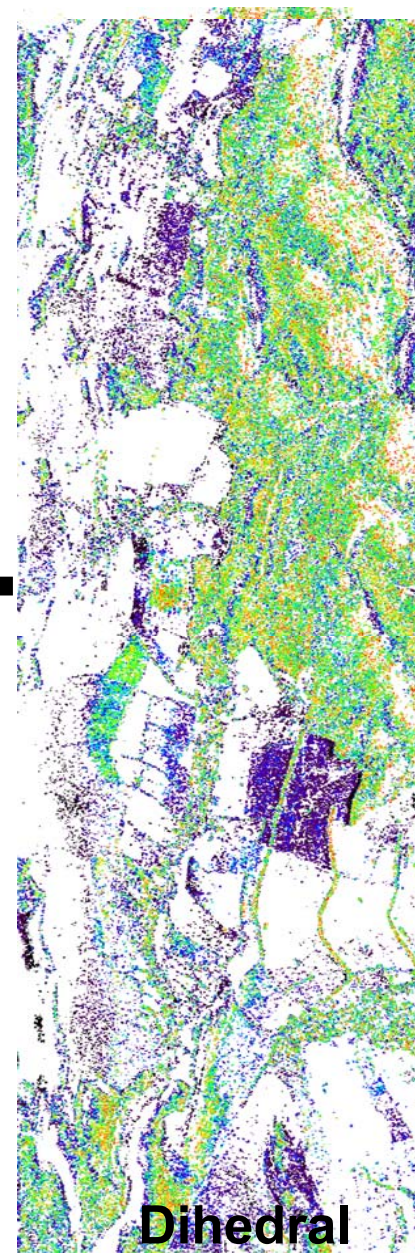
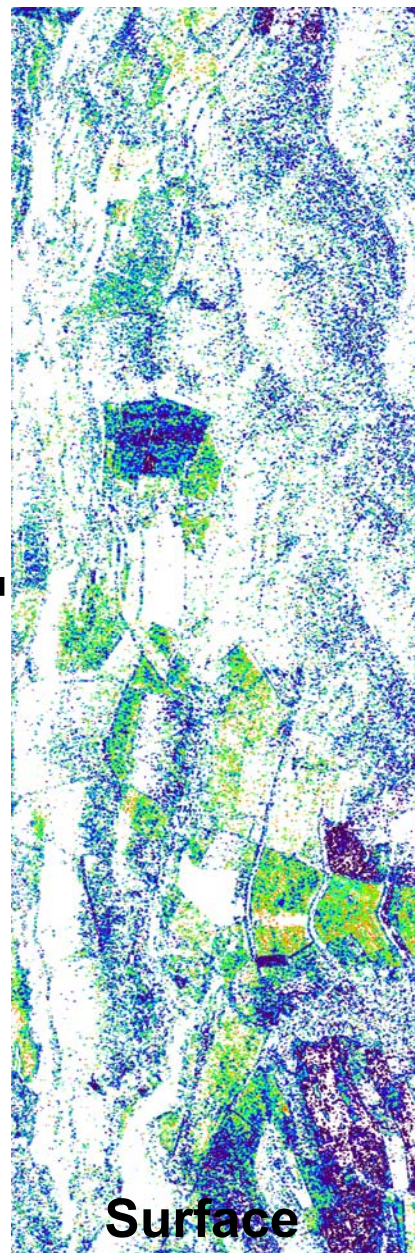
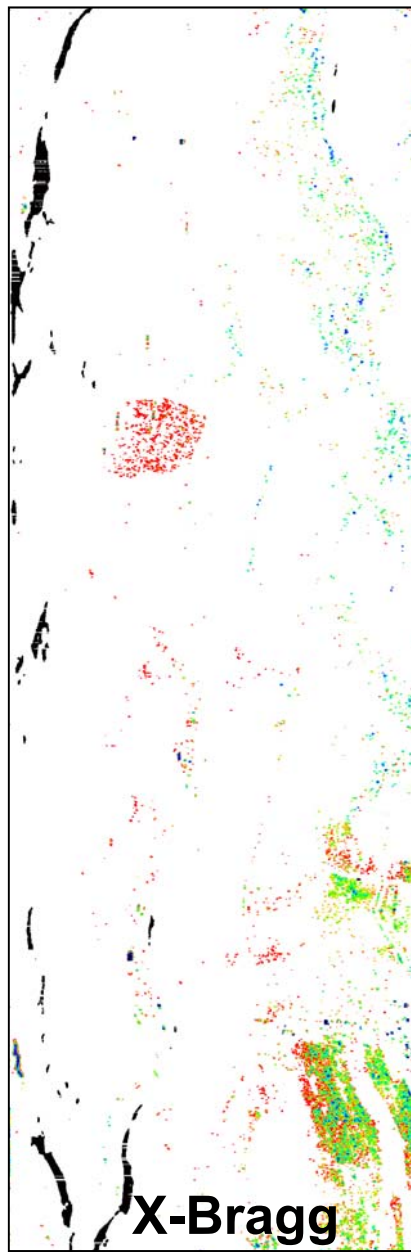
Local incidence

- Winter triticale
- Winter wheat
- Summer barley
- Winter barley
- Grass land
- Winter rape
- Summer corn
- Bare soil



Land use

Inverted Soil Moisture @ L-band



Validation with TDR Measurements on Winter Wheat

Vegetation height:

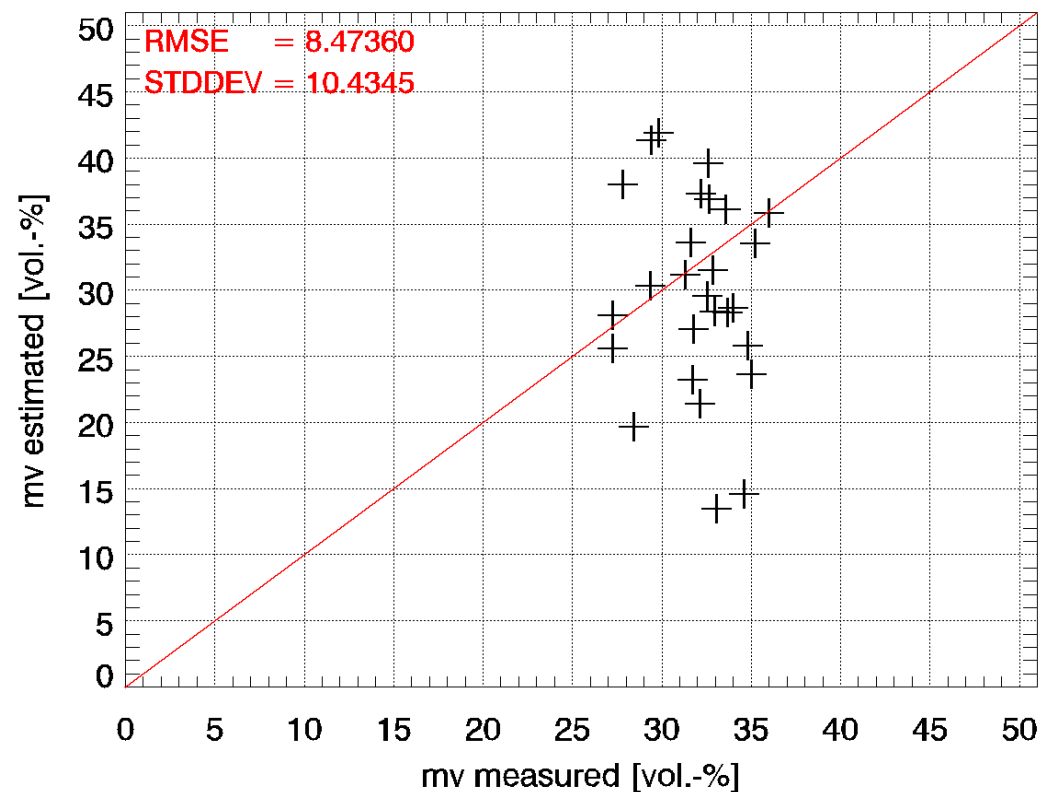
55cm

Row distance:

10cm

Wet biomass:

2,85kg/m²



Validation with TDR Measurements on Summer Barley

Vegetation height:

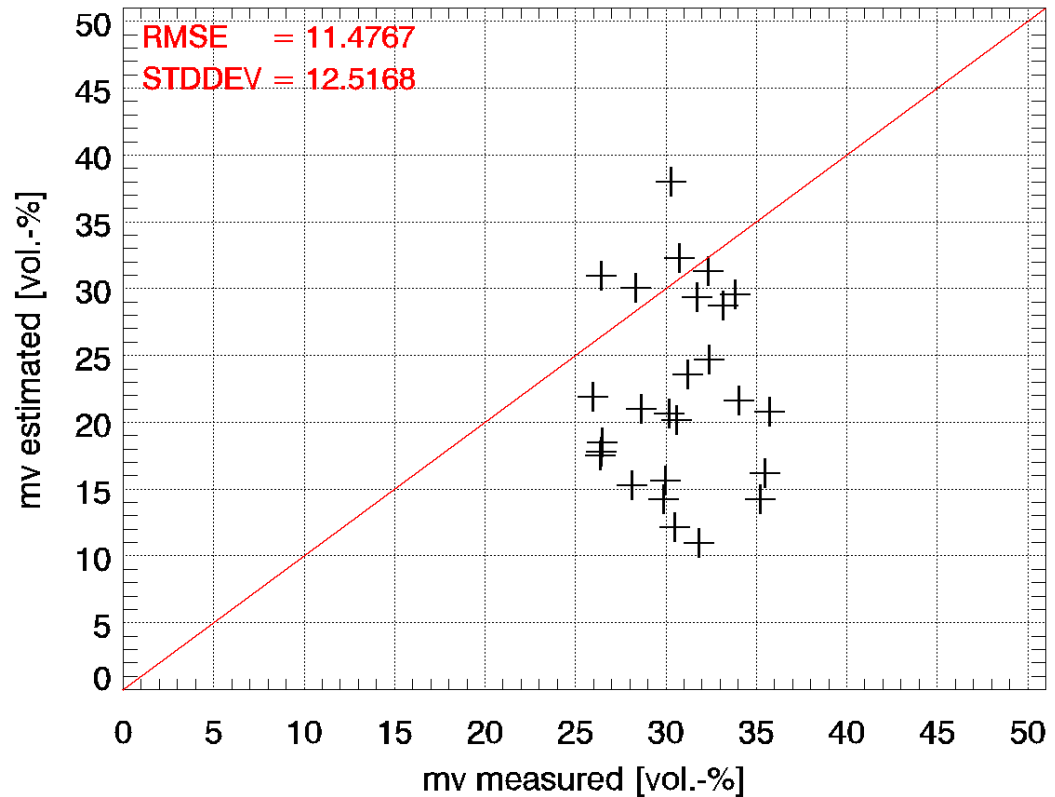
45cm

Row distance:

23cm

Wet biomass:

0,93kg/m²

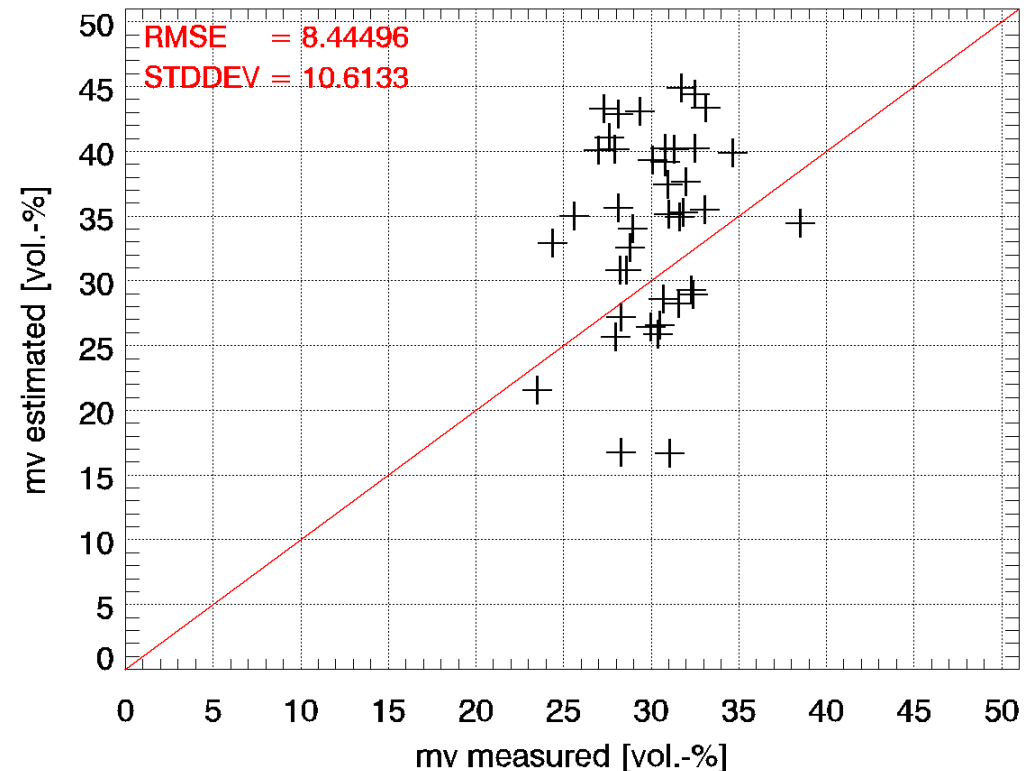


Validation with TDR Measurements on Winter Triticale

Vegetation height:
85cm

Row distance:
10cm

Wet biomass:
3,34kg/m²

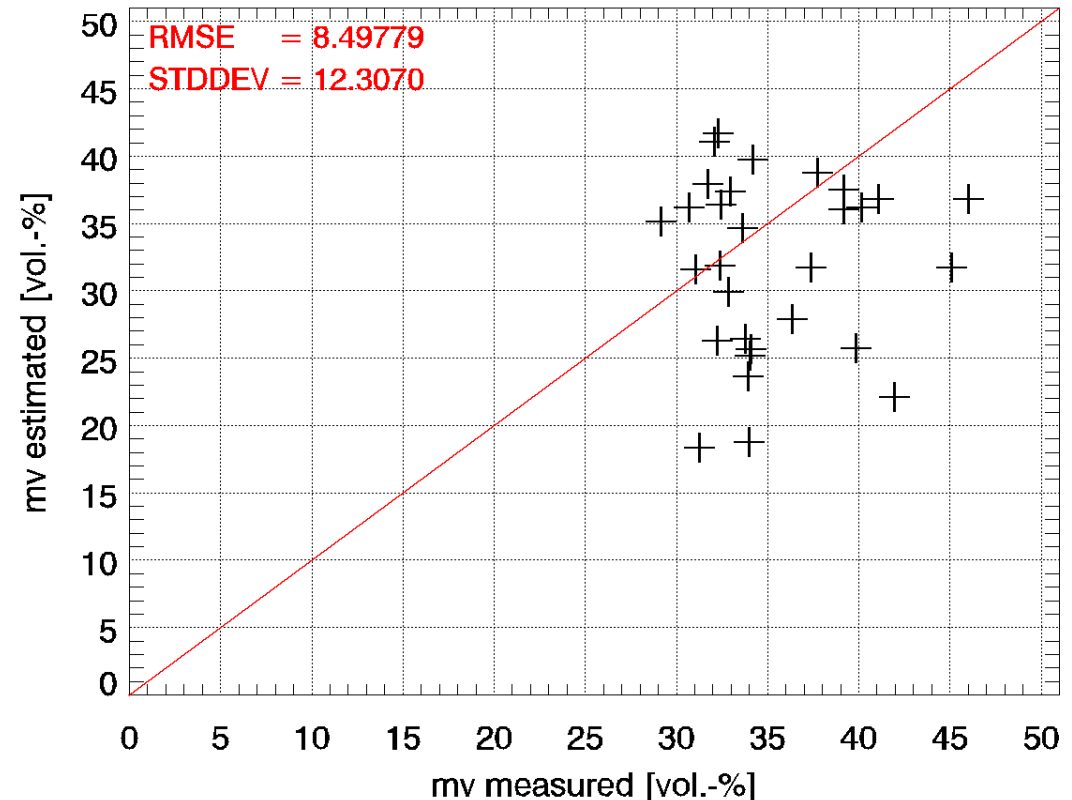


Validation with TDR Measurements on Winter Barley

Vegetation height:
70cm

Row distance:
10cm

Wet biomass:
3,31kg/m²

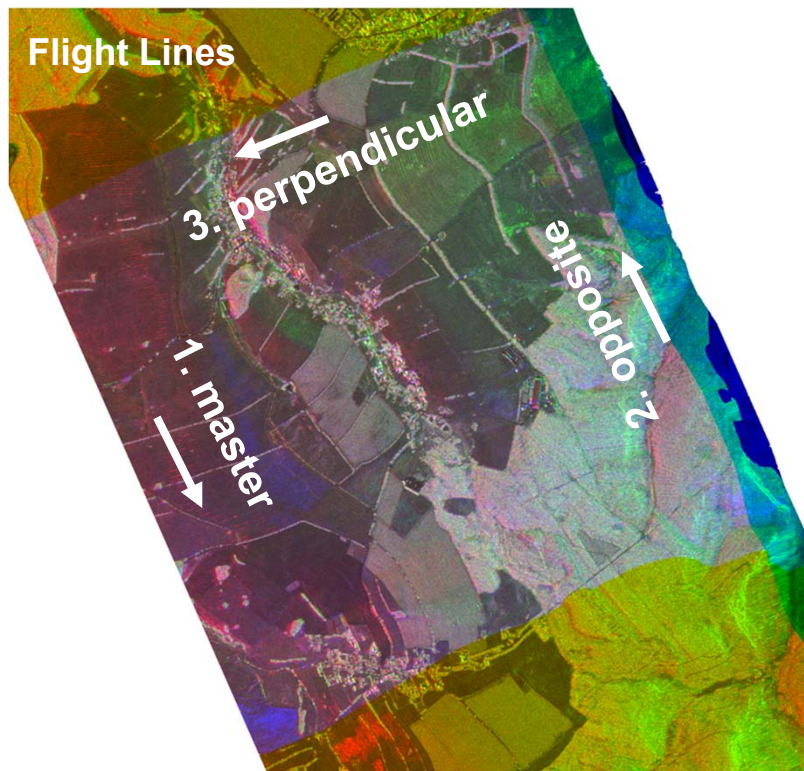


Soil Moisture Estimation

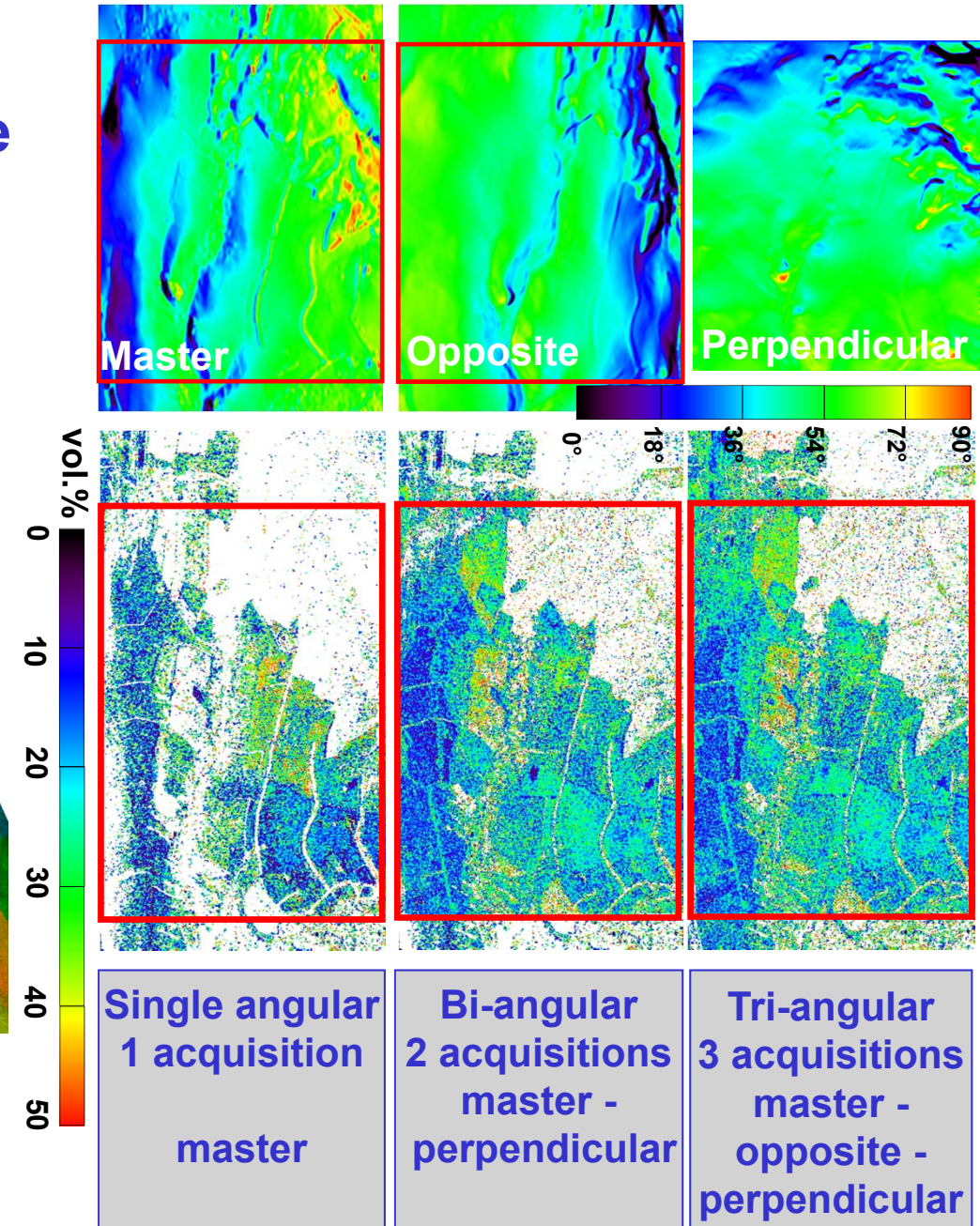
- Surface Characterisation
- mv estimation over bare surface
- **mv estimation under the vegetation**
 - 3 component model decomp.
 - improvement of the 3 component model decomp.
 - **multi-angle approach combined with 3 comp. model decomp.**
 - hybrid decomposition



Multi-Angle Approach for Soil Moisture Inversion Rate Increase



Testsite: Weisseritz Watershed; E-SAR L-band

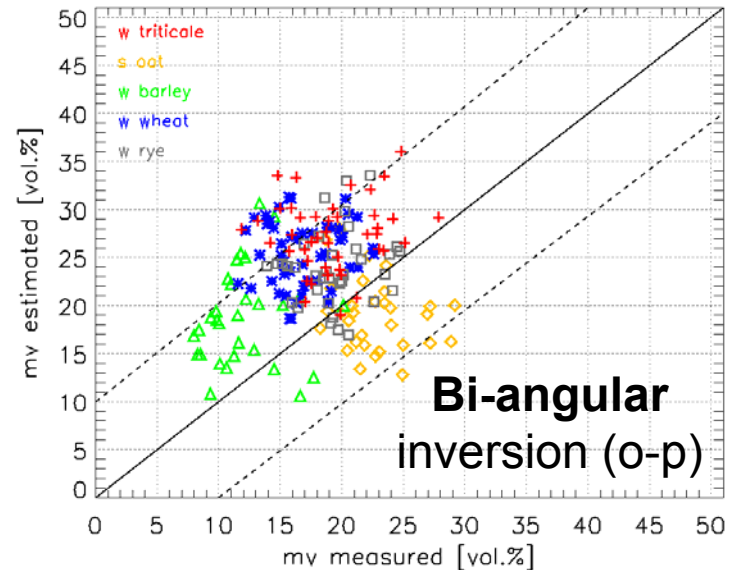
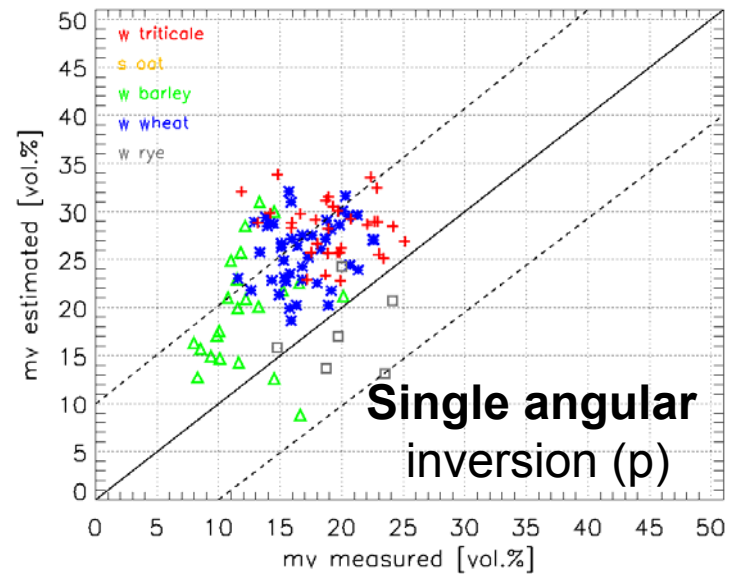
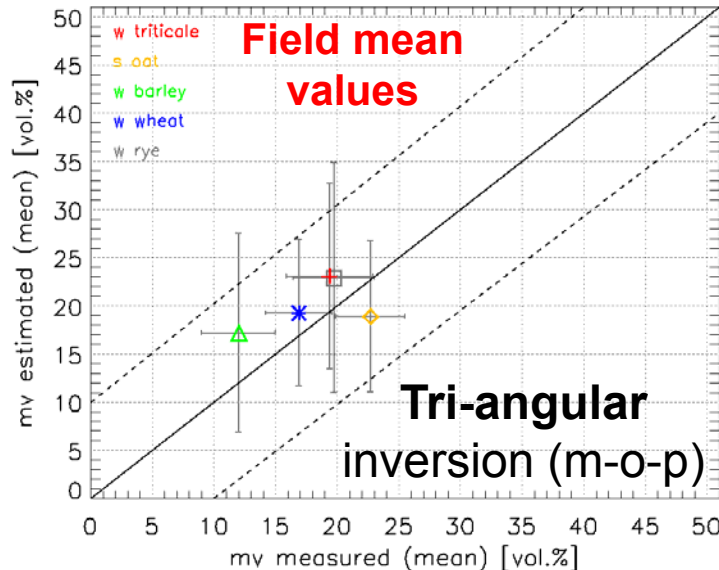
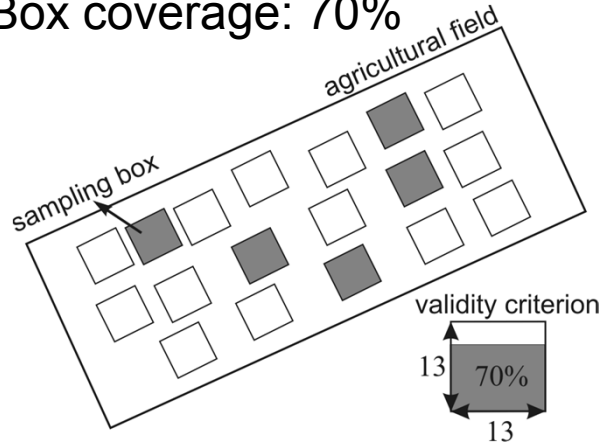


Inversion Rate of Soil Moisture Estimation @ different AOI

	One acquisition 	master	opposite	perpendicular	
		40.32%	29.87%	48.53%	
Two acquisitions 	master-opposite	master-perpendicular	opposite-perpendicular	55.87% 63.39% 60.71%	
	55.87% 63.39% 60.71%		master-opposite-perpendicular		
Three acquisitions 	70.89%				

Validation of Soil Moistures @ different Incidence Angles

Sampling box: 13x13 pixels
Box coverage: 70%



RMSE [vol.%] between Estimated and Measured Soil Moistures for Different Incidence Angle Constellations

Fields	m	o	p	m-o	m-p	o-p	m-o-p
Winter Triticale	6.34	6.34	10.33	5.42	6.27	9.46	5.72
Winter Barley	<	<	9.75	7.76	6.85	8.78	6.94
Winter Rye	5.25	6.11	5.86	5.81	4.89	6.42	5.27
Winter Wheat	4.52	<	9.79	4.41	5.04	9.54	4.98
Summer Oat	8.55	6.43	-	6.35	8.55	6.43	6.35
Mean	6.17	6.29	8.93	5.95	6.32	8.13	5.85
- = out of scene < = too less values for a valid analysis		Single angular			Bi-angular		Tri-angular

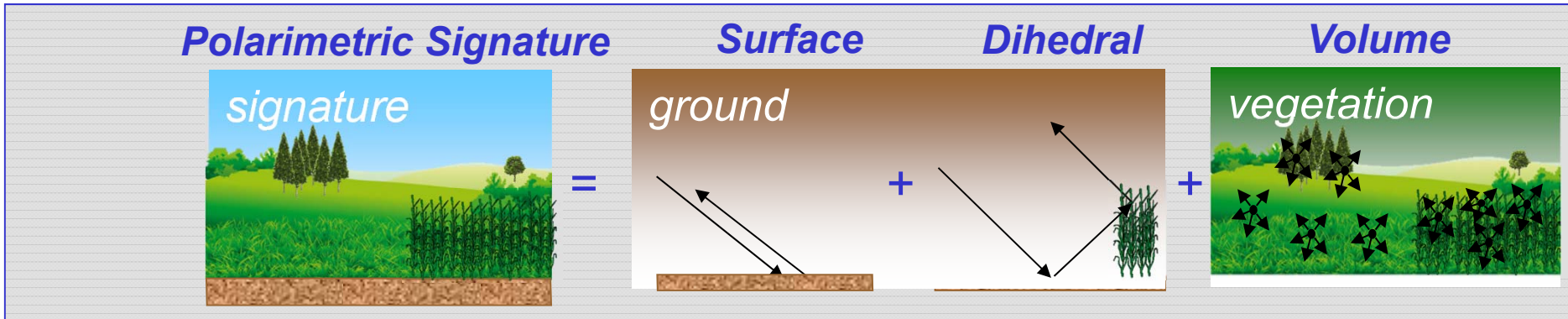


Soil Moisture Estimation

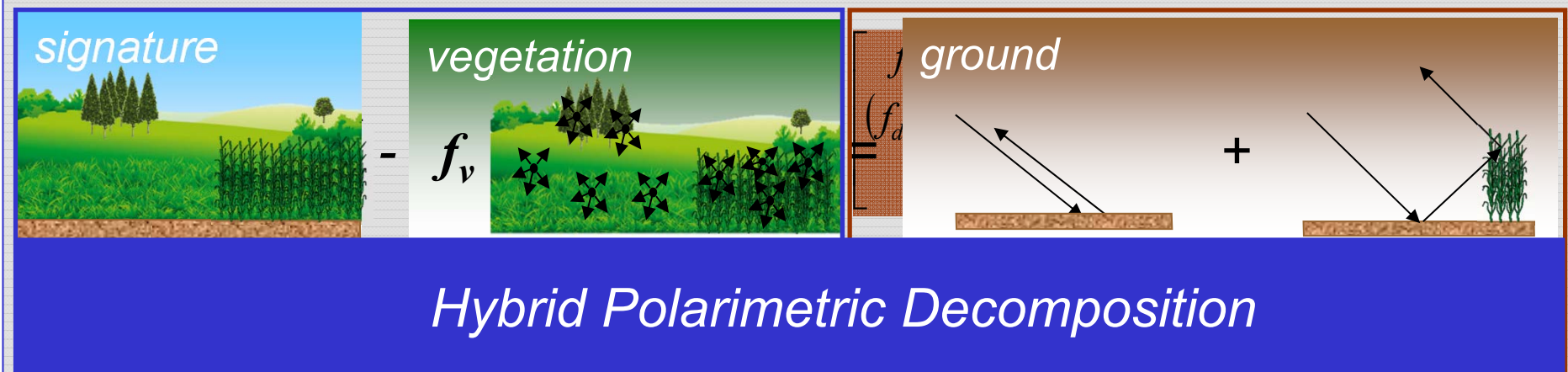
- Surface Characterisation
- mv estimation over bare surface
- **mv estimation under the vegetation**
 - 3 component model decomp.
 - improvement of the 3 component model decomp.
 - multi-angle approach combined with 3 comp. model decomp.
 - **hybrid decomposition**



Basic Principle of Hybrid Polarimetric Decomposition



Removal of Vegetation Component



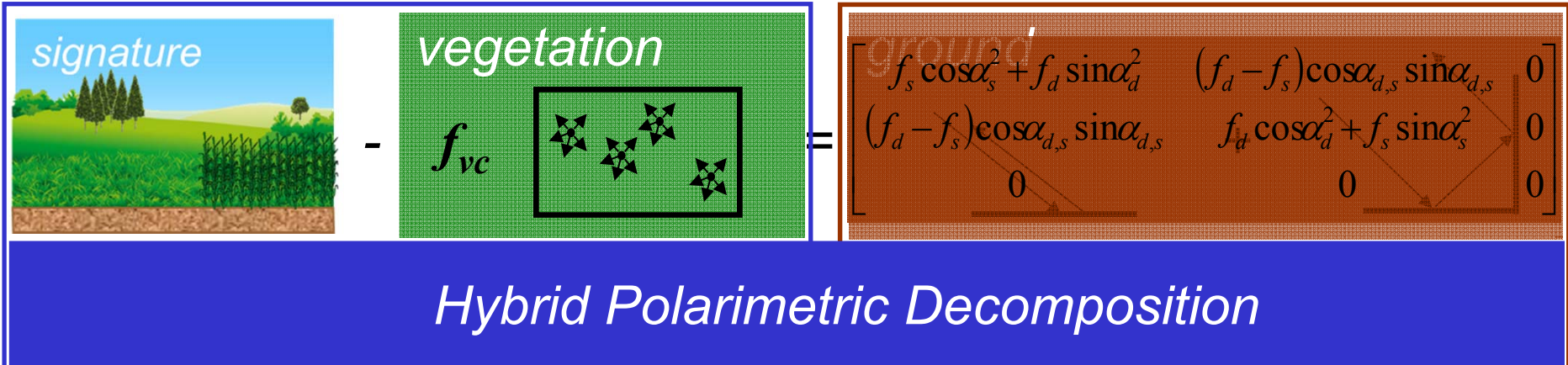
Physically constraint volume intensity (f_{vc}) with surface scattering (α_b)

$$f_{vc} = \frac{1}{2} \text{Im}(\chi_v^2) \quad \text{elements}, \text{surface scattering forward model} (\alpha_s, \alpha_d)$$



Graphics from Google Earth

Retrieval of the Ground Scattering Components



Eigen-based Decomposition of Ground Components

- From eigenvalues: **Intensity of ground (f_d, f_s)**
- From eigenvectors: **Scattering mechanisms of ground (α_d, α_s)**

Physically Meaningful Separation of Scattering Mechanisms (α_d, α_s)

$$\alpha_d + \alpha_s = \pi/2$$

Orthogonality condition

$\rightarrow \left\{ \begin{array}{ll} \alpha \in [0, \pi/4] & \text{Surface scattering} \\ \alpha \in [\pi/4, \pi/2] & \text{Dihedral scattering} \end{array} \right.$

α_s

α_d

103



Graphics from Google Earth API

Slide 103

Soil Moisture Inversion from Surface Scattering Component

Polarimetric SAR data

Surface scattering component
from hybrid polarimetric
decomposition

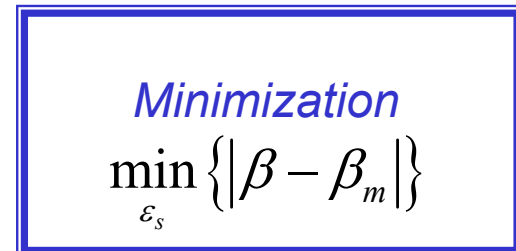
$$\beta = -\tan(\alpha_s)$$

Surface scattering model

Bragg scatter modeling with θ_{loc}
and a variety of soil dielectric
constants ϵ_s

$$\beta_m = \frac{R_{HH} - R_{VV}}{R_{HH} + R_{VV}}$$

$$R_{HH}, R_{VV} = f(\epsilon_s, \theta_{loc})$$

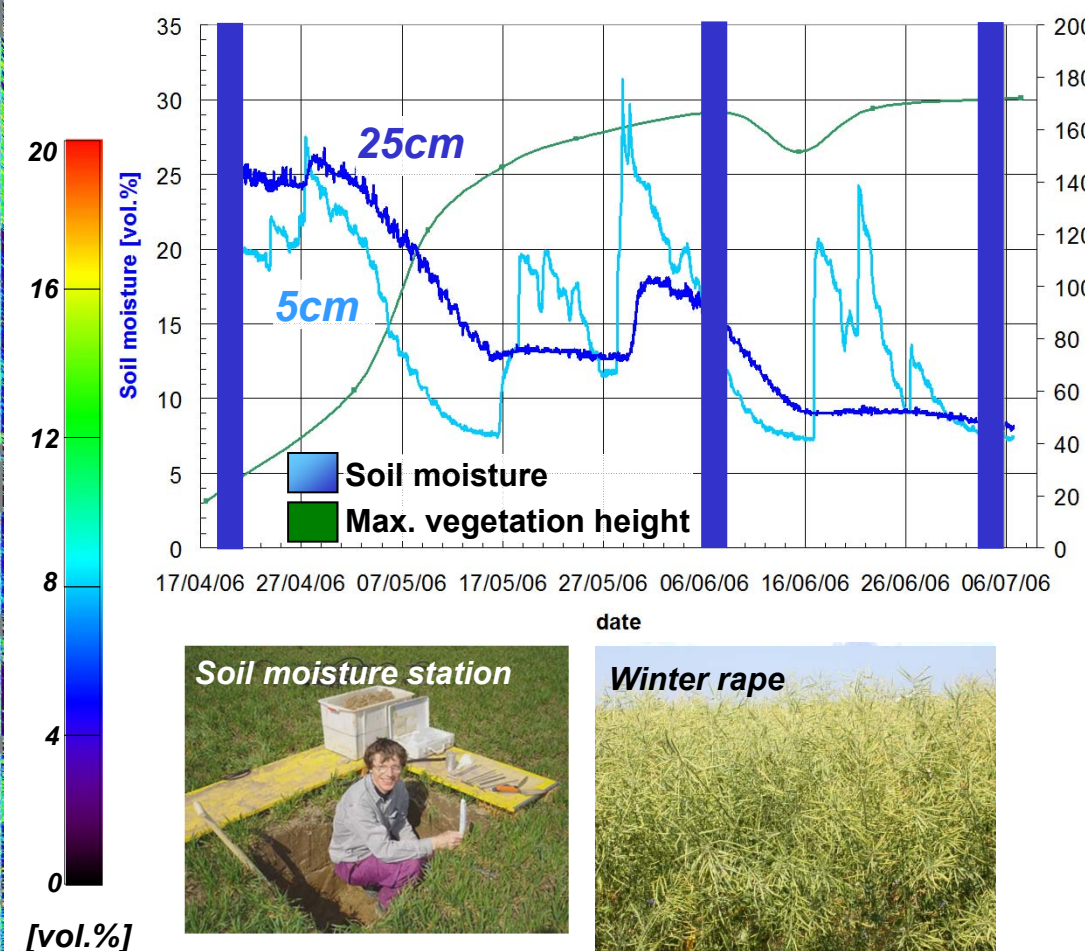
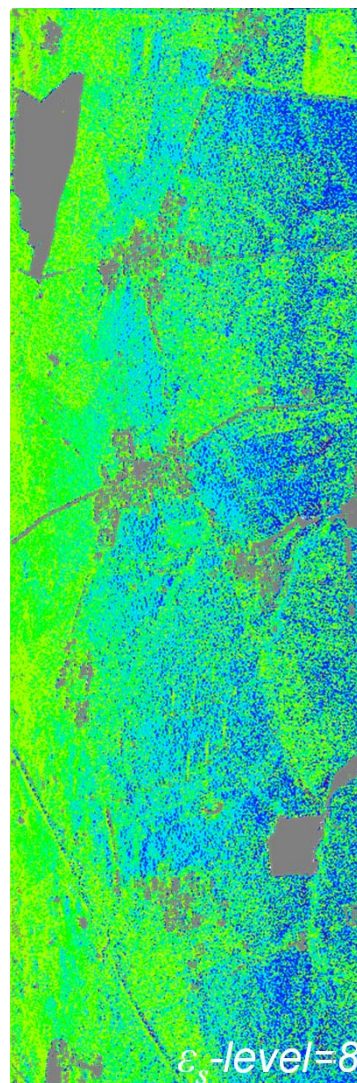
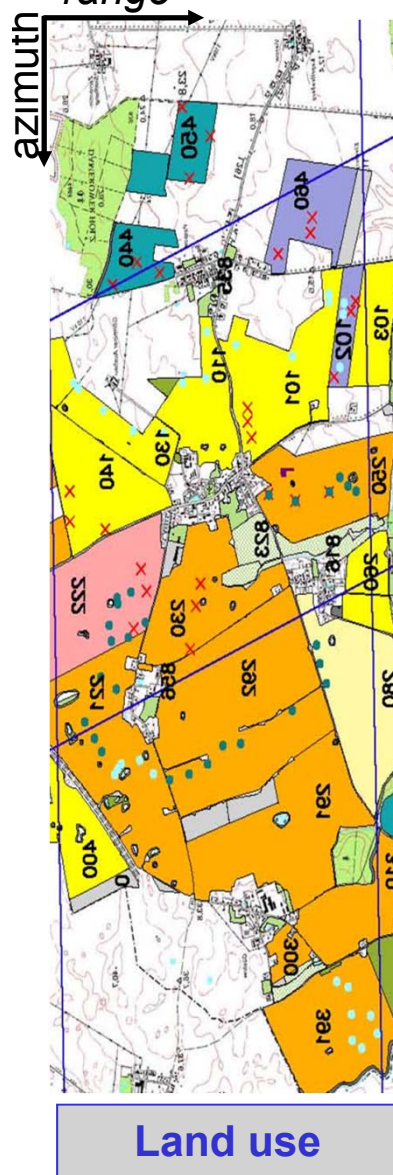


Pedo-Transfer
Function of
Topp et al. ($\epsilon_s < 40$)
Roth et al. ($\epsilon_s > 40$)

Soil moisture [vol.%]



Soil Moisture Inversion along Vegetation Growth Cycle

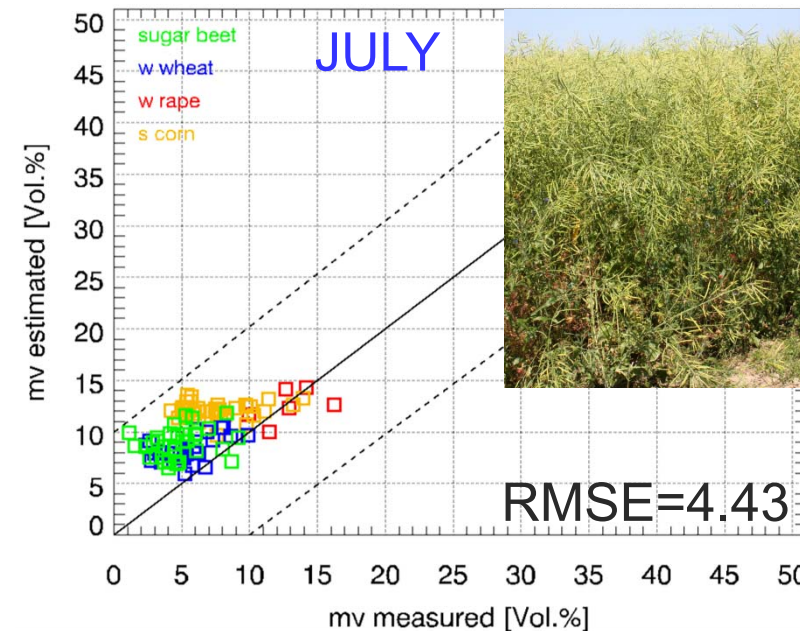
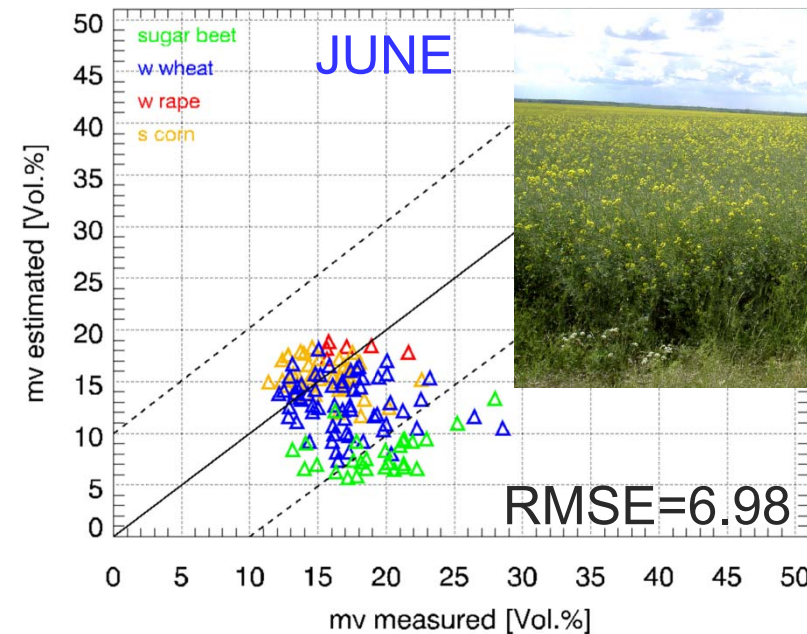
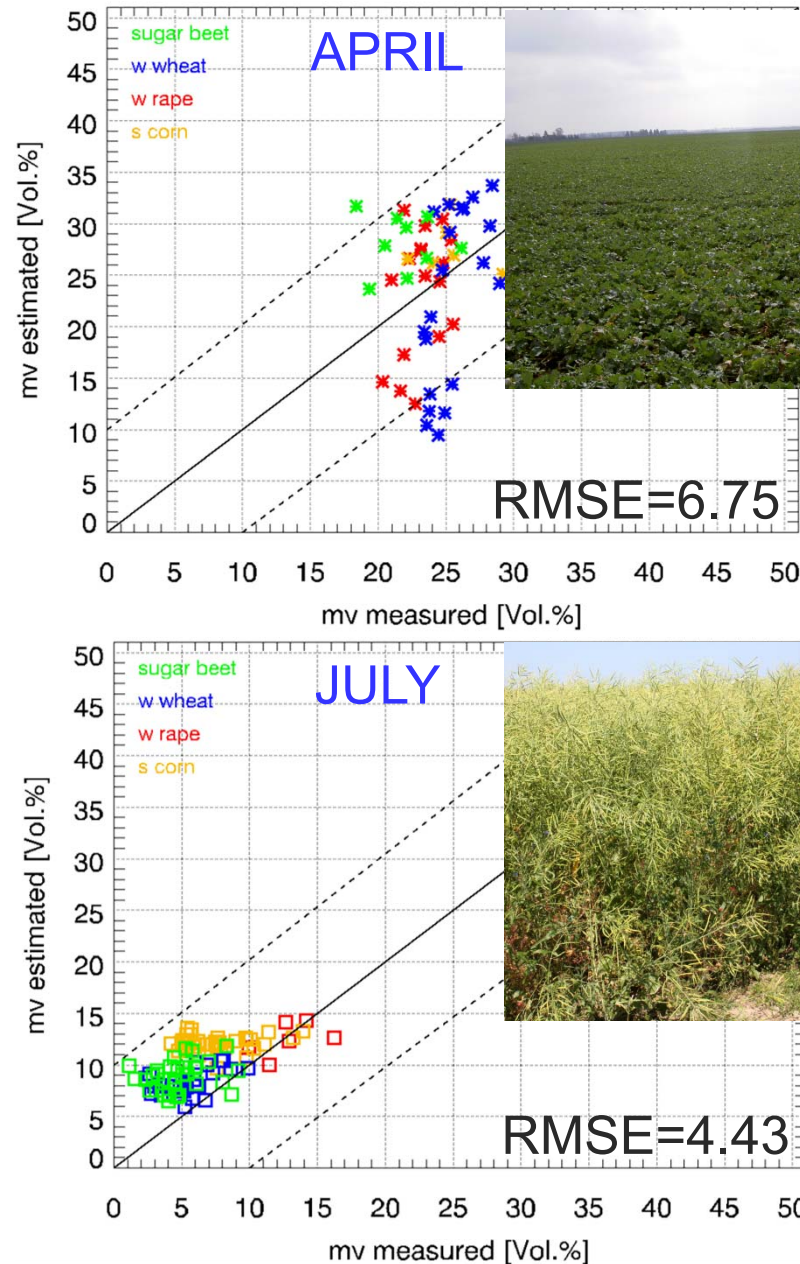


**AgriSAR 2006
L-band
Quad-pol**

**Height:
172cm
Wet biomass:
6.26kg/m²**



Validation of Moisture Inversion with Field Measurements (TDR)

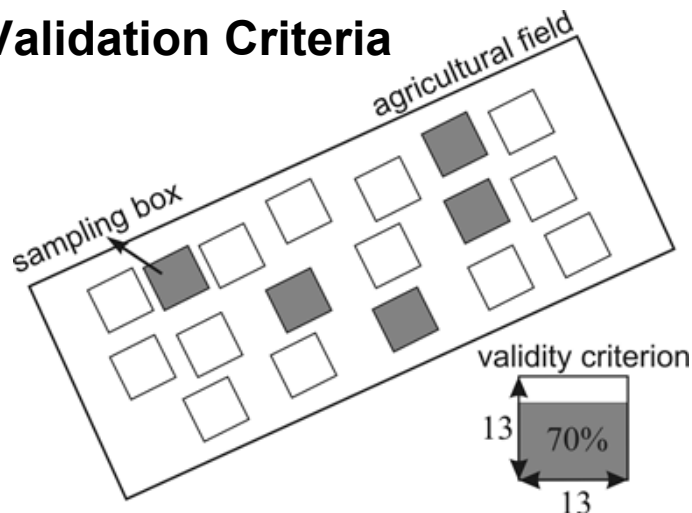


RMSE [vol.%]	APRIL	JUNE	JULY
sugar beet	7.55	11.90	4.68
winter wheat	8.06	6.15	3.40
winter rape	5.70	2.62	2.06
summer corn	5.34	3.20	5.25

validation box: 13x13 pixels

Validation of Soil Moisture Inversion under Vegetation Cover @ L-Band

Validation Criteria

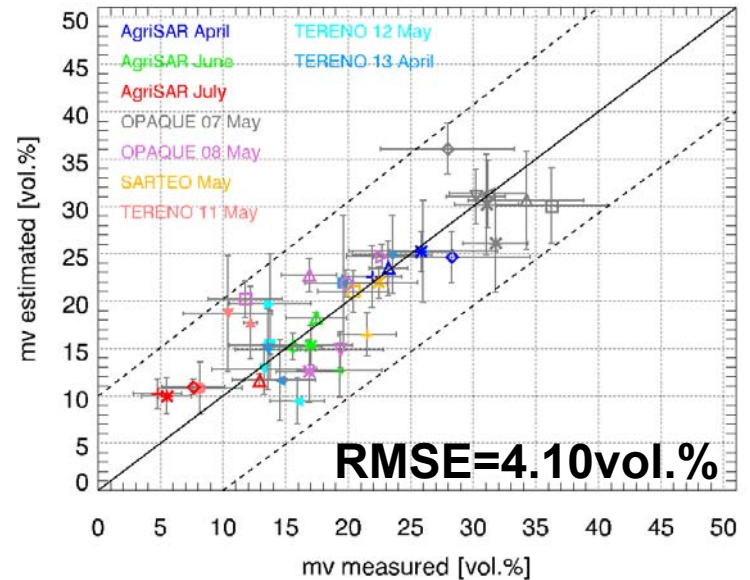


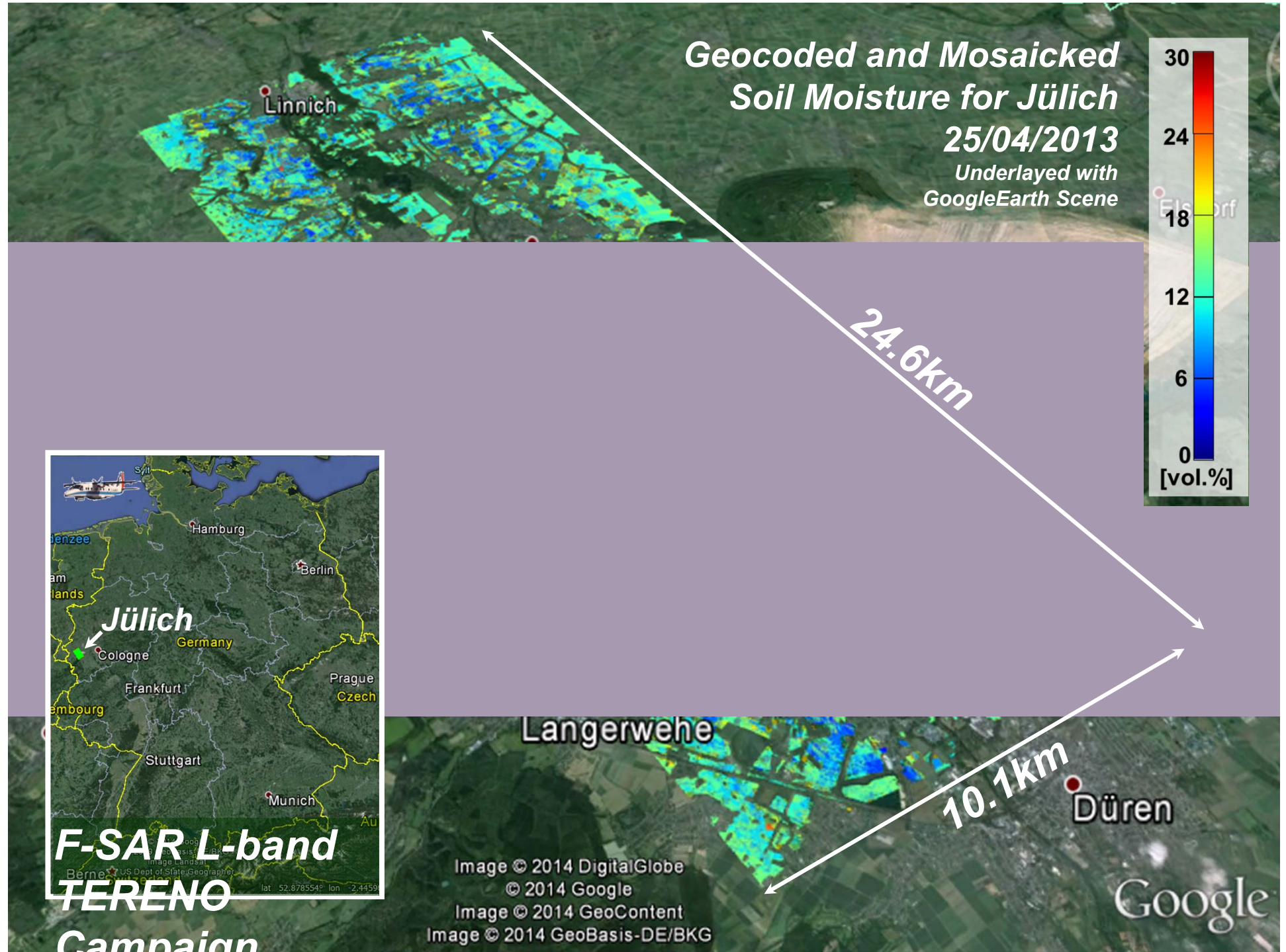
- *winter rye*
- ▽ *summer oat*
- ▷ *winter triticale*
- ◁ *summer barley*
- + *sugar beet*
- ◊ *summer corn*
- *winter barley*
- * *winter wheat*
- △ *winter rape*
- ✗ *grassland*

Variety in Vegetation Cover



9 Campaigns (E-SAR+F-SAR)





Summary Soil Moisture Estimation

- ***Soil moisture inversion is still object of scientific research:***
 - Main research focuses on the estimation of mv under the vegetation
 - One attempt is to use SAR polarimetry for scattering mechanism decomposition in order to characterise and subtract volume from a ground component (surface/dihedral)
 - PolSARPro provides the possibility to invert soil moisture over bare fields and allows a decomposition of scattering mechanisms
 - Outlook: Inversion procedures for vegetated areas are still missing



References (Part I)

Basic Text Books for SAR-Polarimetry and Pol-InSAR:

- ↗ **Cloude, S.**, Polarisation: application in remote sensing, Oxford University Press, p. 352, 2009.
- ↗ **Boerner, W. M. et al.**, 'Polarimetry in Radar Remote Sensing: Basic and Applied Concepts', Chapter 5 in F. M. Henderson, and A.J. Lewis, (ed.), "Principles and Applications of Imaging Radar", vol. 2 of Manual of Remote Sensing, (ed. R. A. Reyerson), Third Edition, John Wiley & Sons, New York, 1998.
- ↗ **Elachi, C. & Van Zyl, J. J.**, 'Introduction to the physics and techniques of Remote Sensing', John Wiley and Sons, p. 552, 2006.
- ↗ **Lee, J.S. & Pottier, E.** 'Polarimetric Radar Imaging: From Basics to Applications', CRC Press, 2009.
- ↗ **Woodhouse, I.**, 'Introduction to Microwaves Remote Sensing', CRC Taylor & Francis, p. 370, 2005.



References (Part II)

Surface Parameter Inversion:

- ↗ Hajnsek, I., Pottier, E. & Cloude, S.R., 'Inversion of Surface Parameters from Polarimetric SAR', *IEEE Transactions on Geoscience and Remote Sensing*, vol. 41, no. 4, pp. 727-745, 2003.
- ↗ Lee, J.-S., Boerner, W.-M., Ainsworth, T. L., Hajnsek, I., Papathanassiou, K.P., Lüneburg, E., 'A Review of Polarimetric SAR Algorithms and their applications', *Journal of Photogrammetry and Remote Sensing*, vol. 9, No. 3, pp. 31-80, 2004.
- ↗ Hajnsek, I. & Cloude, S., 'The Potential of InSAR for Quantitative Surface Parameter Estimation' *Can. J. Remote Sensing*, vol. 31, no.1, pp. 85-102, 2005
- ↗ Hajnsek, Irena; Jagdhuber, Thomas; Schön, Helmut; Papathanassiou, Kostas (2009): Potential of Estimating Soil Moisture under Vegetation Cover by means of PolSAR. IEEE [Hrsg.]: *IEEE Transactions on Geoscience and Remote Sensing*, IEEE, vol 47, no 2, pp. 442 – 454.
- ↗ M. Arii, J.J. van Zyl and Y. Kim: A general characterization for polarimetric scattering from vegetation canopies, *IEEE Transactions on Geoscience and Remote Sensing*, vol. 48, pp. 3349-3357, 2010.
- ↗ M. Neumann and L. Ferro-Famil: Extraction of particle and orientation distribution characteristics from polarimetric SAR data, in Proc. of 8th European Conference on Synthetic Aperture Radar, June 7-10, 2010, Aachen, Germany, VDE, pp. 422-425.
- ↗ Jagdhuber, T., Hajnsek, I., Papathanassiou, K.P.: An Iterative, Generalized Hybrid Decomposition for Soil Moisture Retrieval under Vegetation Cover Using Fully Polarimetric SAR. *IEEE Journal of Selected Topics in Applied Earth Observations and Remote Sensing* , DOI: 10.1109/JSTARS.2014.2371468, p. 1-12, 2014.
- ↗ Jagdhuber, T., 'Soil Parameter Retrieval under Vegetation Cover Using SAR Polarimetry, *PhD Thesis*, University Potsdam, Potsdam, supervised by Prof. Hajnsek and Prof. Bronstert, Date of Defense: 05.07.2012, <http://nbn-resolving.de/urn:nbn:de:kobv:517-opus-60519>, 2012.
- ↗ Bronstert, A., C. Creutzfeldt, T. Gräff, I. Hajnsek, M. Heistermann, S. Itzert, T. Jagdhuber, D. Kneis, E. Lück & D. Reusser, 'Potentials and constraints of different type of soil moisture observations for flood simulations in headwater catchments', *Natural Hazards*, Vol. 60, pp.879–914 , 2012.



Acknowledgement to the AgriSAR Team



Universitat
d'Alacant
Universidad de Alicante

06/06/06



DLR



INTA



Slide 112





Acknowledgement to the OPAQUE Team

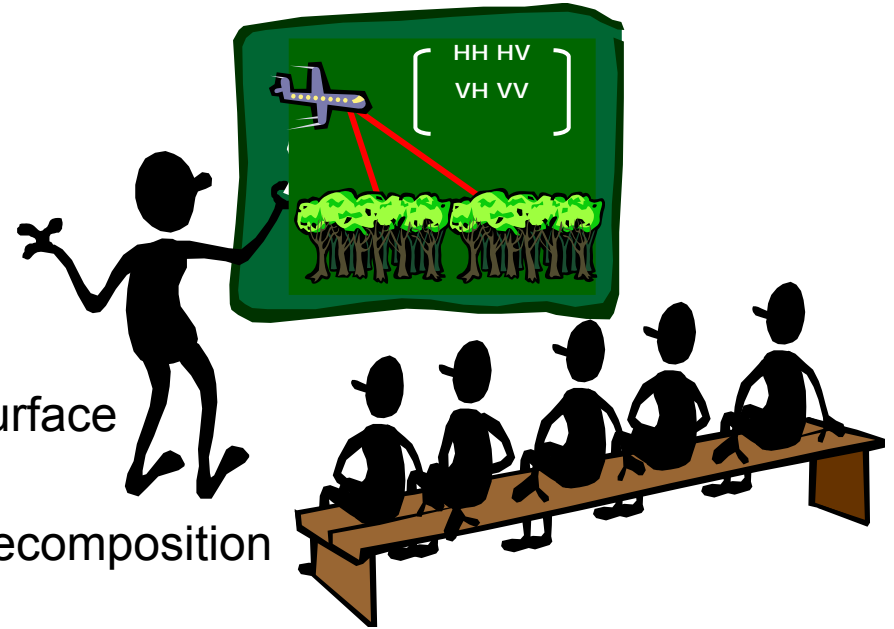
u^b

UNIVERSITÄT
BERN



Part II: Exercises with L-band Airborne Data

- ↗ Read the airborne SAR data
- ↗ Speckle Filtering (refined Lee)
- ↗ Oh, Dubois and X-Bragg Inversion
- ↗ Decomposition Method to extract the surface parameter:
 - ↗ Freeman-Durden Model-based Decomposition
 - ↗ Eigenvector Decomposition



Test Date Used for the Exercise

↗ Testsite: Demmin

- ↗ Location: Northern Germany
- ↗ Acquisition Date: May 2012
- ↗ Frequency: L-band
- ↗ Data size: az: 2.75km rg: 2.2 km
- ↗ Polarisation: 4 SLC
- ↗ Resolution: az: 60cm x rg: 3.8m
- ↗ Rows and columns: 7981 x 1837



Pauli RGB

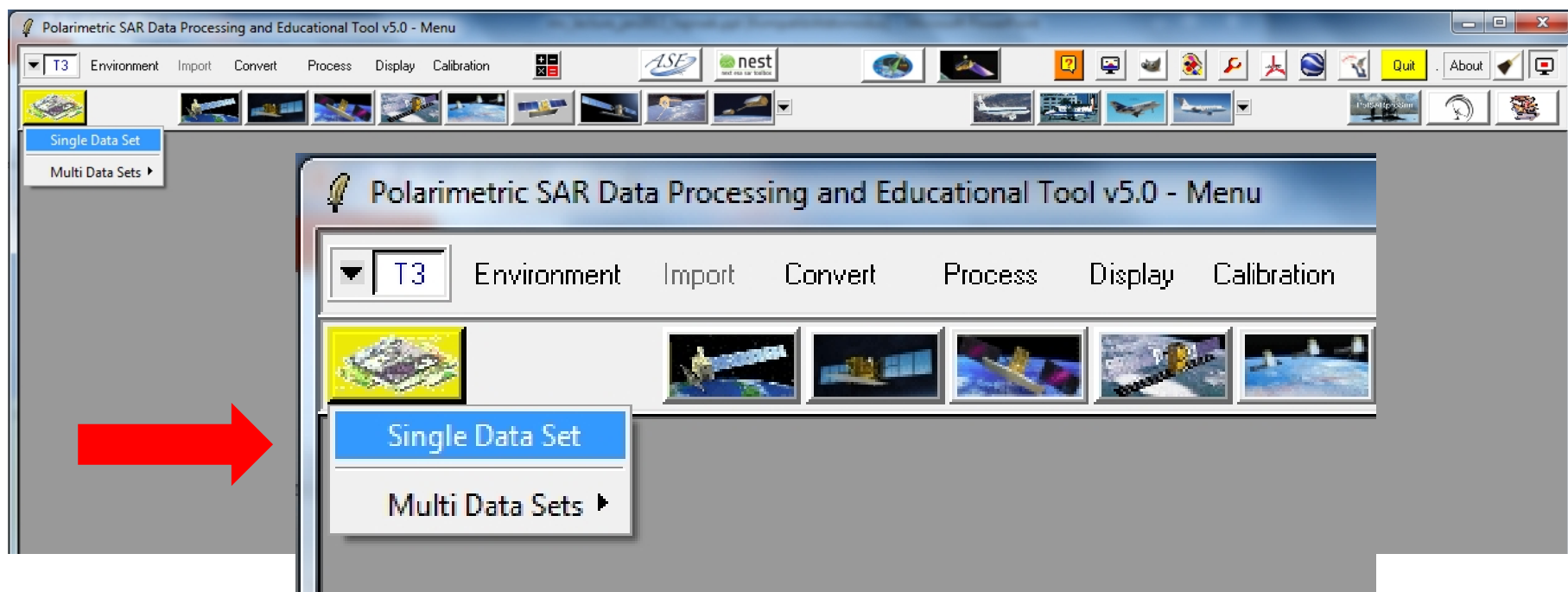


Slide 115

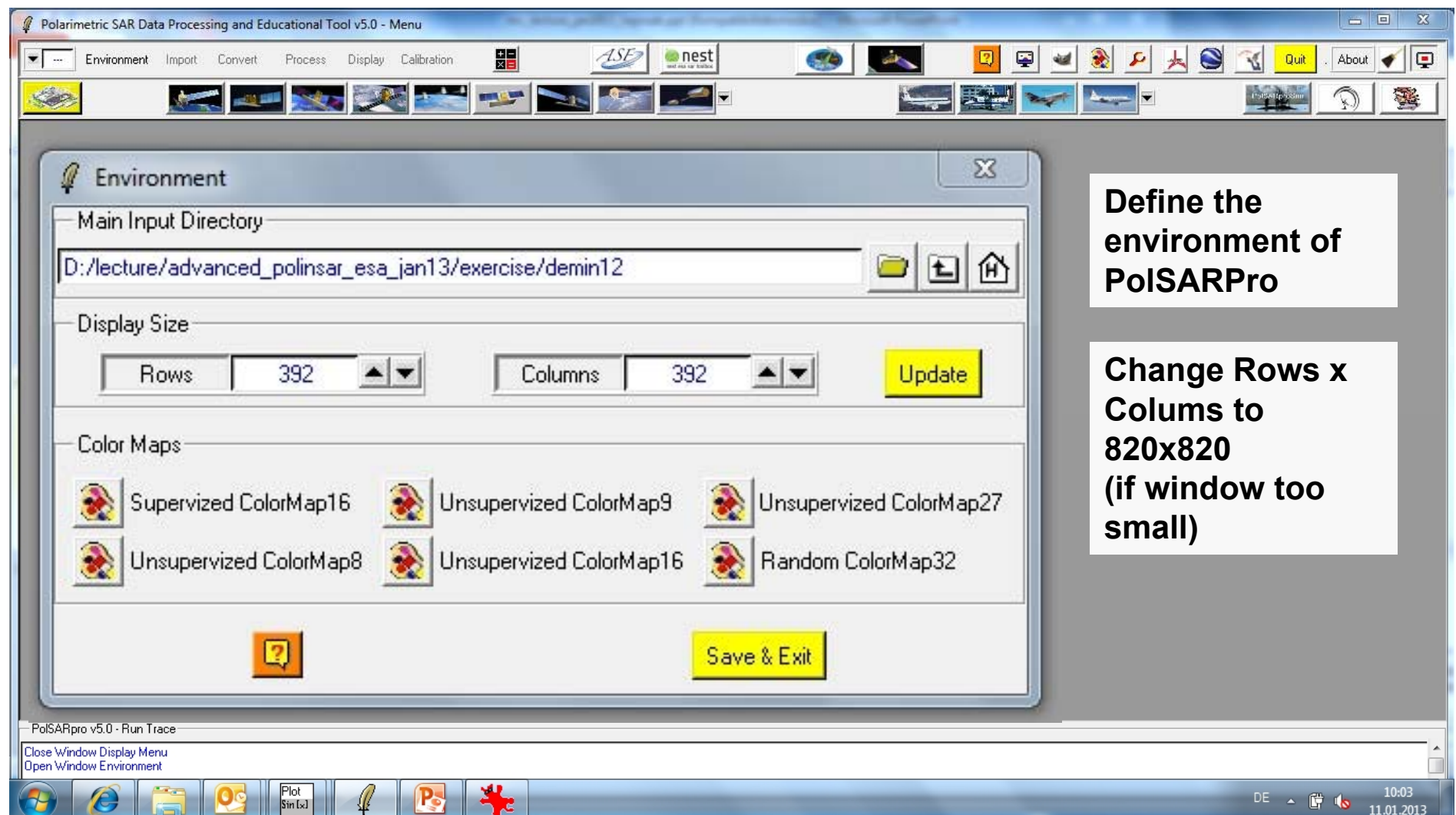


First Steps in PolSARPro

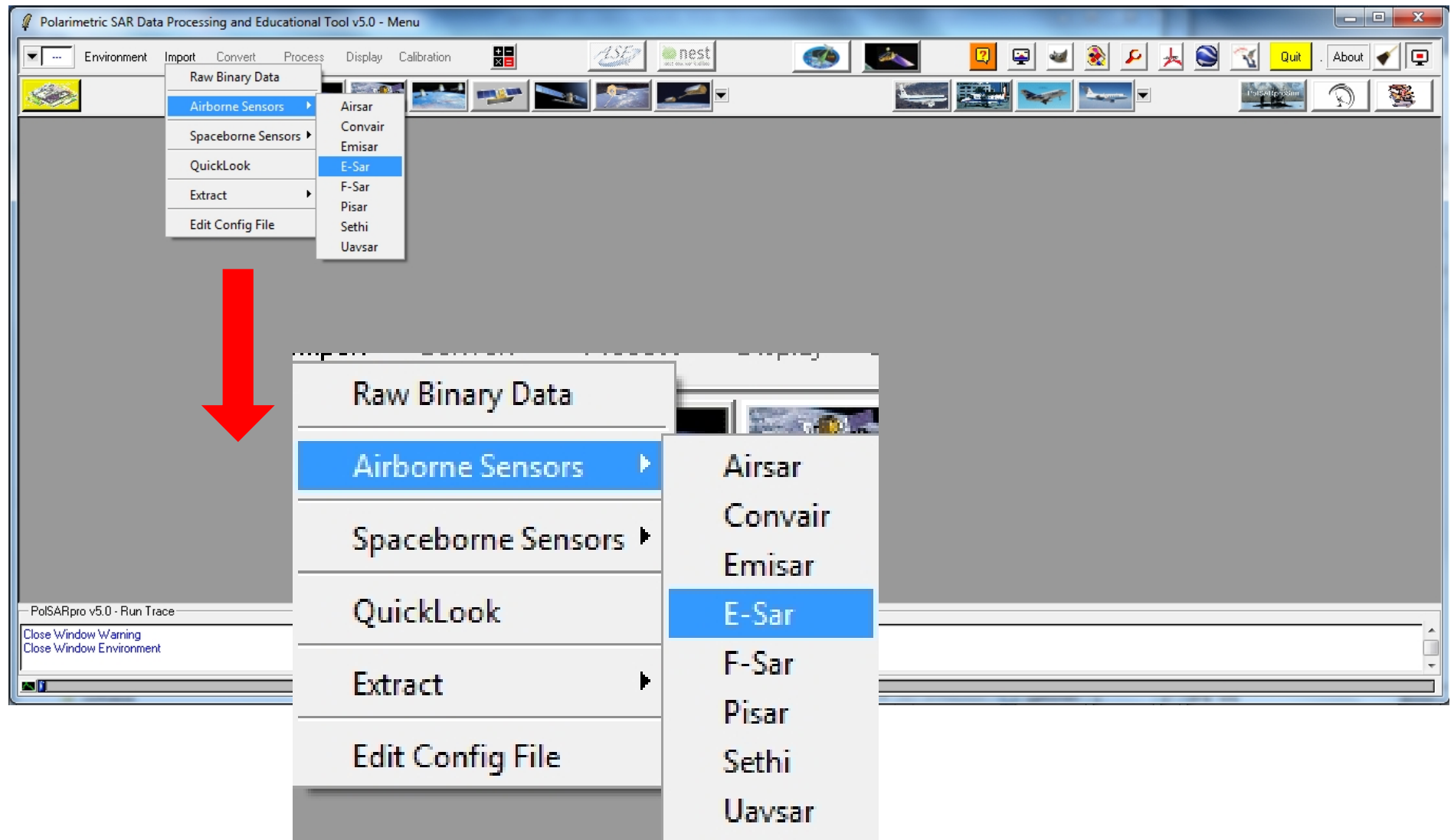
- ↗ Please open PolSARPro
- ↗ Define your environment
- ↗ Open the DLR's acquired test Radar data



First Steps in PolSARPro

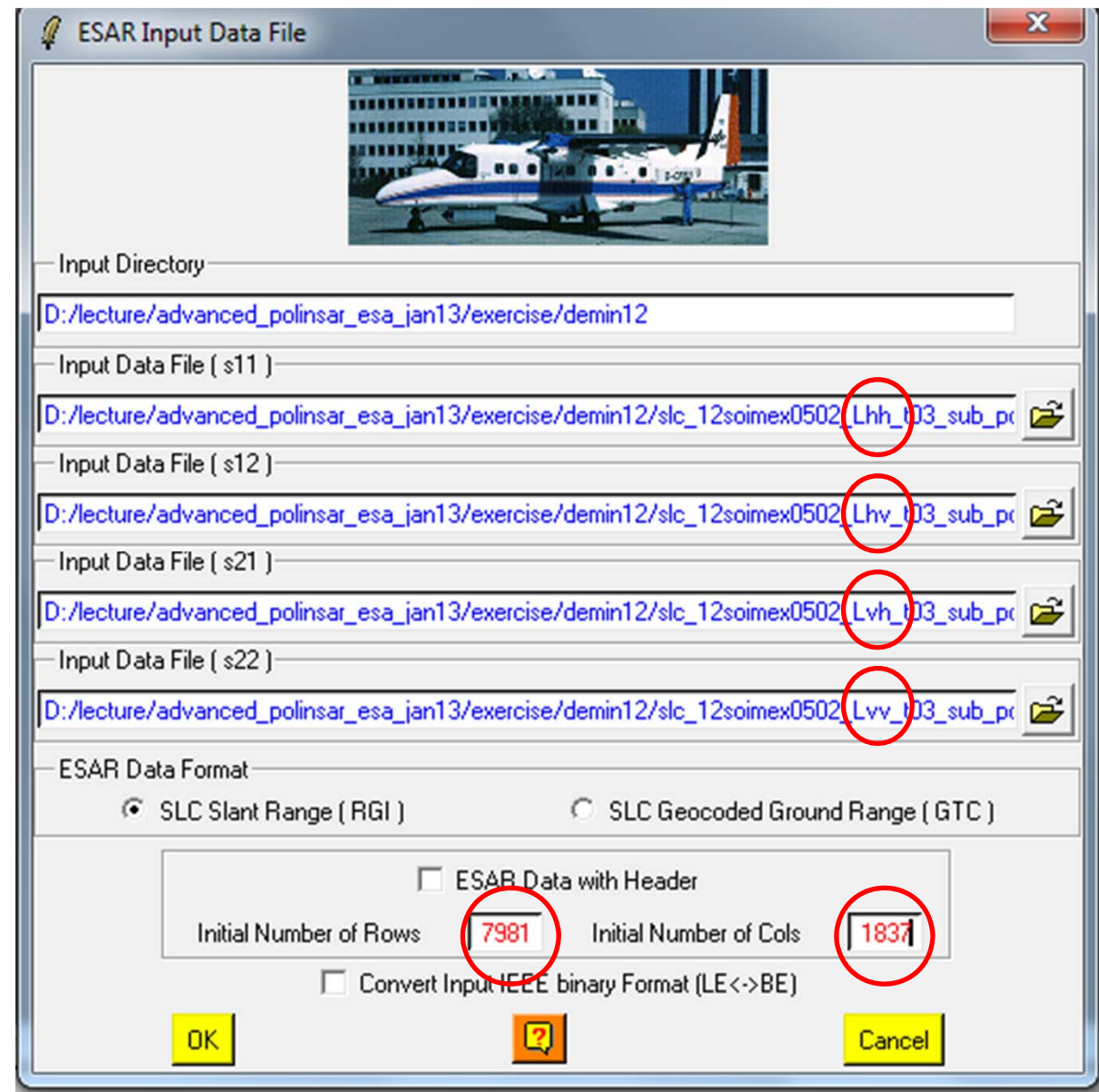


Load the Airborne Data



Fill the Widget with Row and Column

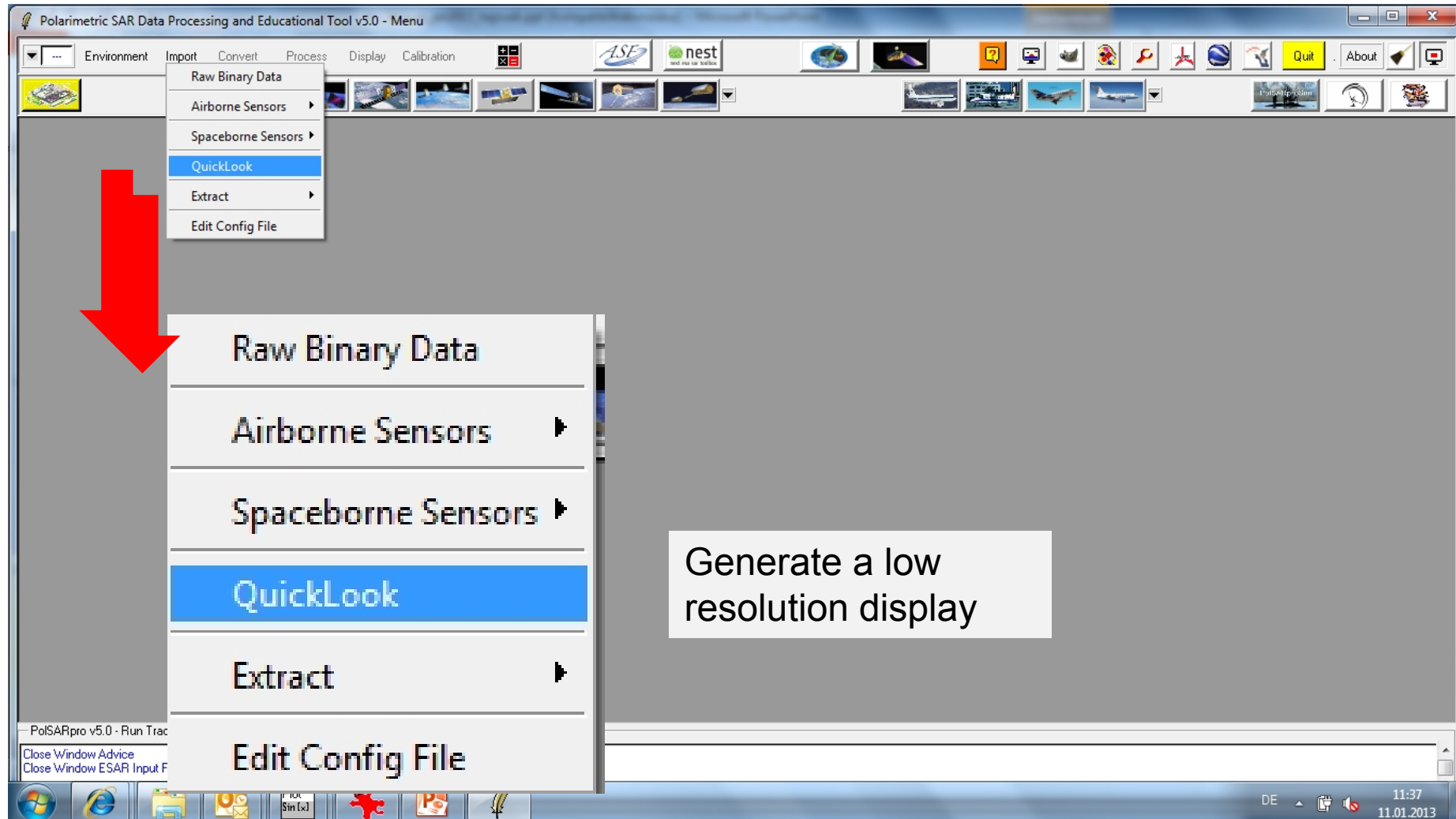
$$[S] := \begin{bmatrix} S_{11} & S_{12} \\ S_{21} & S_{22} \end{bmatrix} = \begin{bmatrix} S_{hh} & S_{hv} \\ S_{vh} & S_{vv} \end{bmatrix}$$



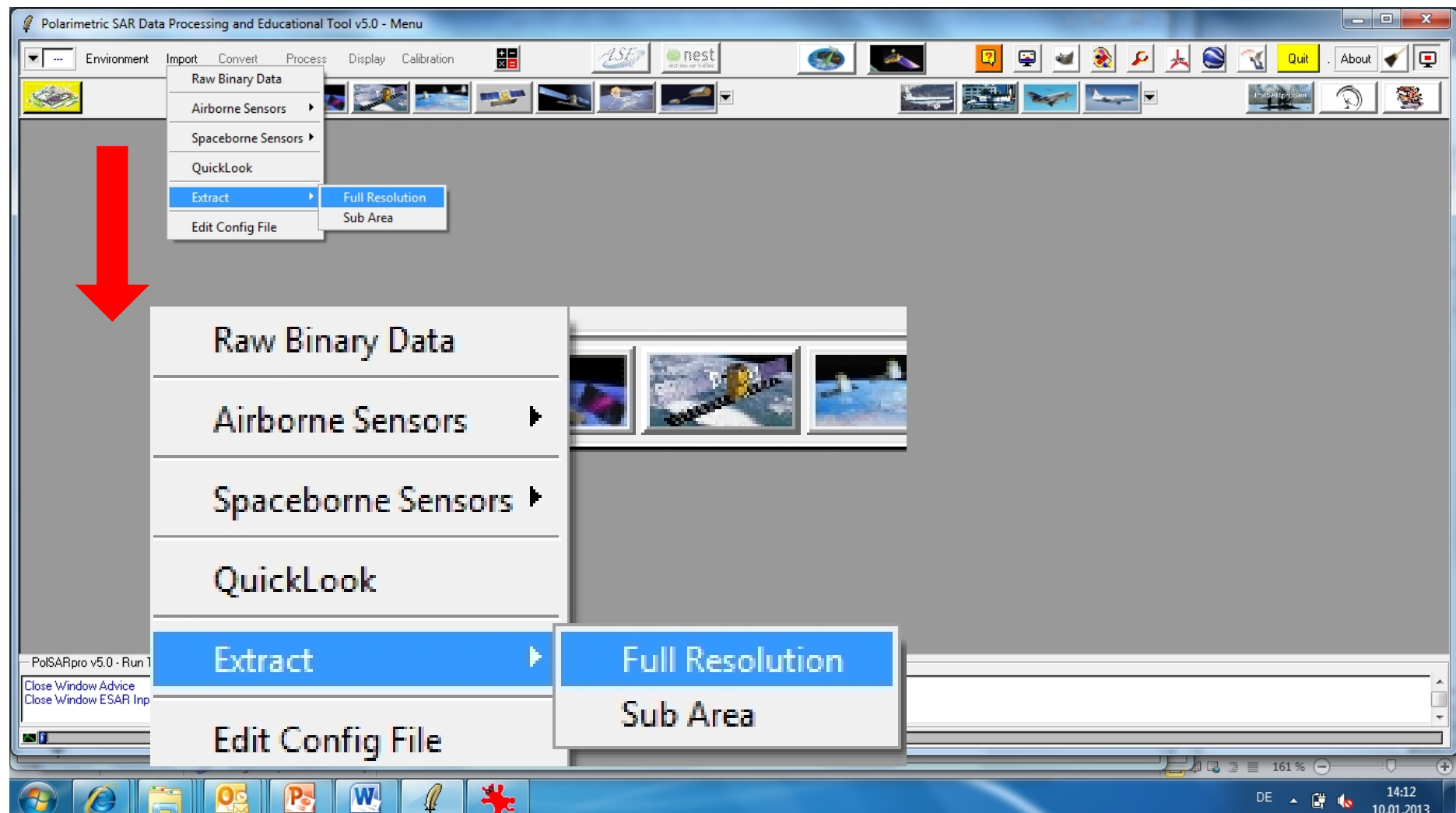
Note: Please add header!



Display the Image

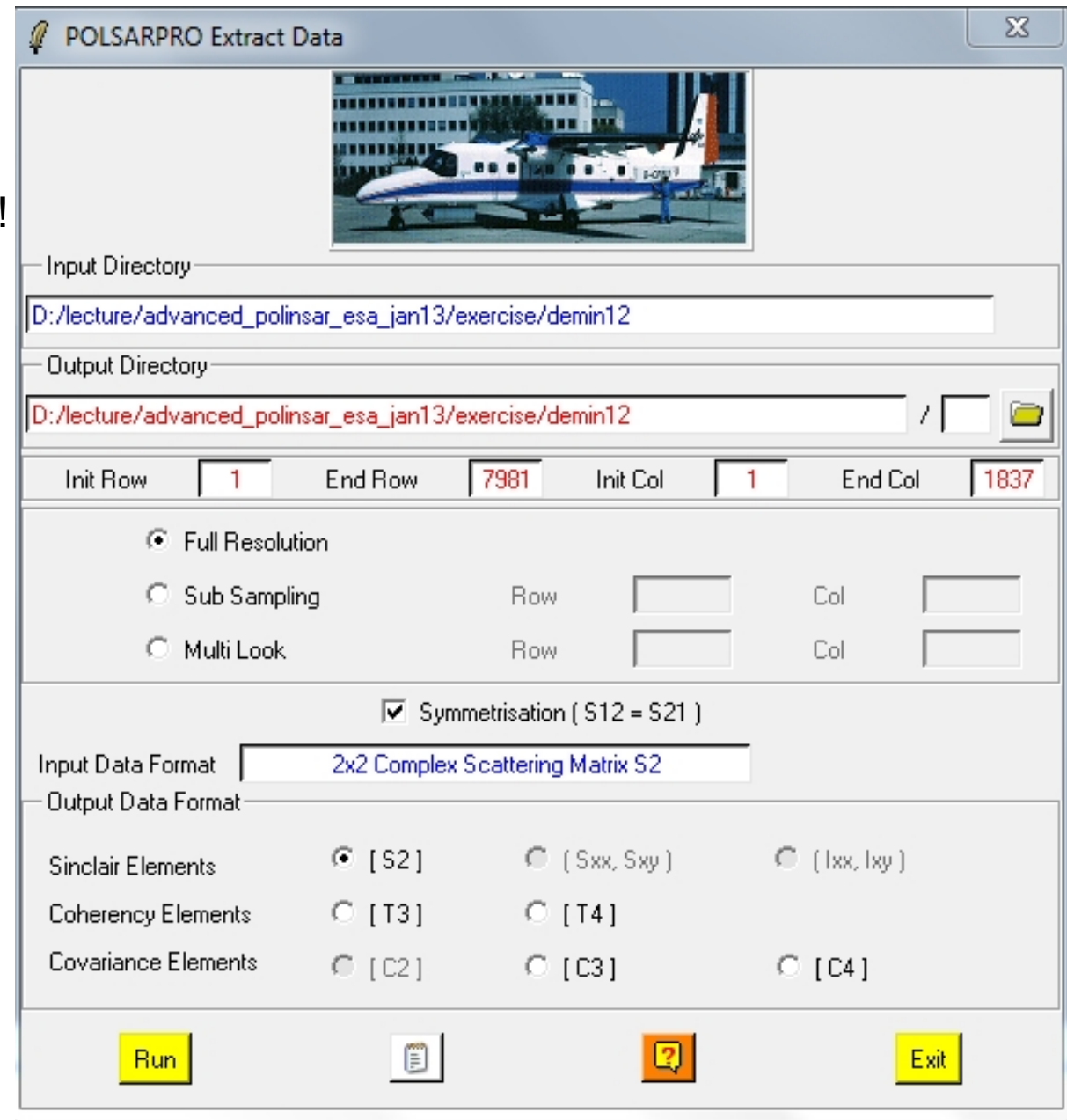


Extract the Test Data



Extract S2 Data

- ↗ Check the header of the file!
- ↗ Full resolution
- ↗ Sinclair Elements [S2]



Display the Data

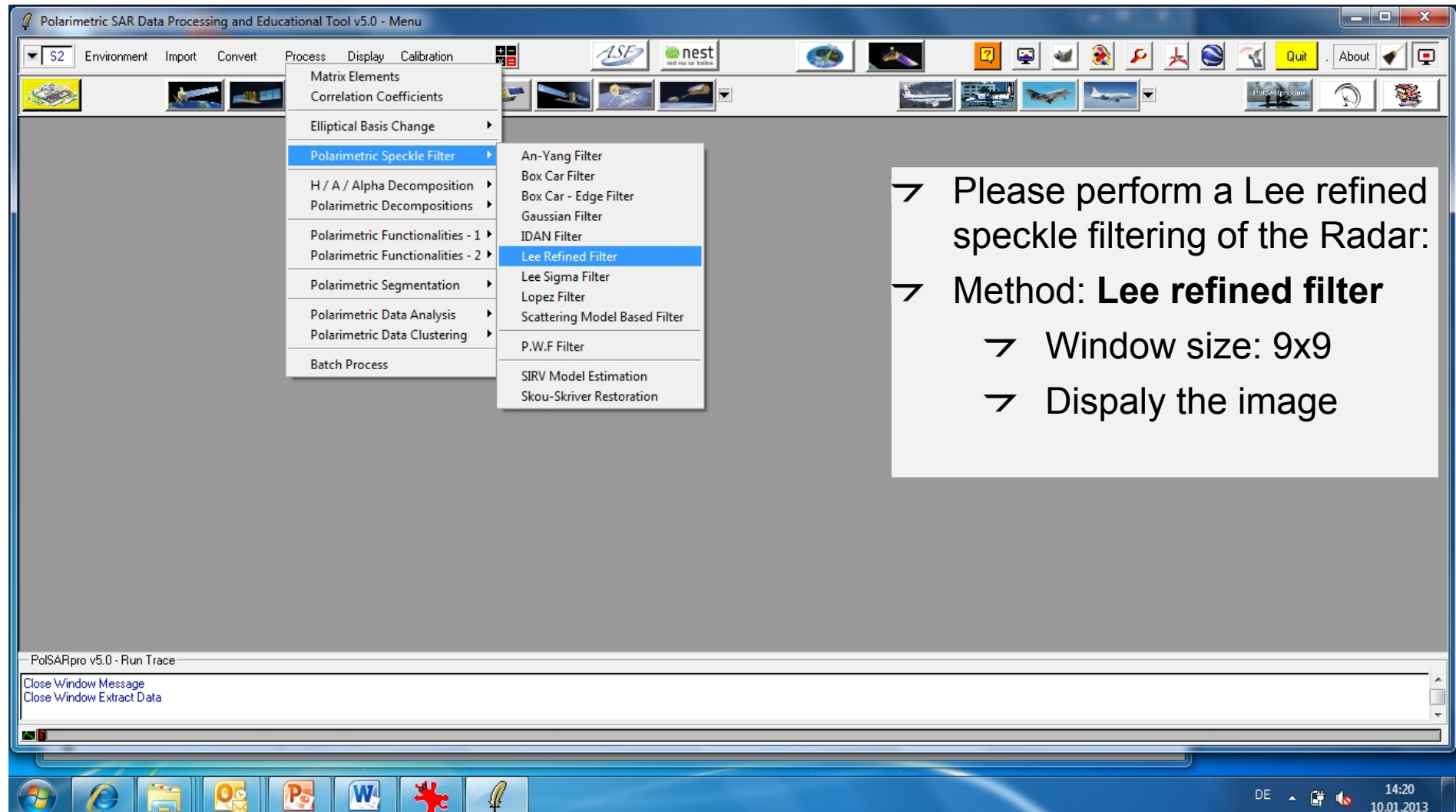
- ↗ Use **GIMP** for image display
 - ↗ What do you see on the image?
 - ↗ What does the colors in the image mean?
 - ↗ Which fields can be potentially inverted to soil moisture content?



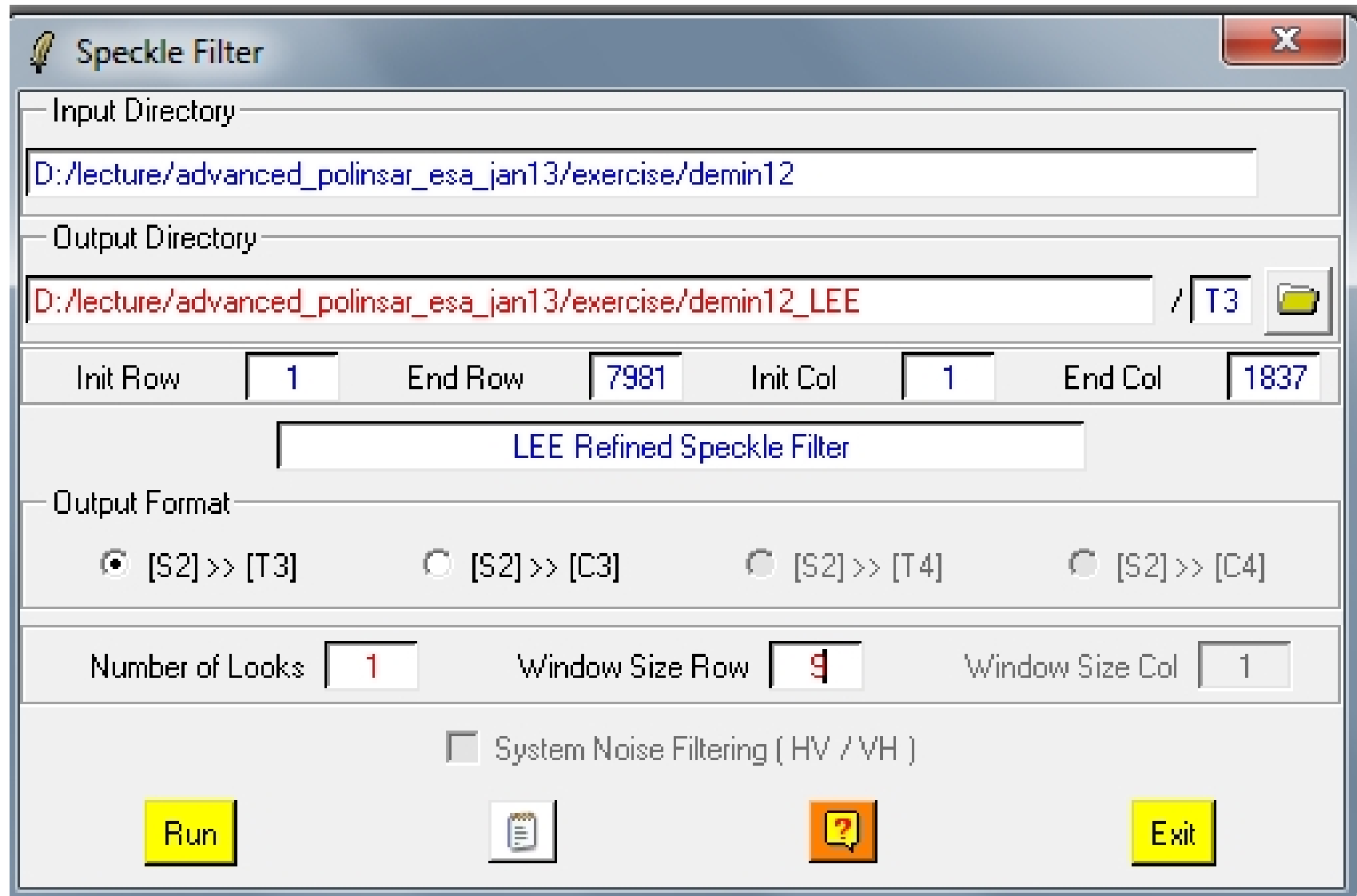
Pauli RGB



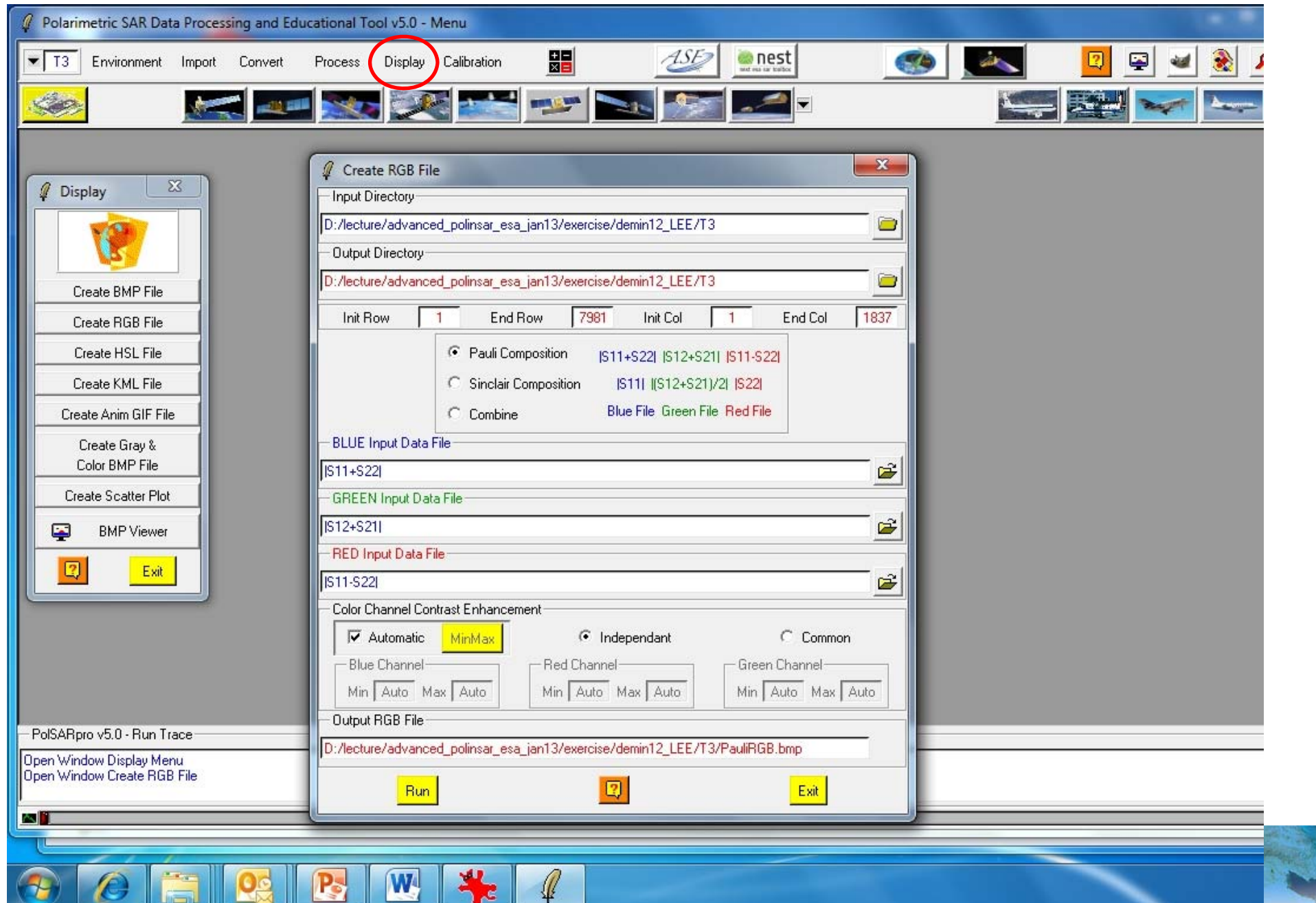
Filtering of the Scattering Matrix



Filtering of the Scattering Matrix



Generate a RGB Image of the Filtered Data



Display the Data

Use **GIMP** for image display



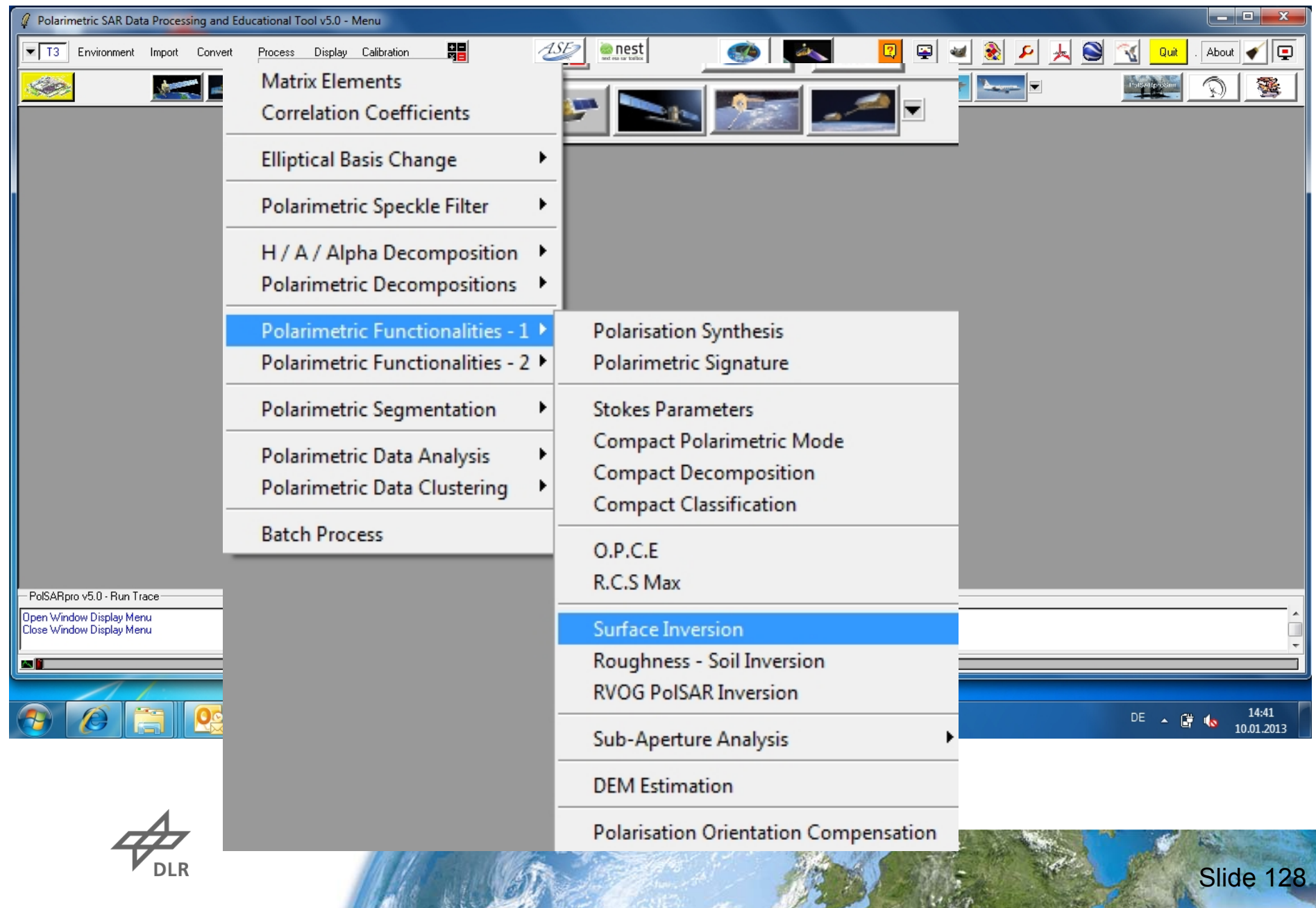
Non Filtered



LEE Refined Filtered
9x9 window

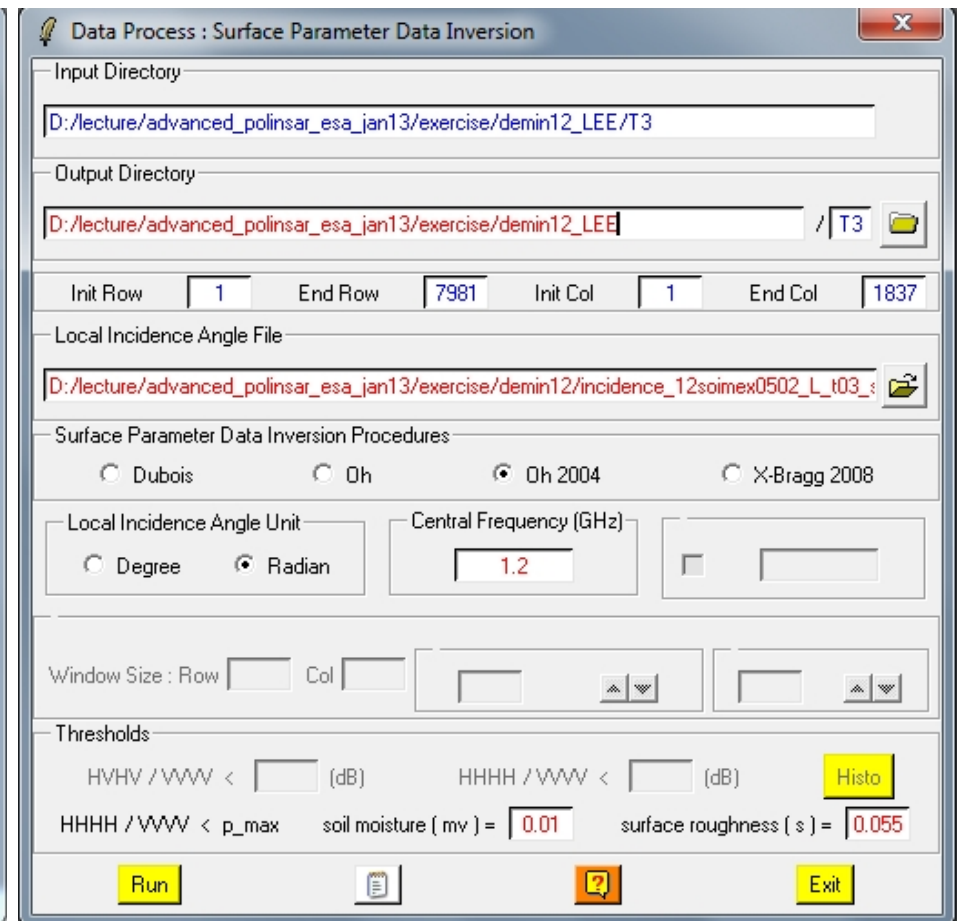
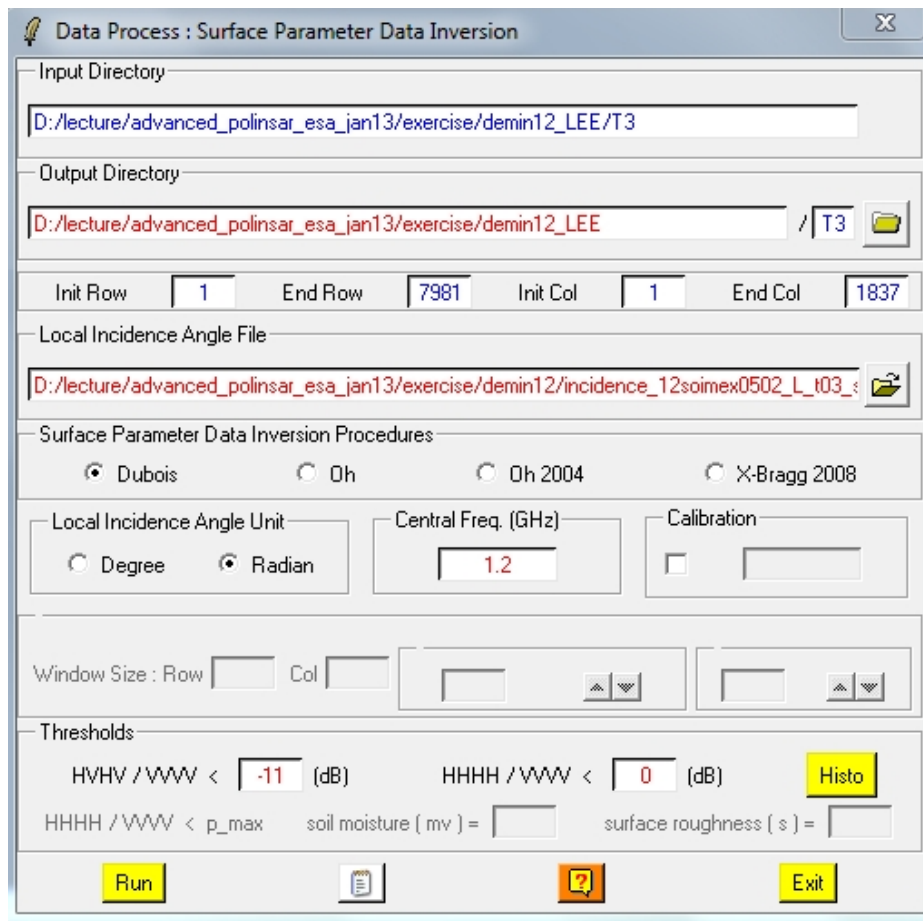


Surface Soil Moisture Estimation (Oh, Dubois & X-Bragg)



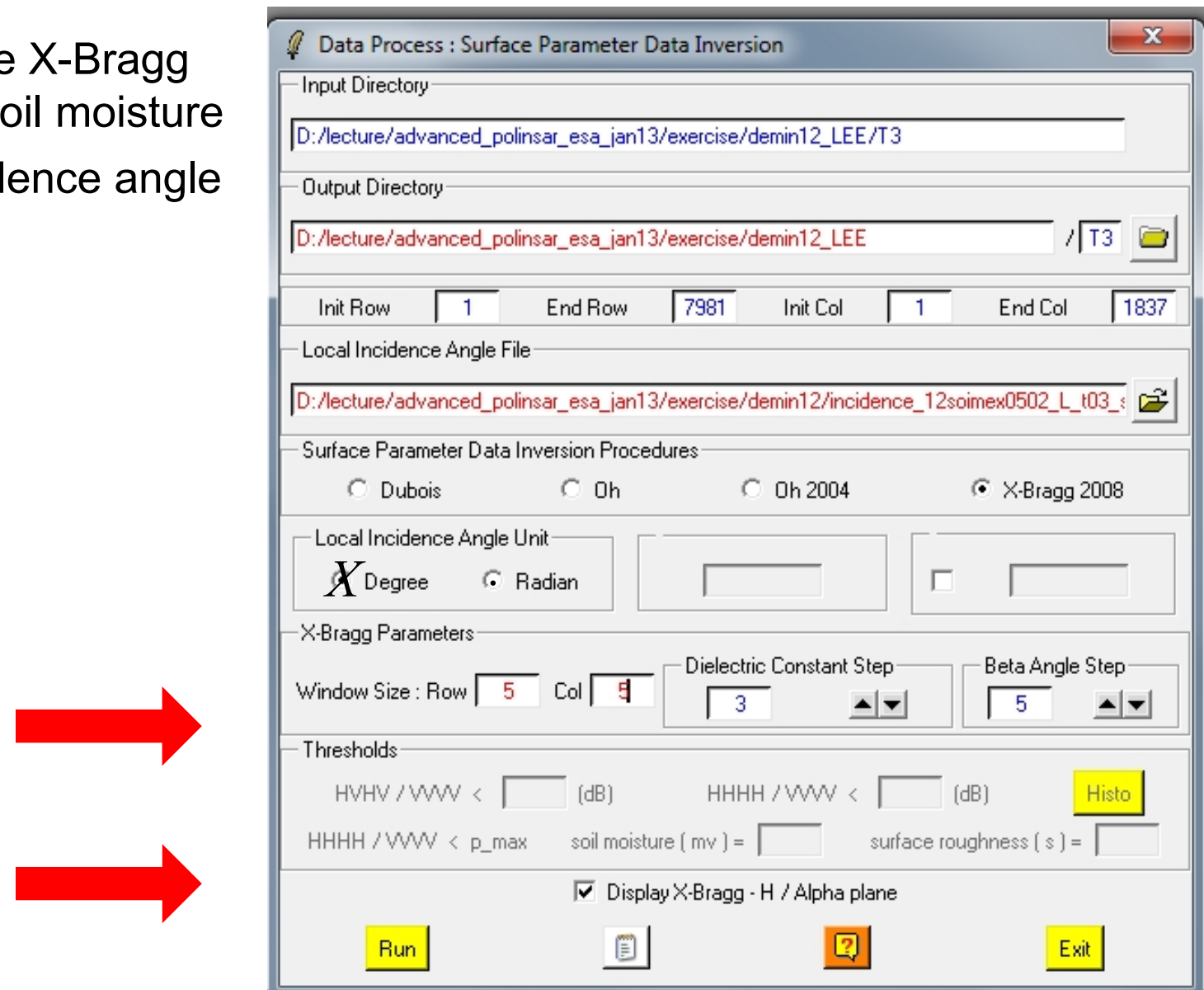
Empirical Models: Dubois @ Oh2004

- Please run the Dubois and Oh2004 inversion for soil moisture
 - Load the incidence angle file (radian)

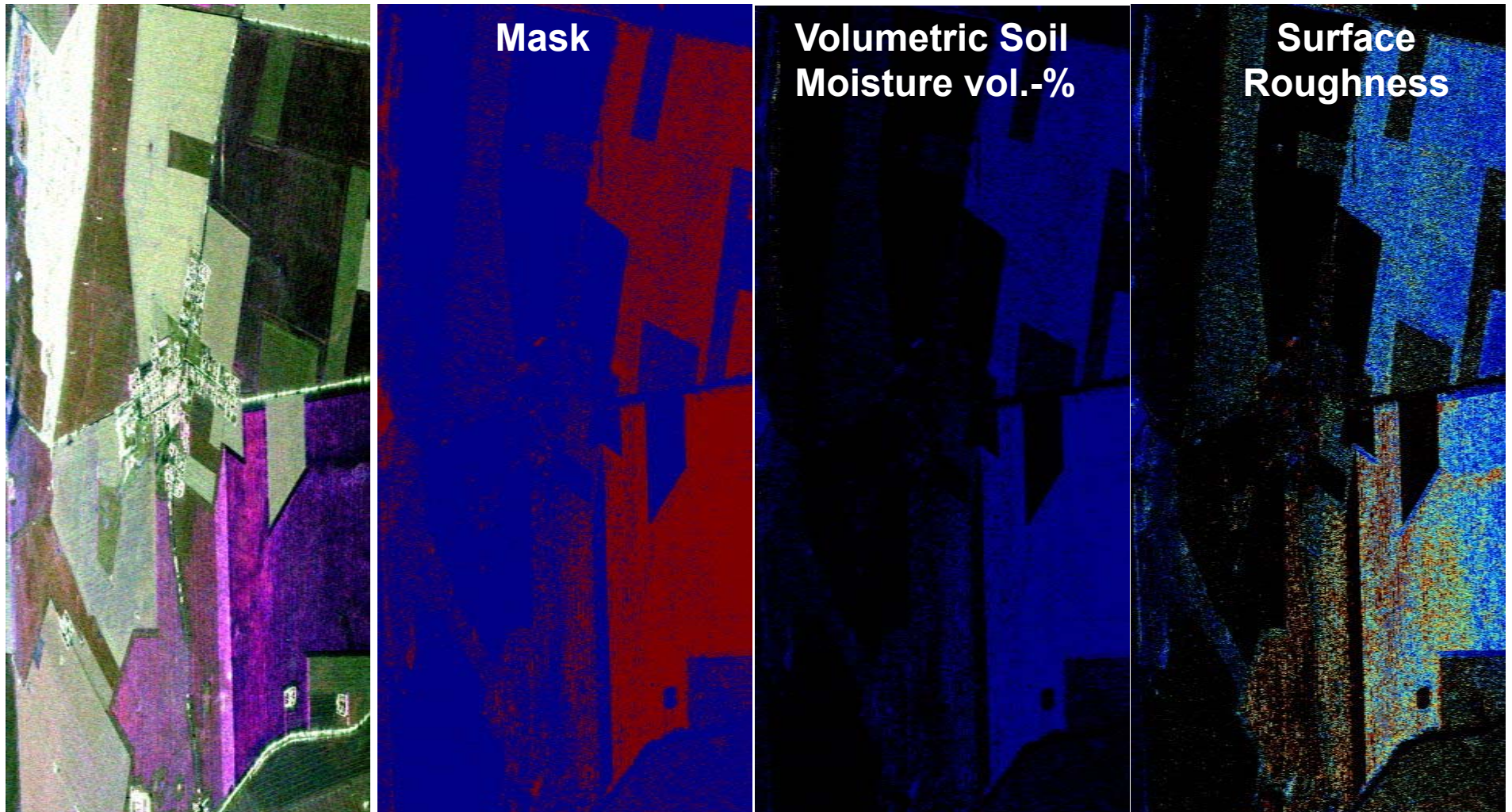


Model Based Models: X-Bragg

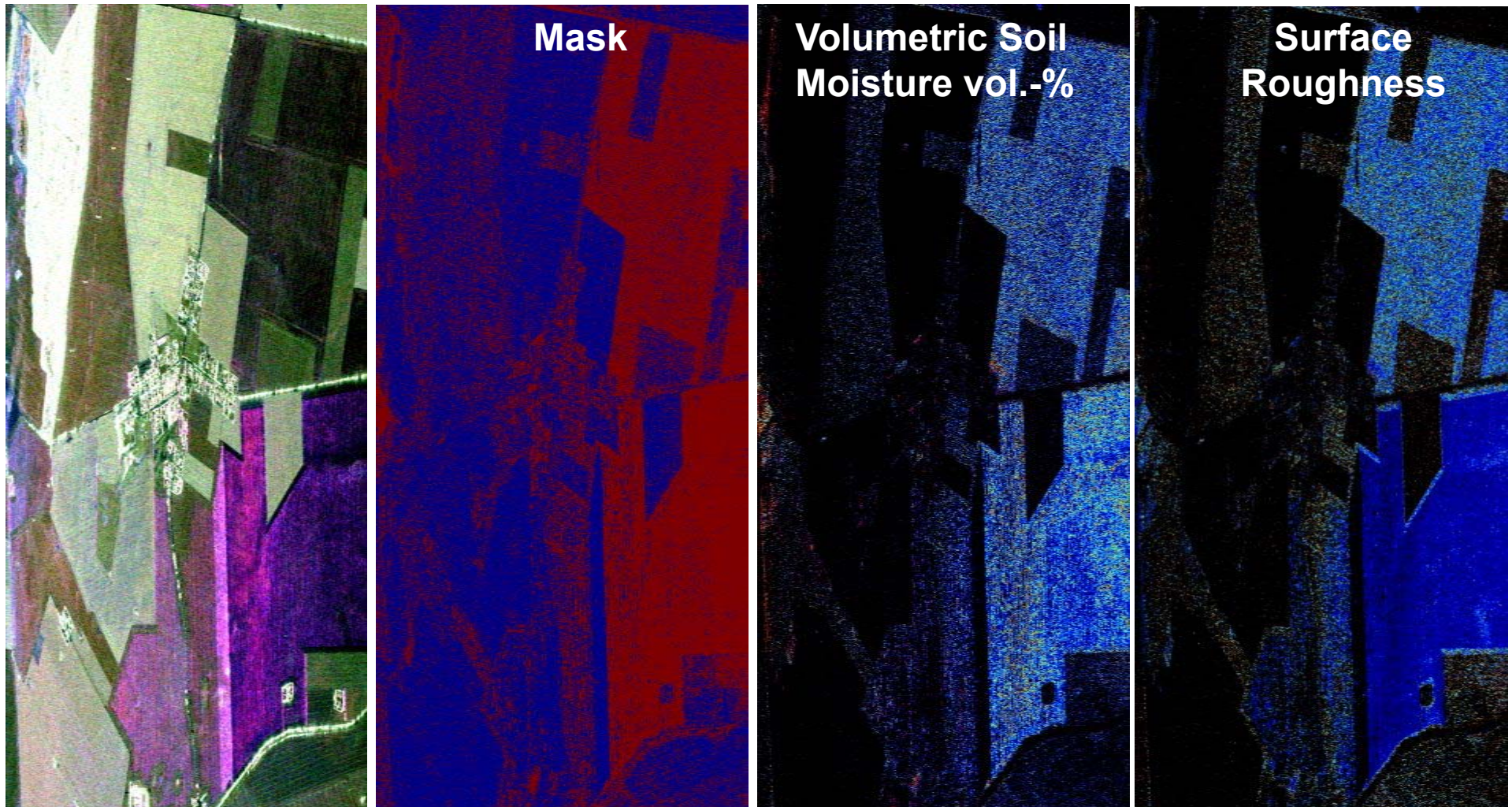
- >Please run the X-Bragg inversion for soil moisture
- Load the incidence angle file (radian)



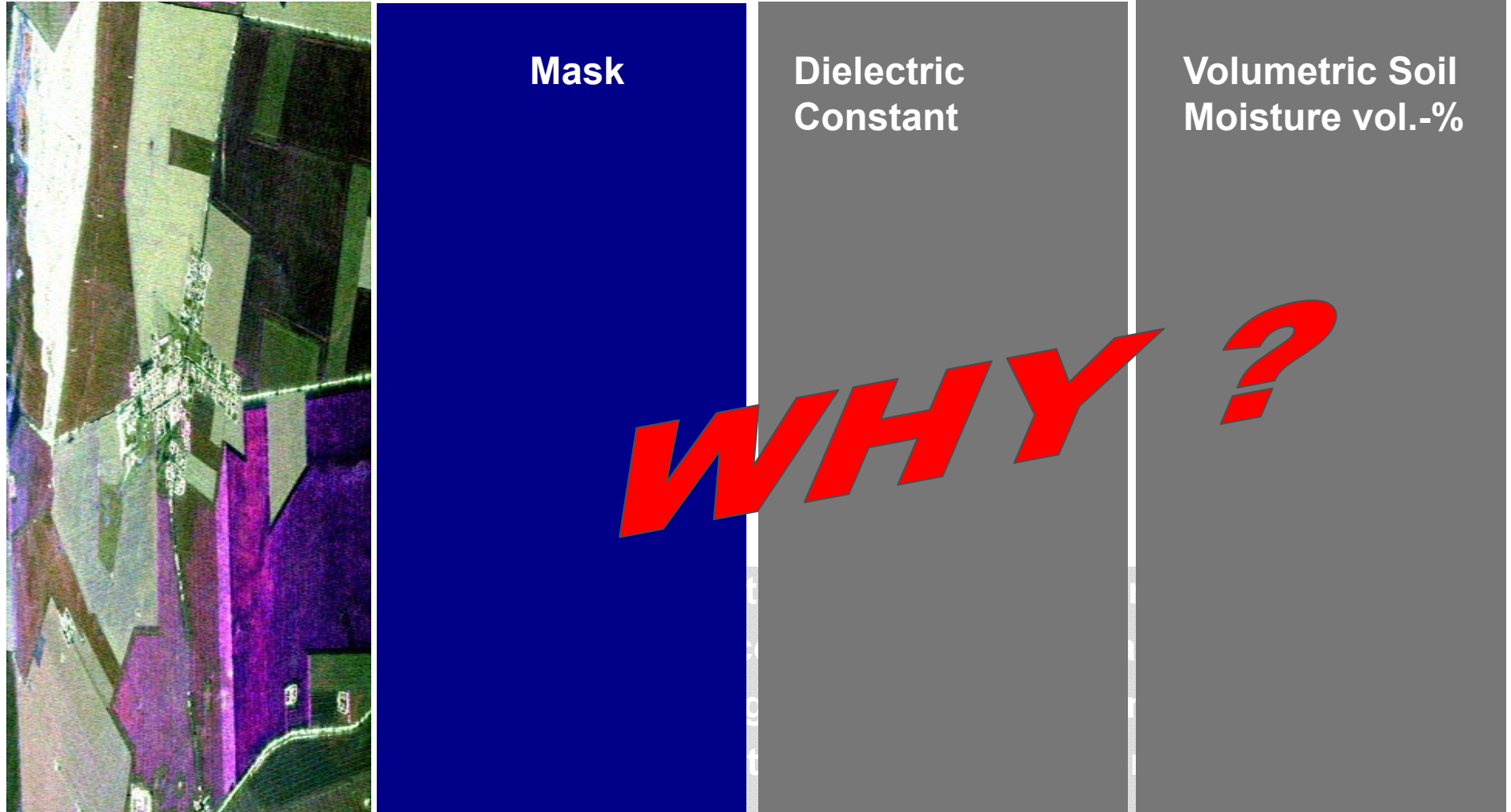
Empirical Models: Dubois – INVERSION RESULTS



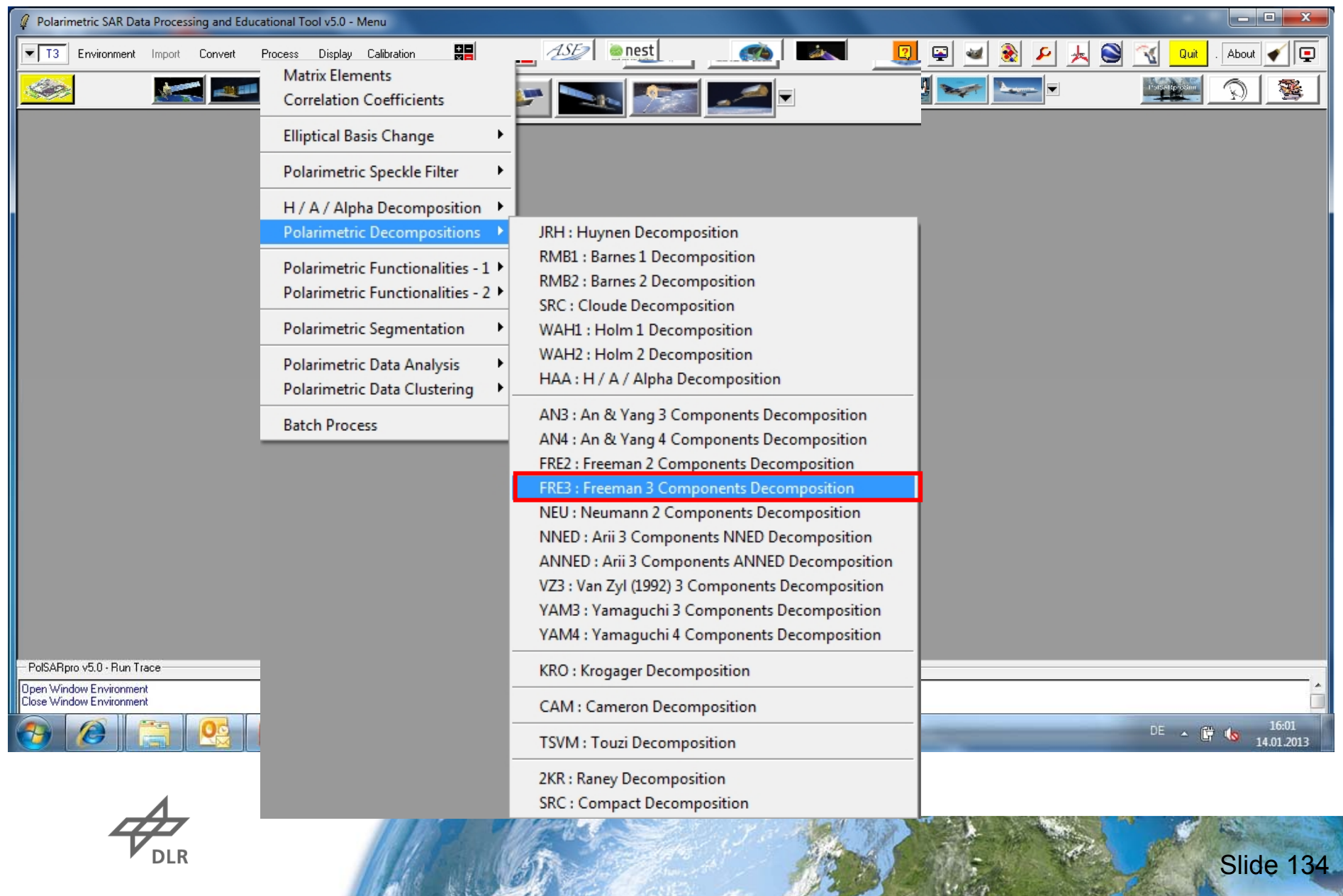
Empirical Models: OH2004 – INVERSION RESULTS



Model Based: X-Bragg – INVERSION RESULTS v4.2

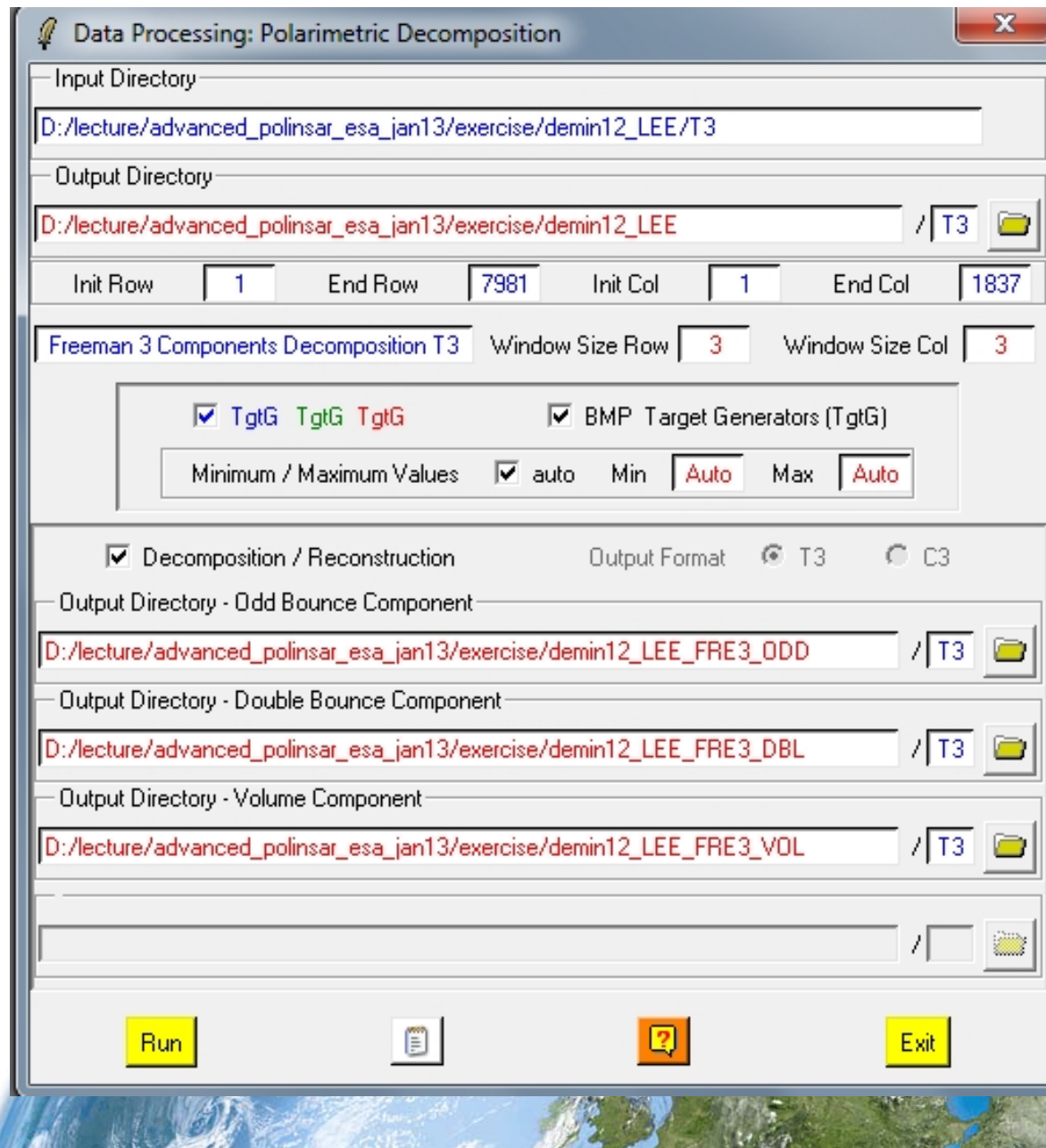


Perform Free3 – Freeman 3 Component Decomposition

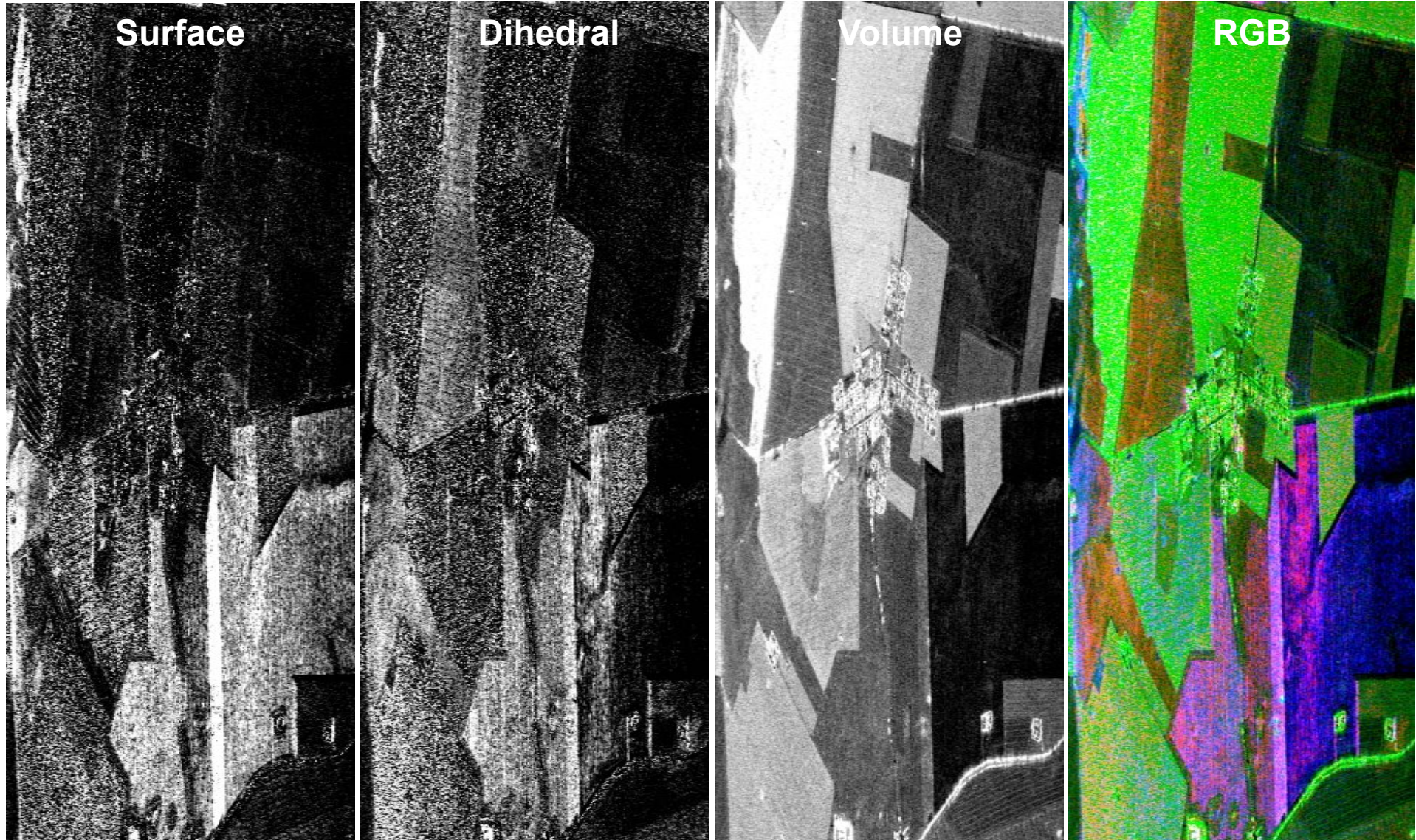


Free3 – Freeman 3 Component Decomposition

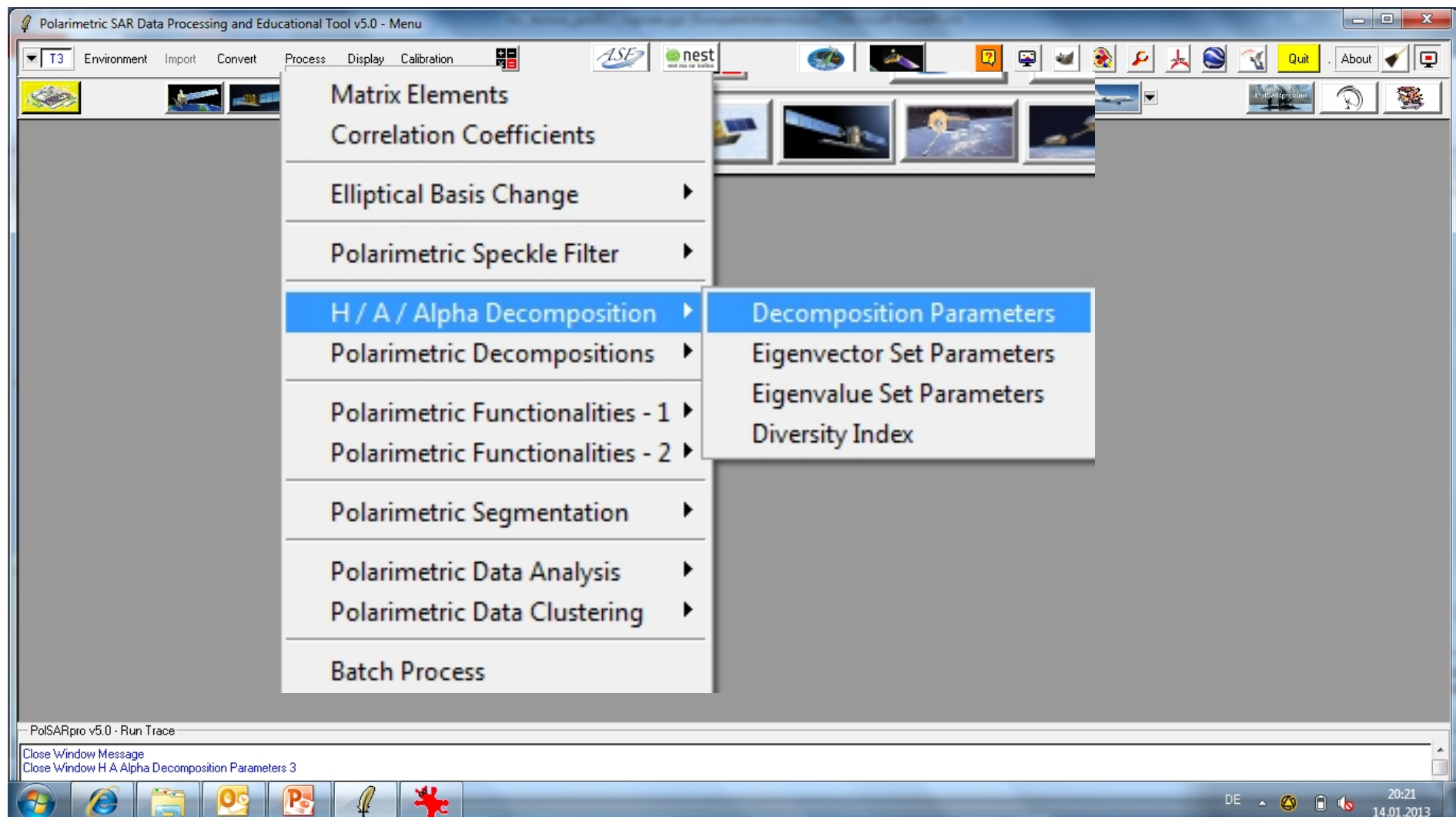
Note: Perform the process on the filtered data



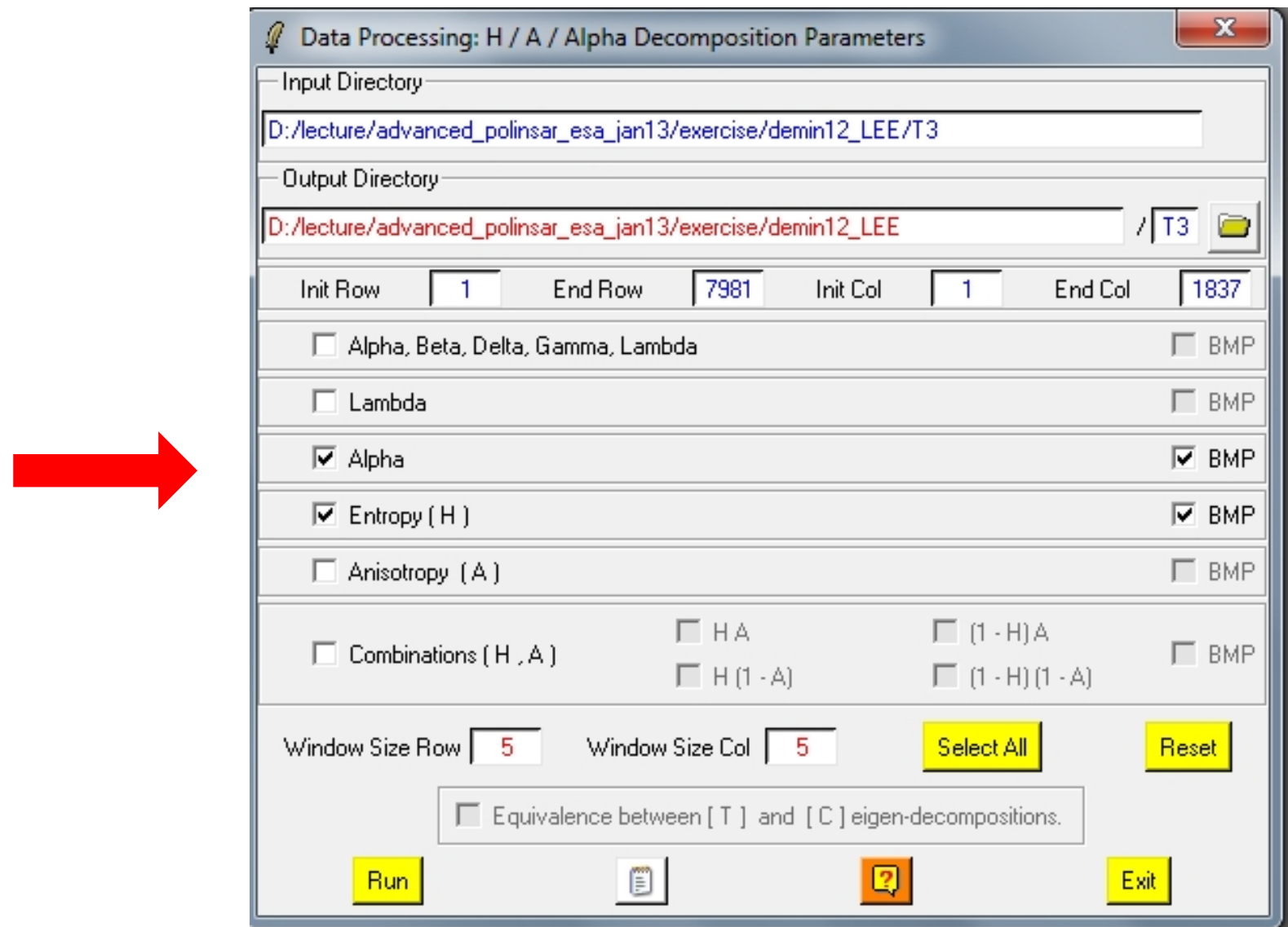
Free3 – Freeman 3 Component Decomposition



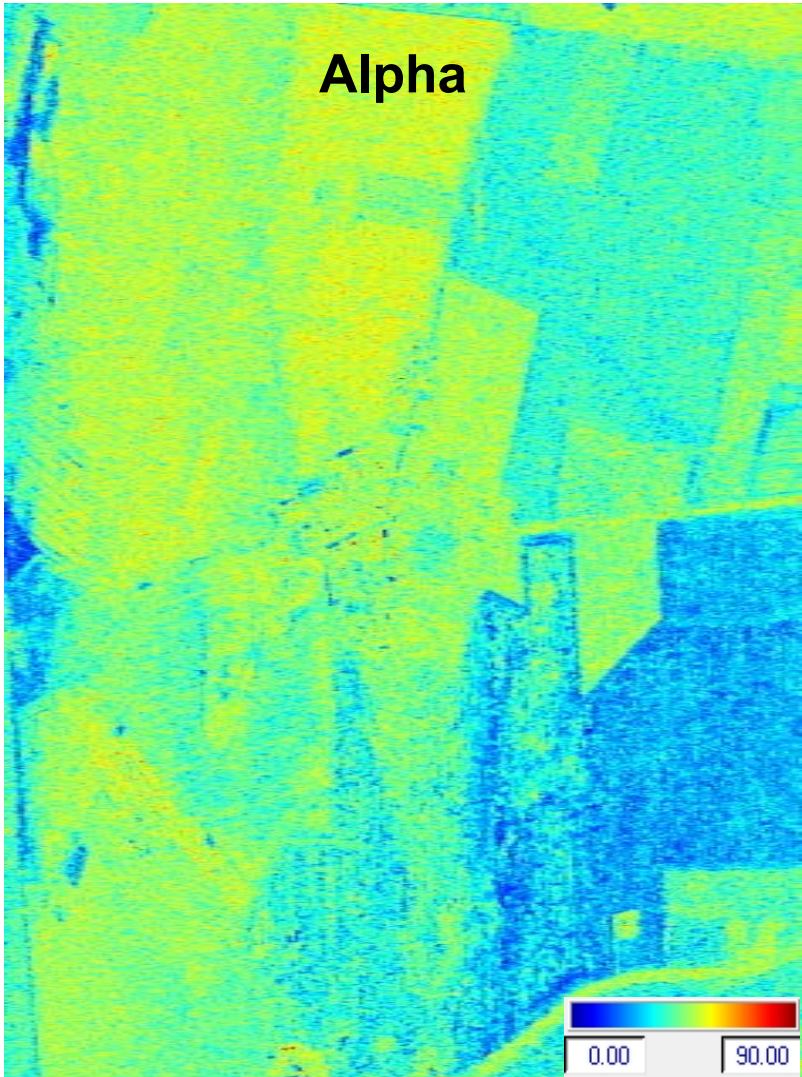
Eigen-decomposition Parameters



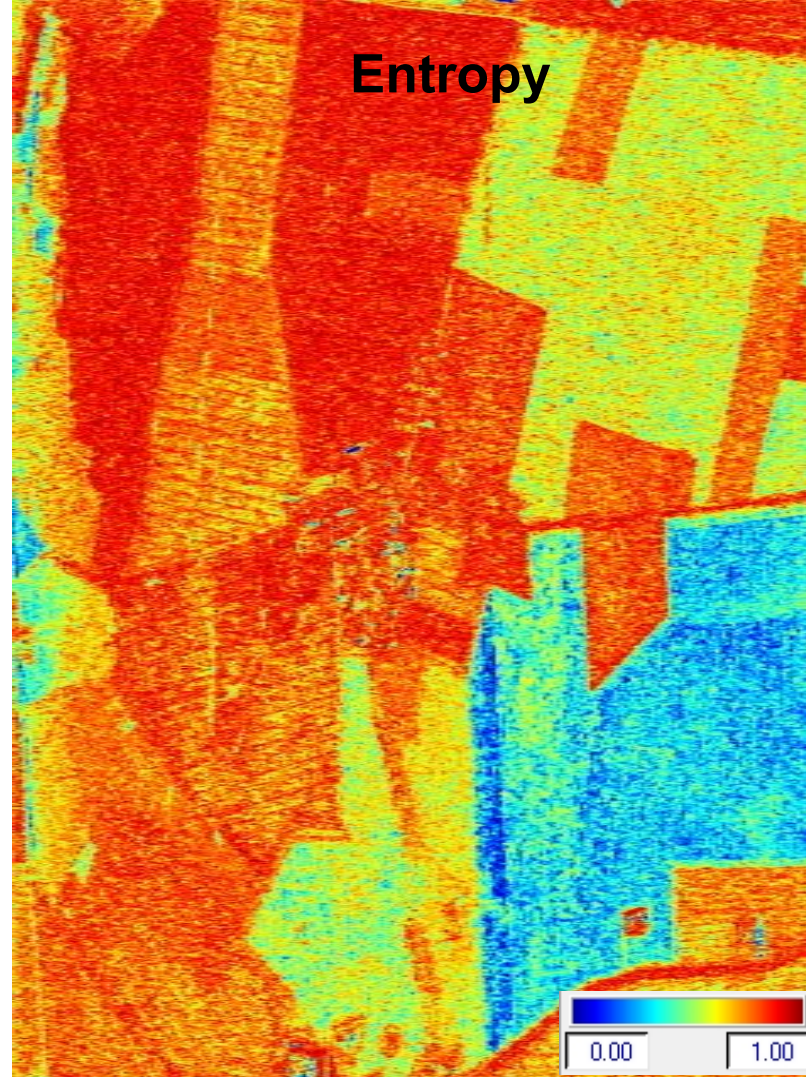
Eigen-decomposition Parameters



Eigen-decomposition Parameters



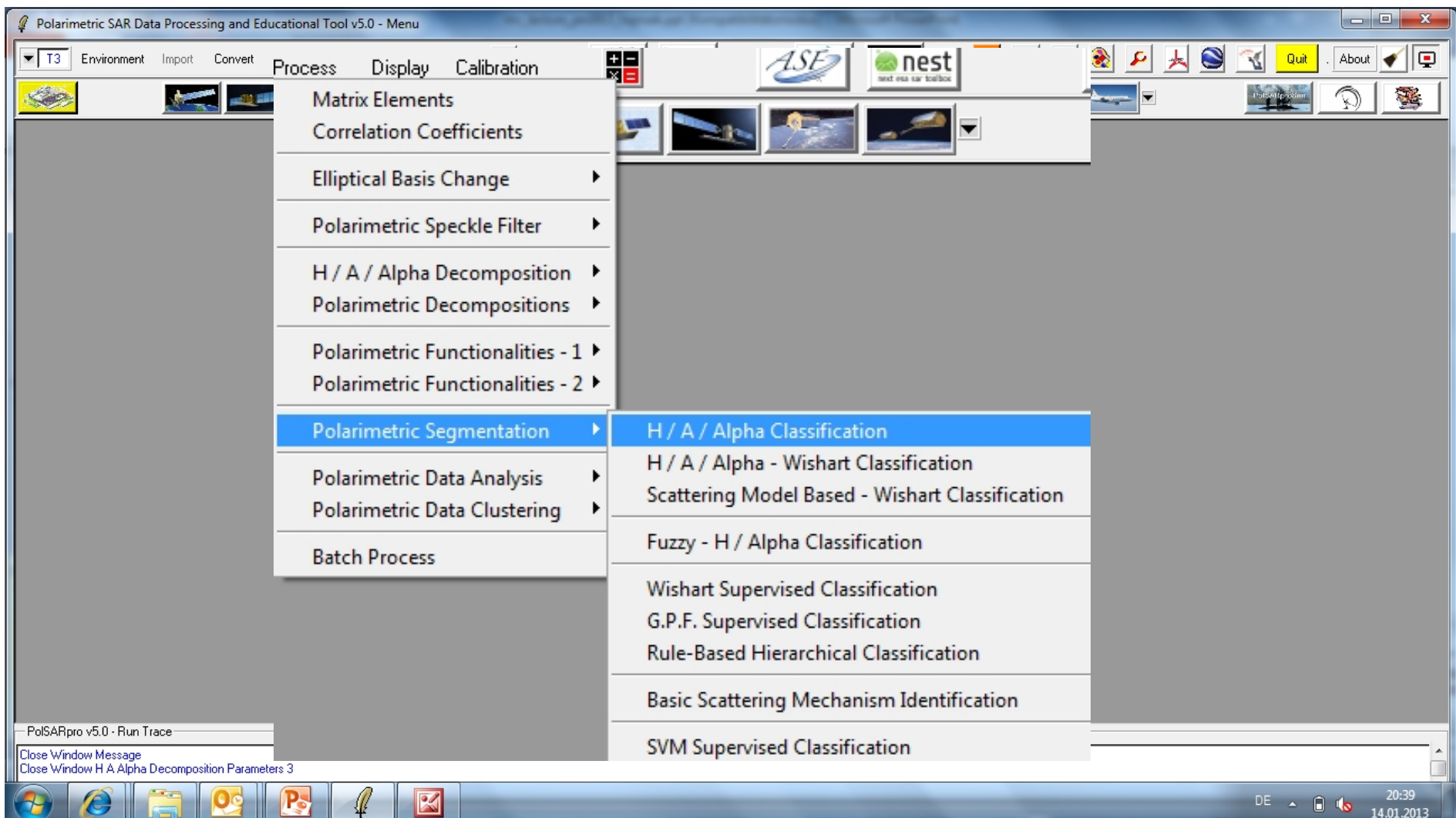
Alpha



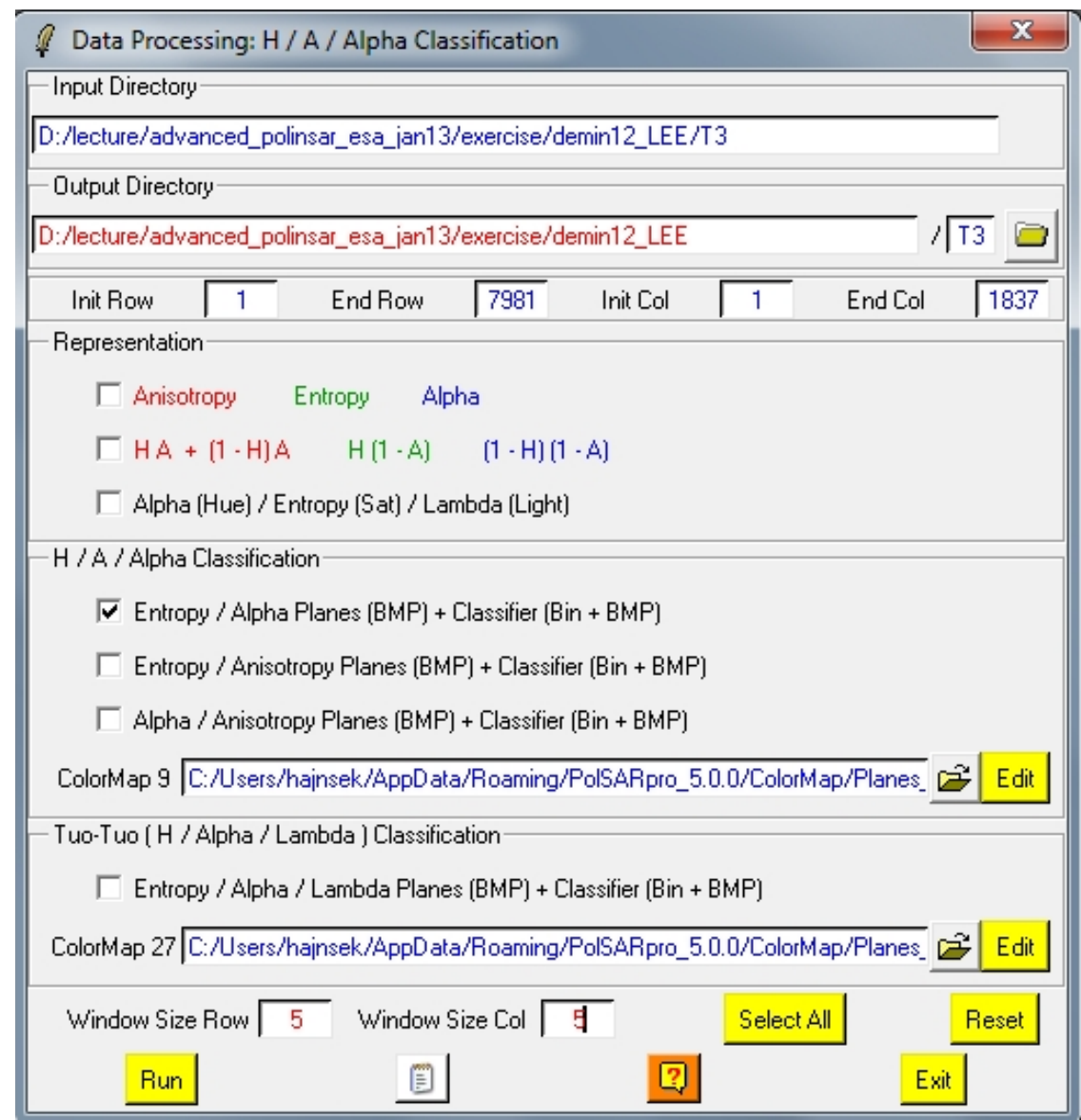
Entropy



2 D Entropy/ Alpha Plot



2 D Entropy/ Alpha Plot



2 D Entropy/ Alpha Occurrence and Segmentation

